UNIVERSITY OF TWENTE.

**Faculty of Electrical Engineering,
Mathematics & Computer Science**

3D Ankle Force and Moment In Ankle Fracture Patients Walking With Instrumented Crutches

Felix J. M. Dransfeld

M.Sc. Thesis
December 2023

Supervisors:
dr. ir. B. F. van Beijnum
prof. dr. J.H. Buurke
dr. E.H.F. van Asseldonk (external)
R. Russcher MSc. (partly)

Biomedical Signals and Systems
Faculty of Electrical Engineering,
Mathematics and Computer Science
University of Twente
P.O. Box 217
7500 AE Enschede
The Netherlands

Preface

"Zo kort als het kan, zo lang als het moet". Which translates to "As short as possible, as long as necessary", is a quote I heard Ellis Folbert use often when talking to patients in the hospital. When patients asked how long it would be before they could go home and how long their rehabilitation would take, this was the answer they repeatedly received. With this research in the field of ambulatory rehabilitation devices, I want to contribute to this adage. The many aspects involved in this thesis, from clinical application and contact with patients to the many hours spent writing code, made it a worthwhile learning experience.

I enjoyed the process of familiarising myself with the problem and coming up with a solution. I also very much appreciated the different views of everyone involved in the project and considered this a valuable addition to the outcome. Bert-Jan for this solution-based way of thinking and his ability to always be one step ahead. Jaap for his valuable input based on years of clinical experience and always making sure people keep a sharp eye by asking 'what if'. Roelien for always being willing to help and for the numerous debates we had about the experimental setup and procedures. Han for the eye-opening experience of seeing patients in the hospital, positivity, and dealing with the exhausting hospital bureaucracy. I hope we can apply the algorithm and instrumented crutches in clinical practice someday.

I want to thank Frodo for building a massive amount of iterations of the instrumented crutches whenever I found something not to my liking and for the many valuable talks we had about anything and everything. And of course Eline for helping with the measurements, her unlimited energy, and her eagerness to learn. And without doubt everyone in the BSS group for the lunch break walks.

I want to thank my girlfriend Rianne for always patiently listening to the many thesis monologues I held, both positive and negative. I want to thank all the friends I made during these study years in Enschede. Studying together surrounded by these meaningful relationships made it much more enjoyable. I want to thank my housemates, in particular Bram and Rejiar who were always there to think about day-to-day struggles and help me put the assignment into perspective. I want to thank my fellow graduation students for our numerous coffee break talks and Teletubbieland lunches.
Finally, I want to thank my amazing parents and brother. Without all your relentless support during my studies I would probably never have finished it.

As I type this text, I realise that the chapter in my life as a student is now closer to the end than I dare to admit. However, for you as a reader, there will be many chapters to come. Enjoy!

Felix Josef Martinus Dransfeld
December 2023
Enschede

Figure 1: The instrumented crutches being used outside.

Additional Research and Contributions

During the course of my thesis research, the project underwent several significant transformations. It initially commenced as a Machine Learning assignment aimed at modeling 3D forces and moments acting on ankle joints using Neural Networks. The input data included information from pressure insoles, Inertial Measurement Units (IMUs), and instrumented crutches, with ForceShoes^{TM} serving as the gold standard reference. The primary goal was to create an ambulatory measurement setup suitable for rehabilitation settings.

However, due to a lengthy 10-month delay in obtaining ethical approval and the constraints imposed by patient availability for measurements, we faced a shortage of training data. Furthermore, the development of the instrumented crutches took 10 months as well before achieving a stable hardware configuration. These challenges prompted us to explore alternative ways to contribute to the field of research.

BRAFO Patient Dataset

The protocol for doing patient measurements was created in a comprehensive way. Measurements contained 10-meter walking tests, figure eight patterns, and performing the activities of daily living of stepping on a raised platform and getting up from a chair, if patients were allowed to do so. Throughout these measurements, patients were equipped with plantar pressure insoles in the ForceShoes^{TM}, instrumented crutches, and Inertial Measurement Units on the feet, lower legs, upper legs, pelvis, sternum, and upper arms. This makes a comprehensive data set, that allows for many more possibilities than discussed in this thesis.

Neural Network Processing Pipeline

Machine learning models made an entry in most scientific research fields in the past years, including biomechanics. In particular artificial neural networks (ANN) have been used in estimating forces and torques of walking. An ANN consist of neurons (nodes) that connect input to an output.

A processing pipeline for training and validating Neural Networks in Python using Jupyter Notebook has been developed. This pipeline included the creation of multiple scripts specifically for the tasks of 10-meter walking tests and figure eight shapes. Models were trained using 200 epochs and a mean squared error optimiser. However, it was ultimately decided not to pursue this direction due to the absence of sufficient patient training data.

Pressure Insole Models

In the study by Mohamed Refai and colleagues, plantar pressure insoles were used to estimate 3D forces and moments of the foot [1]. Patient-specific linear regression models were made, mapping 1D pressure data of 151 pressure sensors to force and moment. This method

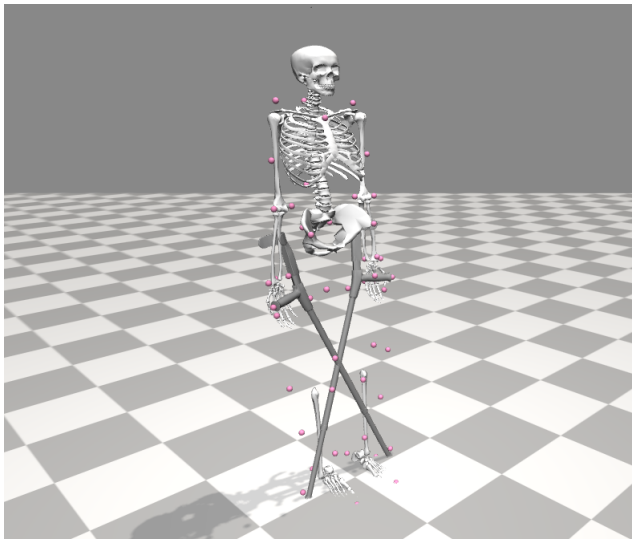

Figure 2: Biomechanical model consisting of skeletal model and crutches developed by Febrer et al. [3]

was applied to and validated on our ankle joints. The model was generalised for all healthy participants and showed good correlations to ForceShoe^{TM} data. However, this model proved unsuitable for both patients. One of the patients had larger feet and consequently an insole with more pressure sensors, making the model unsuitable. The other patient was unique in the data set due to left ankle impairment rather than the right side. The model could not provide accurate estimations in this particular case.

Pressure Insole Centre of Mass

DeBerardinis et al. used plantar pressure insoles to estimate the centre of pressure (CoP) and vertical force under the feet [2]. Outcomes were compared to force plate data and showed good agreement. Vertical force was calculated by multiplying the pressure by the sensor area. CoP was estimated using equation 1 and 2. This method was repeated for measurement data in this thesis and showed good agreement with data obtained from the ForceShoes^{TM}. This allows for the estimation of vertical force, CoP and plantarflexion moment in an ambulatory setting.

$$X_{Ins_t} = \frac{\sum_{i=1}^{n} (D_{t,i})\,(X_i)}{\sum_{i=1}^{n} D_{t,i}} \tag{1}$$

$$Y_{Ins\ t} = \frac{\sum_{i=1}^{n} (D_{t,i})\,(Y_i)}{\sum_{i=1}^{n} D_{t,i}} \tag{2}$$

Biomechanical Model

Another method of estimating 3D force and moments on the ankle joint is by using a biomechanical model. If GRFs of both the feet and crutches are known, internal forces and moments can be calculated. Febrer et al. introduced a 3D full-body skeletal model driven by torque, which incorporated crutches into an excisting full-body OpenSim model (Figure 2) [3]. The IMUs placed on the participants could be used in combination with open-source OpenSense software to calculate ankle force and moments. However, this path was not pursued due to the considerable challenges it posed, making it unfeasible to complete within a reasonable time frame.

Summary

Crutches offer crucial support for lower extremity injuries, transferring body weight to the upper limbs, often aiding those with ankle fractures. Ankle fractures occur at rates between 100 to 150 per 100,000 person-years. After the fracture, patients undergo a six weeks immobilisation period, followed by Partial Weight Bearing (PWB), limiting ankle loading to a percentage of their body weight. Smeeing and colleagues showed an earlier return to work and sports if ankle load began 24 hours after surgery, as opposed to waiting six weeks [4]. Similar research suggests patients should be closely monitored to prevent overloading of the ankle during early weight bearing [5]. This thesis focuses on developing and validating a system for ambulatory measurement and analysis of 3D forces and moments acting on the impaired ankle, highlighting its potential clinical advantages over conventional PWB measurements. The calibration process in Chapter 2 ensures sensor accuracy, establishing a linear relationship between measured forces and applied forces in static settings. Chapter 3 focuses on the design and validation of instrumented crutches using Inertial Measurement Units (IMUs) to track 3D Ground Reaction Forces (GRFs) dynamically. The findings confirm the potential for measuring forces during walking trials, warranting further exploration, particularly regarding crutch tip impact and force validation in real walking scenarios. Chapter 4 introduces a novel method for estimating 3D forces and moments in the ankle joint during crutch gait, significantly improving upon current clinical practices. Emphasising the importance of 3D ankle force and moment beyond PWB, the study calls for additional research on more varied tasks and accurately modelling 3D forces and moments using sensor input. Additionally, the measurements performed during this research contained expanded tests, added patients, and diverse sensors, enhancing dataset value for future gait research within the BRAFO project.

Samenvatting

Krukken vormen een belangrijke ondersteuning bij letsels aan de onderste extremiteiten. Hierbij wordt het lichaamsgewicht gedeeltelijk overgebracht naar de bovenste ledematen, vaak ter ondersteuning van mensen met enkelbreuken. Enkelbreuken komen voor tussen 100 en 150 per 100.000 persoonsjaren. Na de enkelbreuk ondergaan patiënten een immobilisatieperiode van zes weken, gevolgd door Gedeeltelijke Belasting (GB), waarbij de belasting op de enkel wordt beperkt tot een percentage van het lichaamsgewicht. Smeeing en collega's toonden aan dat een sneller herstel en eerder weer beginnen aan werk en sport mogelijk was als de belasting op de enkel 24 uur na de operatie begon, in plaats van zes weken te wachten [4]. Vergelijkbaar onderzoek suggereert dat patiënten nauwlettend in de gaten gehouden moeten worden om overbelasting van de enkel tijdens vroeg belasten te voorkomen [5]. Deze scriptie richt zich op de ontwikkeling en validatie van een systeem voor ambulante meting en analyse van 3D-krachten en -momenten die werken op de gebroken enkel, waarbij de potentiële klinische voordelen ten opzichte van conventionele GB-metingen worden onderzocht. Het kalibratieproces in Hoofdstuk 2 zorgt voor nauwkeurigheid van de sensoren door het vaststellen van een lineaire relatie tussen gemeten krachten en toegepaste krachten in statische omgevingen. Hoofdstuk 3 richt zich op het ontwerp en de validatie van geïnstrumenteerde krukken met behulp van Inertial Measurement Units (IMU's) om dynamisch 3D GRFs te meten. De bevindingen bevestigen het potentieel om krachten te meten tijdens kruklopen. Verder onderzoek kan zich met name richten op de impact van de rubber dop onder de krukken en de validatie van krachten in echte loopscenario's. Hoofdstuk 4 introduceert een nieuwe methode om 3D-krachten en -momenten in het enkelgewricht te schatten tijdens kruklopen, waarbij aanzienlijke verbeteringen worden aangebracht ten opzichte van de huidige klinische praktijken. Door de nadruk te leggen op het belang van 3D-enkelkracht en -momenten ten opzichte van GB, pleit de studie voor aanvullend onderzoek naar meer gevarieerde taken en het nauwkeurig modelleren van 3D-krachten en momenten met behulp van sensordata. Bovendien bevatten de metingen die tijdens dit onderzoek zijn uitgevoerd uitgebreide tests, extra patiënten en diverse sensoren, waardoor de data set een enorme meerwaarde biedt voor toekomstig looponderzoek binnen het BRAFO-project.

Misura ciò che è misurabile, e rendi misurabile ciò che non lo è.

Measure what can be measured, and make measurable what cannot be measured.

Galileo Galilei (1564 - 1642, Pisa)

List of Symbols

Symbol	Definition	Unit
a	Acceleration	m/s^2
a_k	Acceleration error	g
α	Amplification matrix	-
b_k	Gyroscope bias error	rad/s
C	Calibration matrix	N/V
$\times$	Cross product	$-$
F	Force	N
f_c	Cut-off frequency	Hz
$\hat{F}$	Reference force	N
F_{res}	Resulting force	N
g	Gravitational acceleration	m/s^2
G	Calibration matrix values	N/V
h	Height	m
I	Moment of Inertia	kgm^2
m	Mass	kg
M	Moment	Nm
M_{res}	Resulting Moment	Nm
ω	Angular velocity	rad/s
ψ_{crutch}	Reference system of crutch	$-$
ψ_{sensor}	Reference system of sensor	$-$
ψ_{trial}	Reference system of trial	$-$
R	Rotation matrix	$-$
R^2	Coefficient of determination	$-$
τ	Torque	Nm
θ	Angle	rad
θ_k	Orientation error	rad
V	Voltage	V
x_k	Error process	$-$

List of Abbreviations

Abbreviation	Meaning
3D	Three dimensional
10MWT	10-Meter Walking Test
ADC	Analogue-to-digital converter
AP	Anteroposterior
BRAFO	Balanced Rehabilitation after an Ankle Fracture Operation
BW	Body Weight
BWH	Body Weight Height
COM	Center of Mass
COP	Center of Pressure
EQ VAS	EuroQol-Visual Analogue Scales
F&M	Force and Moment
FT	Force Torque
GRF	Ground Reaction Force
vGRF	Vertical Ground Reaction Force
ID	Inverse Dynamics
IMU	Inertial Measurement Unit
MATLAB	Matrix Laboratory
ML	Mediolateral
OMAS	Olerund-Molander Ankle Score
PWB	Partial Weight Bearing
RMSE	Root mean square error
SF-36	Short Form (36)

Contents

I. General Introduction

Chapter 1

Introduction

Crutches are widely used as support for walking with lower extremity injuries. In the United States alone, approximately six million people depend on the use of crutches for ambulation, as indicated by Rasouli [6]. When using crutches, part of the load of the body is transferred to the upper limbs to relieve strain on the lower extremities during both walking and activities of daily living. Crutches stimulate being active and walking with an upright posture, giving benefits for long-term health [7].

The two most common crutch types are forearm crutches and axillary crutches. The latter one features hand grips and a support pad placed in the axilla (the armpit area). Weight-bearing is done on the handle and the axilla pad is designed to enhance stability. In Europe, forearm crutches are more common. Forearm crutches are equipped with a handle and a forearm band that facilitates the transfer of body weight to the crutch [6].

One of the reasons crutches are often needed is ankle fractures. Incidence rates of ankle fractures range between 100 and 150 per 100,000 person-years [8, 9]. Approximately 55% of these ankle fractures result from sports-related activities. Following such a trauma, realignment is often needed. In case of unstable ankle fractures, surgical fixation is needed. This is followed by an immobilisation phase of six weeks while the fracture is healing [10].

Post-immobilisation, a rehabilitation process is started, where a patient is allowed to gradually start loading the affected ankle [11]. During the rehabilitation process, a physiotherapist gives feedback to ensure patients perform exercises correctly. Throughout this process, especially after surgery, patients are restricted to partially loading their ankles. This is called Partial Weight Bearing (PWB) and is expressed in percentage of the body weight. The physiotherapist determines the allowable PWB percentage, tailoring the rehabilitation process to each patient's specific needs. Over time, the percentage PWB is gradually increased on a weekly basis until full load is allowed again. Further stages of rehabilitation involve activities such as walking, squats, and calf raises, all under the supervision of a physiotherapist. The majority of the rehabilitation process, however, is executed by patients at home.

Motivation

Smeeing and colleagues showed an earlier return to work and sports if ankle load began 24 hours after surgery, as opposed to waiting six weeks [4]. Participants were allowed to perform unprotected weight-bearing as tolerated. The study involved 115 participants who underwent surgical fixation of a Lauge-Hansen supination external rotation stage 2-4 ankle. See Chapter F in the Appendix for a detailed overview of ankle fracture classifications. Dehghan et al. found early postoperative weight bearing in ankle fracture surgery patients to enhance range of motion and increase physical and mental SF-36 scores six post-operation [11]. Neither study reported complications or infections arising as a result of early weight bearing.

Park et al. compared early weight bearing with non-weight bearing 12 months postoperatively. Early weight bearing was allowed two weeks post-surgery. The comparison involved Olerund-Molander ankle scores (OMAS) for both groups and the time required to return to pre-injury activities. The study concluded that the early weight-bearing group featured a shorter recovery time to pre-injury activities. OMAS scores after 12 months for early weight bearing showed no significant difference between the two groups.

In a research of Schubert et al. two groups were investigated after surgery on an unstable rotational-type ankle fracture. The first group was allowed weight bearing two weeks postoperatively, and the second group after six weeks. OMAS scores as well as general health status (EQ-5D VAS) scores were compared for both groups, 2, 6, 12, and 26 weeks after surgery. Results showed higher mean EQ-5D VAS scores at a 6-week follow-up for the early weight-bearing group. OMAS scores were similar after 26 weeks for both groups. It was concluded there is a clinically relevant and statistically significant benefit in patient general health status in the early weight-bearing group compared to the reference group [12]. Similar research additionally concluded that patients doing early weight bearing should be closely monitored at home to prevent overloading during early weight bearing [5].

The Balanced Rehabilitation after an Ankle Fracture Operation (BRAFO) project focuses on developing an ambulatory measurement system for rehabilitation of ankle fracture patients outside of the clinic [13]. For this purpose, regular forearm crutches are equipped with a 6 DOF force/torque sensor (ATI Mini 45 SI-580-20) just above the crutch tip and an Inertial Measurement Unit (IMU, MPU9250) to measure linear acceleration and angular velocity. The crutches transmit data wirelessly over Bluetooth. Additionally, the system included insoles for foot pressure measurement, inertial measurement units (IMUs) placed on different body parts, and a ForceShoe^{TM} system for quantifying 3D force and moments exerted on the feet.

Within the BRAFO project, there are two main topics. The first one is to investigate balance and gait parameters during crutch walking in patients after an ankle fracture. The second one, which this thesis is about, focuses on forces on the affected ankle during crutch walking. In this pilot study, the system was clinically validated in a patient group of two patients with ankle fractures and four healthy subjects simulating fractures. This study provides valuable insights into the system's usability, applicability, and potential clinical applications.

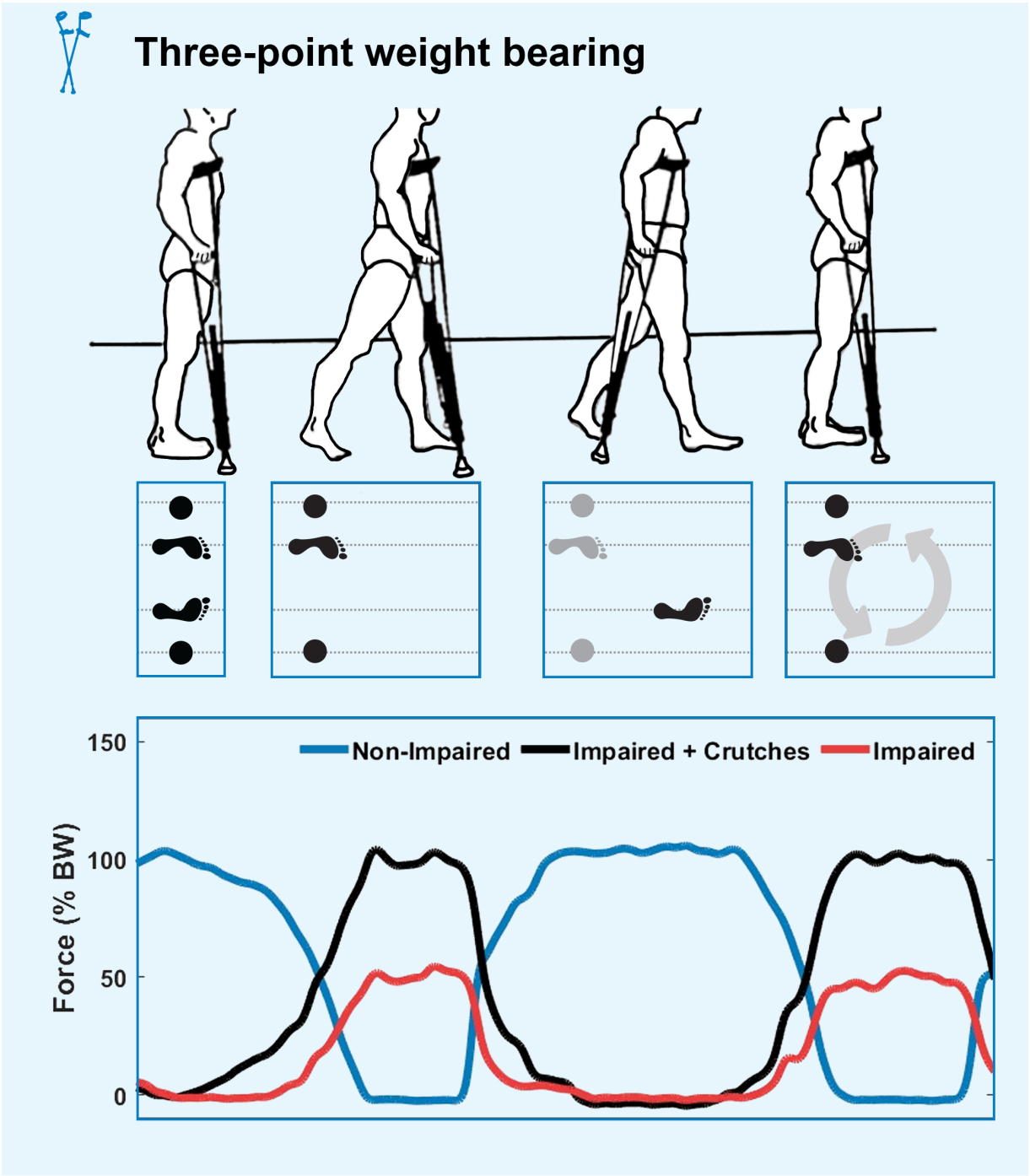

Figure 1.1: Three-point weight bearing is often used for rehabilitation [14]. It provided for varied levels of weight-bearing. Both crutches are moved forward at the same time as the impaired side, followed by advancing the non-impaired side. The image shows axillary crutches, in this research, forearm crutches were used. The top image was adapted from Utah's Joint Replacement Specialist [15], the middle image is adapted from Rasouli [6].

Problem Statement

This research focuses on the forces on the impaired ankle during crutch walking. To get full insight into the load, both force and moment are investigated. Forces during crutch gait are measured using instrumented crutches. ForceShoes™ are used as force and moment reference in this research.

Next to the design and validation of the instrumented crutches, the net 3D force and moments on the ankle joint are assessed. Crutches are used for weight-bearing introducing differences between the impaired and non-impaired ankle in terms of load. Figure 1.1 shows an overview of three-point weight-bearing gait, the placement of feet and crutches, and the vertical forces involved.

The main objective of this thesis is to develop and validate a system that allows for ambulatory measurement and analysis of forces and moments acting on the ankles of patients with ankle fractures. In addition to this, an important part is to investigate ankle loading patterns. This included identifying the dominant force and moment directions and comparing the differences between 3D information and the current clinical measure of PWB.

The initial step in this process involves calibrating the force sensors used in the custom-designed instrumented crutches. This includes making specific adjustments to ensure the accuracy of the sensors. The central question posed in this context is: 'What is the relationship between measurement from the instrumented crutches and presented forces?'

Subsequently, the procedure for measuring Ground Reaction Forces (GRFs) of the instrumented crutches was presented. Crutch GRFs needed to be transformed from a local reference system to a general reference system. To validate the accuracy of this instrumented crutch system, it was compared to data obtained from force plates, which served as the reference standard. The question addressed here is: 'How can 3D GRFs be measured using instrumented crutches in combination with an IMU?'.

The BRAFO project focuses on the applicability and clinical possibilities of the measurement system. In addition to evaluating the patterns of ankle and crutch loading in both healthy participants and patients with ankle fractures, the clinical measure of PWB is also assessed. PWB exclusively focuses on the vertical force and therefore potentially misses crucial information. The question that arises is: 'What information does 3D net ankle force and moment contain compared to PWB?'.

Thesis Organisation

To answer the main and sub-questions, the thesis is divided into parts. The General Introduction is followed by Part II, where Chapter 2 describes the calibration of force sensors and Chapter 3 the design and validation of the instrumented crutches. In Part III, Chapter 4 presents the comparison of net 3D ankle force and moments to Partial Weight Bearing. The population consisted of four simulated ankle fracture and two ankle fracture patients. In part IV, Chapter 5 gives the General Discussion of the whole thesis.

In Appendix A additional results to Chapter 4 are presented. Appendix B elaborates on the hardware design of the crutches and serves as documentation for future medical research. Appendix C assesses the drift that was present in the force sensors due to increasing temperature.

In D research is presented where optical markers were used to determine the orientation of the crutches, instead of IMUs.

Finally, in Appendix E and F, a short overview of different crutch walking patterns as well as ankle fractures are presented respectively. Appendix G contains the documents of ethical approval and Appendix H the measurement protocol.

II. Crutch Calibration, Design and Validation

Chapter 2

Static Calibration of ATI 45 Mini Force Sensor

In this chapter, the calibration of the force sensor that is located at the tip of the instrumented crutches is described. The purpose of calibrating the force sensor is to determine the relationship between the values measured by the sensor and the actual forces that are applied at the crutch tip. In order to do so, forces are presented to both force sensors in a static situation using a test setup. A description of the hardware design of the crutches can be found in Appendix B Hardware Design. Measurement changes due to temperature changes can be found in Appendix C.

2.1 Introduction

The first research question asked in the introduction chapter is: "What is the relationship between measurements from the instrumented crutches and present forces?" Answering this question requires determining the relationship between the raw sensor readings and present forces. To determine this correlation, a calibration procedure is necessary, consisting of applying known forces to the force sensor situated at the crutches' tips. After the calibration, forces present at the crutch tip can correctly be measured and expressed in the reference frame of the crutch.

Previous work by Sesar et al. used a piezoelectric force sensor in an instrumented crutch [16]. Calibrating the force sensor was done by placing the crutch vertically on an already validated force plate. Random forces were applied to find the relationship between sensor voltage measurements and force plate force readings. A coefficient of determination value of $\boldsymbol{R^2}$ = 0.996 was found, and a Root Mean Square (RMS) error of 8.78 N.

Chamorro-Moriana and colleagues used a similar method for the calibration of the force sensor in their instrumented crutches [17]. A rate of determination of $\boldsymbol{R^2}$ = 0.993 was found and it was concluded this is sufficient for accurately monitoring gait. The research by Sesar and colleagues additionally introduced the existence of non-linearities in their system due to friction and the dynamics of the amplifier conditioning the voltage output of the sensor. Despite non-linearities, both studies concluded readings were accurate enough for gait monitoring.

The relationship between measured values of the force sensors and the present forces is originally linear. A calibration matrix supplied by the sensor manufacturer can be used to calculate these forces. However, for various reasons, an additional scaling factor may be introduced. In

addition, a non-linear relationship may have arisen due to the components used in the crutches.

The instrumented crutches used in this study both contain an ATI Mini 45 SI-580-20 (Schunk, Arnhem, NL) Force/ Torque (FT) sensor, that were left over from an older project. Specifications can be found in table 2.1. A calibration matrix is required for this sensor, which translates the voltages of the six channels of strain gauges into forces and moments. This is specific to each sensor, however, the matrix of one of the sensors is lost, so the same matrix for both sensors is used. A sensor can also change over time, requiring a new calibration matrix to be created. Finding a new calibration matrix can be a laborious and time-intensive task. Although the sensor manufacturer may offer such a service, it can be costly. Thus, in this report, it was decided to manually search for a scaling factor that correlates the forces with the existing calibration matrices of the sensors. In addition, the sensors had an internal rotation of the axes that needed to be compensated. Applying a known moment is more difficult and has been omitted from this analysis.

In addition to the variations resulting from the usage of outdated calibration matrices, there are other contributing factors that make the implementation of an additional scaling factor necessary. The first reason for introducing a scaling factor is the use of a sensor-amplifier pair that differs from what the manufacturer provided. Secondly, an Analog-Digital Converter (ADC) is used in the instrumented crutches. This converts voltages into 14-bit digital values and introduces scaling as well. When walking with the crutches, the forces measured can become so large that the ADC's limit is reached. To prevent this, an offset voltage can be set on the amplifier, lowering values going into the ADC. These offsets can cause non-linear behavior between measured values and forces when approaching the limits of the amplifier. In the event that both sensors and the amplifier behave linearly at different offsets, a linear relationship can be established between measured values and forces by introducing a scaling factor for each force direction. The ultimate objective is to understand the forces within the crutch's reference system. Since the sensor is mounted at a rotated angle with respect to the crutch, an extra force rotation is necessary to align the sensor's shear forces with those of the crutch.

This chapter presents a calibration procedure for the force sensor, where known weights are applied along the x, y, and z directions. First, it is examined whether there is a linear relationship between the offered weights and measured values. This is done for different voltage offsets on the amplifier. Then, a scaling factor is determined to translate sensor-measured values into forces. Finally, the rotation angle required to rotate the shear force directions of the sensor in the frame of the crutches is determined.

2.2 Background

A 6x6 matrix is used to convert sensor readings V_0 - V_5 to actual forces. This matrix is specific per sensor and is supplied by the manufacturer. Conversion is done by multiplying the voltages with the matrix:

$$\mathbf{F = C\ V} \tag{2.1}$$

Where **F** is the array of 3D forces and 3D torques, **C** is the 6x6 calibration matrix and **V** are the voltages measured from the strain gauges. Written out:

$$\begin{pmatrix} Fx \\ Fy \\ Fz \\ Tx \\ Ty \\ Tz \end{pmatrix} = \begin{pmatrix} FxG0 & FxG1 & FxG2 & FxG3 & FxG4 & FxG5 \\ FyG0 & FyG1 & FyG2 & FyG3 & FyG4 & FyG5 \\ FzG0 & FzG1 & FzG2 & FzG3 & FzG4 & FzG5 \\ TxG0 & TxG1 & TxG2 & TxG3 & TxG4 & TxG5 \\ TyG0 & TzG1 & TyG2 & TyG3 & TyG4 & TyG5 \\ TzG0 & TzG1 & TzG2 & TzG3 & TzG4 & TzG5 \end{pmatrix} \begin{pmatrix} V_0 \\ V_1 \\ V_2 \\ V_3 \\ V_4 \\ V_5 \end{pmatrix} \tag{2.2}$$

Where $F_{x,y,z}$ are the forces in x, y and z direction and $T_{x,yz}$ are the torques around the x, y and z direction. The specific calibration matrix used in this report for both FT sensors is:

$$C = \begin{pmatrix} -2.11240 & 32.15269 & 0.96205 & -34.17360 & 0.01723 & 0.30383 \\ -1.95287 & 18.87434 & -0.55920 & 19.27552 & 2.37414 & -36.52639 \\ -19.14735 & 0.85372 & -18.49781 & 0.48799 & -18.97113 & 0.74205 \\ 35.98018 & -1.59886 & -34.23936 & 1.08167 & -0.66967 & -0.06261 \\ 20.57191 & -1.12269 & 19.78786 & -0.61574 & -39.59170 & 1.86745 \\ -1.29831 & 17.79016 & -0.96511 & 18.70644 & -0.77576 & 17.41219 \end{pmatrix} \tag{2.3}$$

This matrix is originally provided by ATI in 2004 for sensor FT05489, corresponding to the sensor in the right crutch.

A linear scaling factor can be introduced for every force and torque direction to relate forces at the crutch tip and measured voltage values.

$$F = \alpha CV \tag{2.4}$$

This equation holds true in case all components in the crutches behave linearly in case of static forces. That is the ATI 45 Mini force sensor, amplifier, and ADC. α is a 6-by-1 array.

$$\alpha = \begin{bmatrix} \alpha_{Fx} \\ \alpha_{Fy} \\ \alpha_{Fz} \\ \alpha_{Tx} \\ \alpha_{Ty} \\ \alpha_{Tz} \end{bmatrix} \tag{2.5}$$

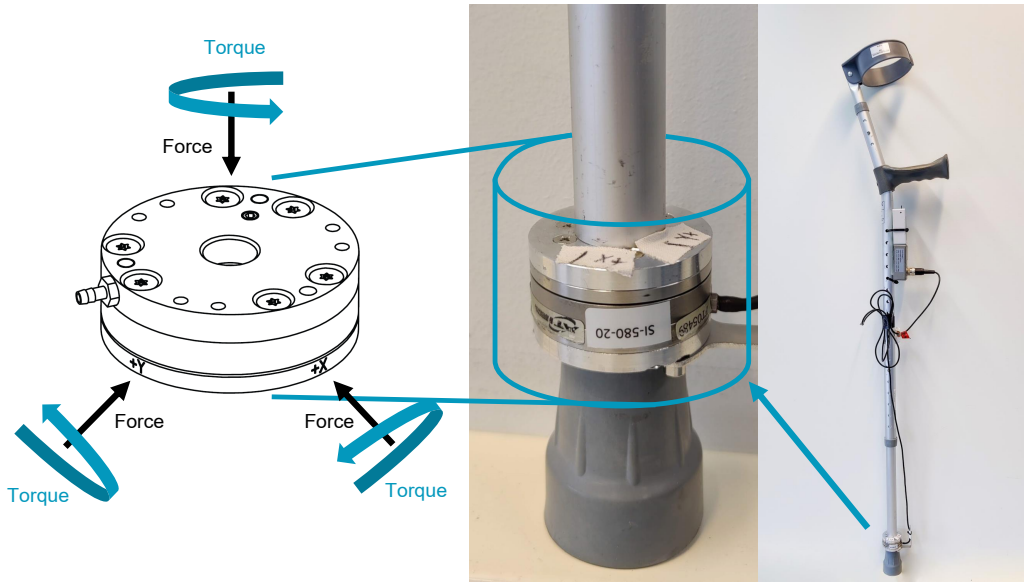

Figure 2.1: Overview of an instrumented crutch and the 6 DOF force torque sensor. An ATI Mini 45 force-torque sensor is used. The FT sensor needs to be calibrated.

The force sensor is positioned within the crutch with a specific rotation. In the design of the crutches, a deliberate choice was made to align the force sensor cables along the walking direction to minimise obstruction for the user. Consequently, the internal axes of the sensors (ψ_{sensor}) do not directly align with both the walking direction and the sideways orientation of the crutch (ψ_{crutch}).

In the crutch's frame of reference (ψ_{crutch}), the z-axis is rungs along its shaft. The y-axis corresponds to the handrest direction and the x-axis extend sideways, perpendicular to both. Refer to Figure 2.1 for a visual representation of the sensor placement within the crutch. An angle of rotation needs to be calculated to align the internal x- and y-axes of the force sensor with those of the crutch.

$$\psi_{crutch} = \boldsymbol{R} * \psi_{sensor} \tag{2.6}$$

Where ψ_{crutch} defines the reference system of the crutch, $\boldsymbol{R}$ is a rotation matrix, and ψ_{sensor} the reference system of the force sensor. A horizontal rotation is defined by:

$$\boldsymbol{R}_z(\theta) = \begin{bmatrix} \cos\theta & -\sin\theta & 0 \\ \sin\theta & \cos\theta & 0 \\ 0 & 0 & 1 \end{bmatrix} \tag{2.7}$$

With $\boldsymbol{R}$ the rotation matrix and $\boldsymbol{\theta}$ the rotation angle. Thus, the total equation to determine forces from sensor measurements becomes:

$$\boldsymbol{F} = \boldsymbol{R}\boldsymbol{\alpha}\boldsymbol{C}\boldsymbol{V} \tag{2.8}$$

With $\boldsymbol{R}$ the rotation matrix, $\boldsymbol{\alpha}$ the scaling matrix, $\boldsymbol{C}$ the calibration matrix, and $\boldsymbol{V}$ the measured voltages.

Table 2.1: Metric specifications of ATI Mini 45 SI-580-20. Adapted from [18].

Fx,Fy	**Fz**	**Tx, Ty**	**Tz**	**Fx, Fy**	**Fz**	**Tx, Ty**	**Tz**
580 N	1160 N	20 Nm	20 Nm	1/4 N	1/4 N	1/188 Nm	1/376 Nm
Sensing range				Resolution			

Table 2.2: Table overview of known z-direction weights.

	Weight applied (kg)	**Cumulative sum of weight (kg)**	**Cumulative sum of force (N)**
1	Unloaded	0	0
2	4.4	4.4	43.16
3	4.3628	8.7628	85.96
4	4.3814	13.1442	128.94
5	4.4332	17.5774	172.43
6	4.3712	21.9486	215.32
7	4.3661	26.3147	258.15

2.3 Method

The aim of this calibration procedure was to 1) Establish the linearity between measured forces and actual forces, 2) Determine the amplification factor for x-, y-, and z-direction forces and 3) Determine the rotation angle of both sensors to align with axes of the crutch. This was assessed by applying known weights in normal and sideways force direction of the FT sensor. A linear fit was determined between the measurements and known forces. Amplification factor of the amplifier resulted from the slope of the linear fit. Internal rotation angle of the FT sensors resulted from finding the angle that maximizes force in a single sideways direction. Accuracy of the fit was estimated using the root-mean-square-error (RMSE) and coefficient of determination ($\boldsymbol{R^2}$).

Data collection
Both crutches were consecutively placed in a holder on a workbench in an upright position. The bottom part of the crutch with the rubber tip attached was facing up. See image 2.2 for an overview of the test setup. Crutches were loaded with 7 known weights successively up to 27 kg. An overview of the weights can be found in table 2.2. Loading was repeated for three offset pairs per crutch, giving a total of 6 measurements. Firstly, offsets were determined that are suitable for use in actual measurement scenarios, ensuring that there is no clipping during an individual's gait. The phenomenon of clipping was attributed to the range limit of the ADC. Secondly, offsets were set to 0 for all six channels and finally, offsets values were determined in the middle of the aforementioned two offsets.
Next, both crutches were successively placed in a setup where a known shear force could be applied. A metal wire was placed around the end of the crutch where the rubber tip was attached. 9 known weights were sequentially added to this wire. An overview of the weights can be found in table 2.3. Loading was done firstly with the x-direction of the crutch pointing up, i.e. walking direction. After unloading the crutch, it was rotated 90° counter-clockwise and the experiment was repeated. Offsets were used where no clipping occurred.

Table 2.3: Overview of known shear forces.

	Weight applied (kg)	Cumulative sum of weight (kg)	Cumulative sum of force (N)
1	Unloaded	0	0
2	2	2.0	19.62
3	2	4.0	39.24
4	2	6.0	58.86
5	1.99	7.99	78.3819
6	4	11.99	117.6219
7	5	16.99	166.6719
8	5	21.99	215.7219
9	5	26.99	264.7719

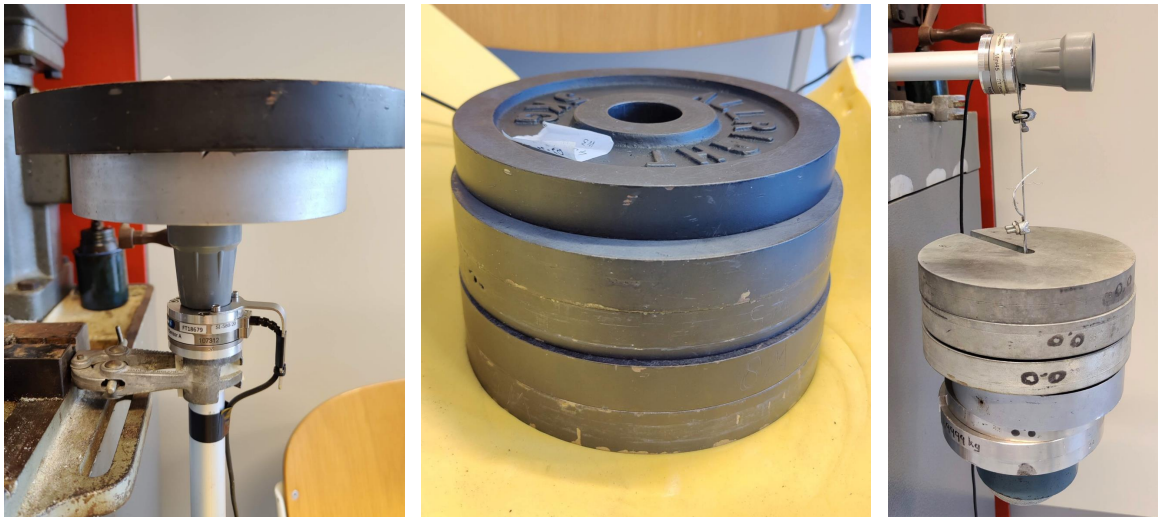

Figure 2.2: **Left:** Measurement set-up for applying known forces/weights to the sensor in z-direction. **Middle:** Weights for z-direction measurement. **Right:** Measurement set-up for applying known forces/weights to the sensor in sideways direction.

Table 2.4: Overview of z-direction fitting parameters.

Measurement	Linear fit	R^2	RMSE	Determined α (Neglect y-intercept)
Right - 0	y = 0.52x + 0.25	0.99997	0.19	1.92
Right - half	y = 0.51x + 0.12	0.99999	0.12	1.96
Right - full	y = 0.51x + 0.62	0.99991	0.47	1.96
Left - 0	y = 0.48x + 0.22	0.99999	0.16	2.08
Left - half	y = 0.48x + 0.13	0.99995	0.35	2.08
Left - full	y = 0.48x + 0.25	0.99999	0.18	2.08

Data Analysis
Data was analysed using MATLAB (Mathworks, USA). Data of the crutch was made equidistant and resampled to 100 Hz. Voltage readings from the force sensor were multiplied by the calibration matrix according to

$$\boldsymbol{F = R\alpha CV} \tag{2.9}$$

With **F** the force and torque values of the sensor, $\boldsymbol{R}$ the rotation matrix around the z-axis, $\boldsymbol{\alpha}$ the scaling array, **C** the calibration matrix, and **V** the voltage readings from the ADC. The specific calibration matrix used can be found in chapter 2.2. A linear fit was then determined for every weight loading experiment to relate known static forces to force reading from the sensor. The linear fit was determined using the least-squares method and scoring metrics to evaluate the data fit were the Root Mean Square Error (RMSE) and $\boldsymbol{R^2}$.

Factor $\boldsymbol{\alpha}$ is determined via linear fit using the least-squares method and derived as the reciprocal of the slope ($\mathbf{1}$/Slope number). Internal rotation angles of the FT sensors' axes with respect to the crutch are also determined. The y-direction of the FT sensor is rotated such that it is aligned with the walking direction of the crutch, i.e. the handle pointing forward. The mediolateral direction of the crutch is in that case aligned with the x-axis of the FT sensor. Angles were determined by finding the angle that maximizes the force in the y-direction and sets the x-direction to 0. When the crutches were rotated 90° counter-clockwise, the x-direction is maximised and y-direction is set to 0.

2.4 Results

Z-direction force
For the FT-sensor on the right crutch, the slope number is 0.52 when offsets of 0 are chosen, and 0.51 for offsets half and full. The FT-sensor on the left crutch shows a slope number of 0.48 for all offsets. The y-intercept is 0.25 or smaller in all cases, except for the right crutch with full offsets. There a y-intercept of 0.62 is found. $\boldsymbol{R^2}$ values are equal to 1 in all cases. RMSE is 0.35 or lower in all cases, except for the right crutch with full offsets, where the RMSE is 0.47. To relate actual forces to measured forces in z-direction using different offsets, an $\boldsymbol{\alpha}$-value of 1.9333 ± 0.0231 is found for the right crutch. An $\boldsymbol{\alpha}$-value of 2.08 ± 0 is found for the left crutch. See figure 2.3 for an overview of fitting known forces to measured force values. An example of what the loading experiment looked like for the right crutch with offsets 0 can be found in figure 2.4. Table 2.4 presents an overview of all linear fit results.

X- and y-direction force
The linear fit between the measured and applied forces in the x- and y-direction all had an $\boldsymbol{R^2}$-value of 1. The FT sensor of the left crutch showed and RMSE of 1.9N in case of 0° and 1.5N

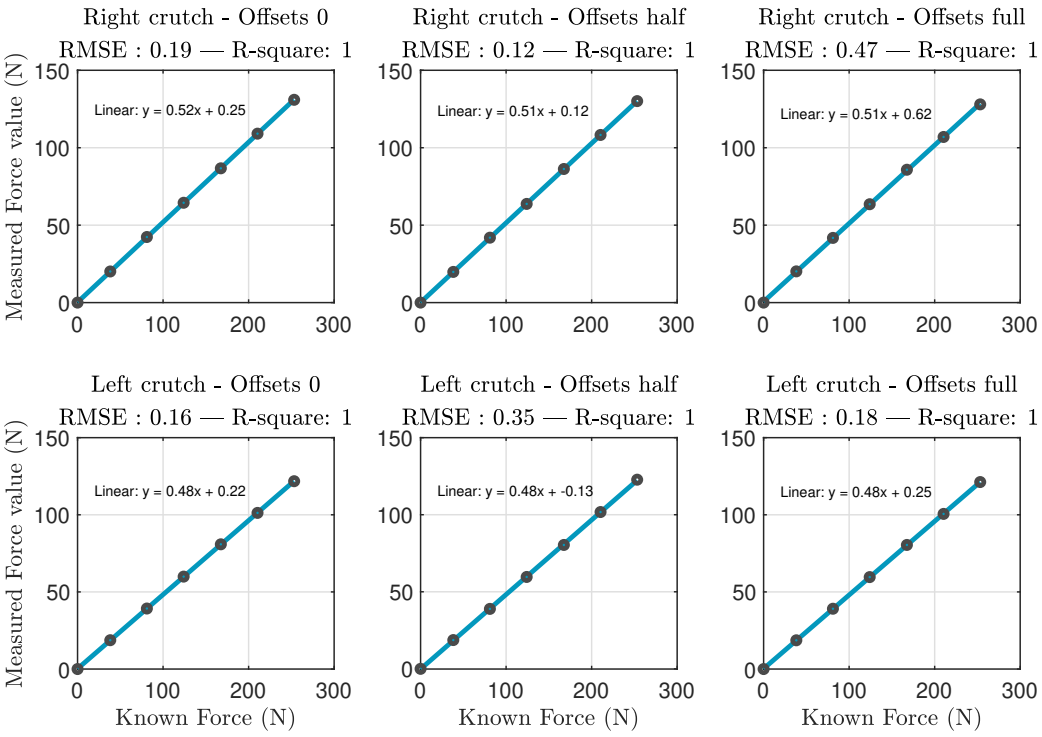

Figure 2.3: Results of linear fit using *polyfit* with right and left crutch. $\boldsymbol{R^2}$-values are all 1.

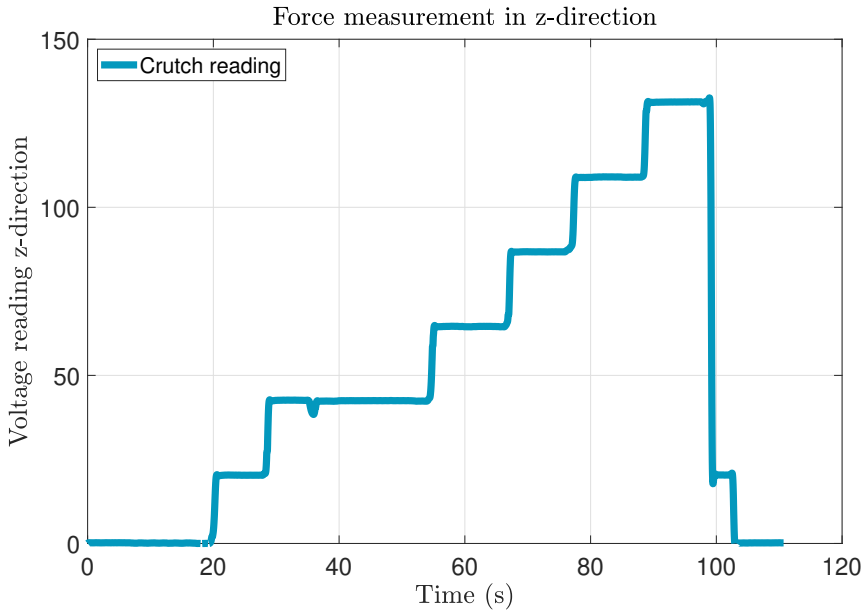

Figure 2.4: The loading experiment for the right crutch with offsets 0. Loading every individual weight can be clearly distinguished as well as removing the weights.

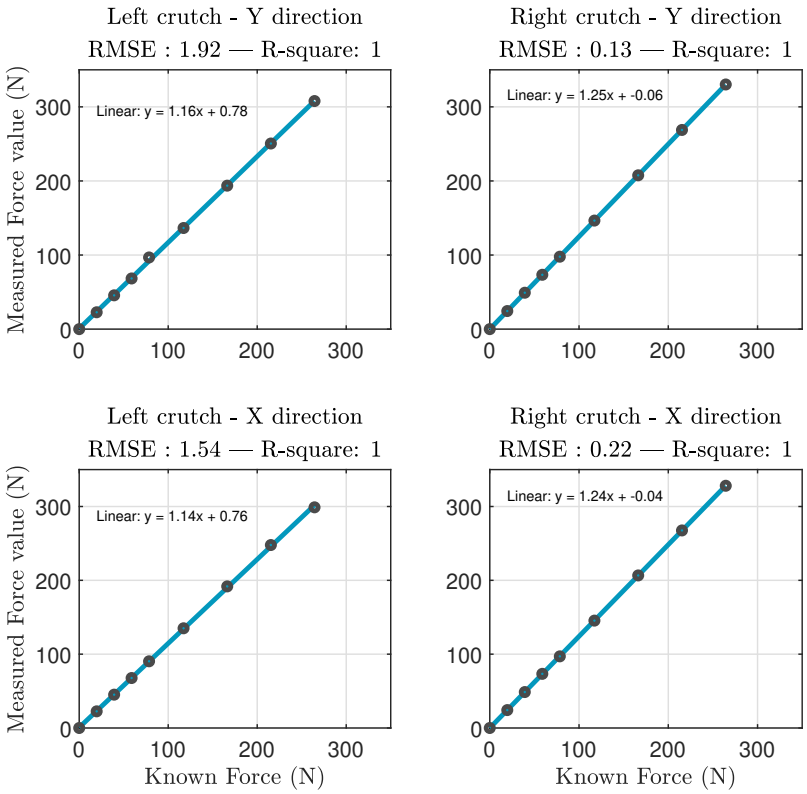

Figure 2.5: Results of linear fit using *polyfit* with right and left crutch. $\boldsymbol{R^2}$-values are all 1.

Table 2.5: Overview of x- and y-direction fitting parameters.

Measurement	**Linear fit**	**R^2**	**RMSE (N)**	**Angle θ**	**Determined α (Neglect y-intercept)**
Left crutch - 0°	y = 1.16x + 0.78	0.9997	1.922	**45°**	0.862
Left crutch - 90°	y = 1.14x + 0.76	0.9998	1.536	**40°**	0.877
Right crutch - 0°	y = 1.25x - 0.06	0.9999	0.126	**-22°**	0.800
Right crutch - 90°	y = 1.24x - 0.04	0.9999	0.225	**-21°**	0.806

in case of 90°. The FT sensor of the right crutch showed and RMSE of 0.126N in case of 0° and 0.225N in case of 90°. A full overview can be found in table 2.5 and figure 2.5.
Angles found to align left FT sensor axes with crutch axes are 45° and 40°. Angles found to align right FT sensor axes with crutch axes are -22° and -21°.
Scaling factor of the left FT sensor was found to be 0.8065 $\pm$ 0.0106. Scaling factor of the right FT sensor was found to be 0.8030 $\pm$ 0.0042. This results in the α-matrices found in equation 2.10. For computational purposes, the amplification factors related to Tx, Ty, and Tz are set to 1.0. These are however not determined in this experiment.

$$\boldsymbol{\alpha_{FT,Left}} = \begin{bmatrix} \mathbf{0.8065} \\ \mathbf{0.8065} \\ \mathbf{2.0800} \\ \mathbf{1.0} \\ \mathbf{1.0} \\ \mathbf{1.0} \end{bmatrix} \quad \boldsymbol{\alpha_{FT,Right}} = \begin{bmatrix} \mathbf{0.8030} \\ \mathbf{0.8030} \\ \mathbf{1.9333} \\ \mathbf{1.0} \\ \mathbf{1.0} \\ \mathbf{1.0} \end{bmatrix} \tag{2.10}$$

2.5 Discussion

This chapter presented a calibration procedure for the force sensors in the instrumented crutches. The relationship between known static forces applied to the FT sensor and sensor readings was determined. Metal weights with a known mass were used to apply the static forces. Figure 2.3 and 2.5 showed a linear relationship between known and applied forces.

First of all, it was questioned whether there was a linear relationship between applied forces and measured values. And if this condition remains applicable even with varying voltage offsets at the amplifier. Known normal forces were applied to check this condition. As the normal force is a linear combination of voltage readings from different strain gauges, linearity can be assumed for all force directions. Experiments with 3 offset pairs showed $\boldsymbol{R^2}$ values of 1 and RMSE values of 0.47N or lower. Linearity under different conditions can therefore be assumed.

Second, the amplification factor for all three force directions was determined. Linear data fits gave scaling factors of 0.8 for shear forces in case of both sensors. Forces in the z-direction gave a scaling factor of nearly 2. Looking at table 2.1, the range of Fz is indeed twice as large as Fx and Fy. One possible reason for this could be that the sensor has been designed to have lower sensitivity in the normal force direction, which allows for a higher range in that direction. This compensation was incorporated into the original sensor-amplifier pair.

The research by Chamorro-Mariona and colleagues found a coefficient of determination of $\boldsymbol{R^2}$ = 0.993 [17]. Sesar and colleagues found a coefficient of determination $\boldsymbol{R^2}$ = 0.996 and an RMSE of 8.78 N [16]. This research found a value close to 1, indicating a strong correlation, and an RMSE of maximally 1.92 N. However, Sesar et al. used a larger force range of 0 to 500 N, compared to 0 to 260 N in this study. Additionally, it should be noted, Sesar et al. overcame non-linearities by making a separate fit for different force ranges. This study did not experience non-linearities due to the dynamics of the amplifier in the tested force range. A single fit could therefore be used for the whole force range.

In order to align the internal sensor axes with the crutches, rotation angles were computed. A rotation angle around the z-axis of -22° was found for the right crutch, corresponding with the manufacturer's technical drawings. An angle of 43° was found for the left crutch. The difference between the two sensors may be explained by the custom designs ATI offers. The sensor placed in the left crutch may be made to order and deviate from the standard design.

Using $\boldsymbol{F = R\alpha CV}$, forces in x-, y-, and z-direction ranging from 0 - 260N can be reproduced well. It should be noted, however, that applying force in a single direction is difficult. If the weights are put slightly tilted, force is also exerted in other force directions. It could be the explanation for the differences found between scaling factors of the left and right FT sensors. To ensure scaling factors are correct, a real-life walking situation should be recreated with known forces.

Forces considered in this chapter are in the local reference system $\boldsymbol{\psi_{crutch}}$ of the crutch. This means they cannot directly be related to ground reaction forces (GRFs) of the crutches. To reconstruct GRFs, orientation information of the crutches is needed. Forces must be decomposed in x-, y-, and z-direction in a global reference system. Orientation information can be obtained using an optical marker system or using IMUs. Chapter 3 describes the validation of determining GRFs using an IMU mounted on the crutches. The dynamic walking setting might additionally introduce nonlinearity. The rubber crutch tip for example could act as a damper

and introduce a damping factor.

Torques are not considered in this study, as they are more difficult to validate. Applying a specific torque to a sensor requires a custom setup. Also, when validating the crutches in a dynamic setting where force plates are used, relating torques to the FT sensor is not trivial. In the α-matrix, the amplification factors corresponding to the torques are set to 1.0 for computational purposes. This is a shortcoming of the current state of the instrumented crutches. In a future study, torques could be validated as well. It gives interesting information about how the crutches are used.

2.6 Conclusion

A calibration procedure and corresponding steps for the force sensors found in the instrumented crutches were described in this chapter. The relevant research question in the chapter was "What is the relationship between measurements from the instrumented crutches and present force?". First of all, linearity was assessed between sensor readings and forces presented to the sensors in a test setup. Following this, it was determined how forces could be properly computed in a static situation.
In case of z-direction force, $\boldsymbol{R^2}$-values of 1 are found, and RMSE values all under 0.5N. A scaling factor of 2.08 is found or the left FT sensor and 1.92 for the right FT sensor.
The linear fit for sideways force also resulted in $\boldsymbol{R^2}$-values of 1 and RMSE values all lower than 2N. For the left FT sensor, a scaling factor of 0.8065 is found with a rotation angle of 43°. A scaling factor of 0.8030 is found for the right FT senor with a rotation angle of -22°. It can be concluded the relationship between force measurements and applied forces is linear. With the scaling factors and rotation angles found in this chapter, forces can be reproduced by the crutches. The experiment was performed in a range of 0 - 260N. In contrast to static forces, ground reaction forces (GRFs) during walking are of greater interest. Subsequently, the validation of the measured forces in a dynamic walking scenario would be necessary. Chapter 3 covers this topic.

Chapter 3

Design and Validation of Instrumented Crutches for Measuring 3D Ground Reaction Forces

This chapter describes the steps needed to measure ground reaction forces using instrumented crutches. This is important, as the forces measured by the sensor directly are in a local reference system while the needed forces are in a reference system defined before every trial, called the trial reference system (ψ_{trial}). To do so, the orientation of the crutches was tracked using an IMU, and forces were converted to ground reaction forces. Measurements were compared to force plates. Detailed force sensor calibration is discussed in Chapter 2 Static Calibration of ATI 45 Mini Force Sensor. Measurement changes due to temperature variations can be found in Appendix C.

3.1 Introduction

Three-dimensional ground reaction forces (GRFs) of crutch gait are an important measure of stress on the lower limbs, as highlighted in Li's study on 'Three-point weight-bearing' [14]. Walking with crutches means the GRFs are distributed between the feet and crutches. In an ambulatory setting, specialised lab equipment may not be available, as is the case within the BRAFO (Balanced Rehabilitation after an Ankle Fracture Operation) project. It becomes necessary to obtain measurements directly from the crutches. To address this need, an ATI Mini 45 force sensor placed at the tip of both instrumented crutches measures forces locally at the tip of the crutch. This means when walking, the sensors' orientation with respect to the ground changes. To keep track of forces during a walking trial, GRFs are expressed in a three-dimensional coordinate system that is fixed with respect to the ground. If the orientation of the crutches is tracked continuously, it is possible to convert the locally measured forces of a crutch to the trial frame. An Inertial Measurement Unit (IMU) in combination with a Kalman filter can be used to keep track of orientation during a walking trial. This chapter describes how to execute this transformation and compares outcome values to force plate measurements. The research question answered in this chapter is therefore: "How can 3D GRFs be measured using instrumented crutches in combination with an IMU?"

Previous studies have explored various approaches to equip crutches with 3D force-sensing capabilities. These methods involve two components: a force-sensing mechanism and a method of monitoring the crutch's orientation. Merrett et al. developed a forearm crutch system to monitor tilt and force placed on the crutch [19]. Force-sensing resistors were used. Despite be-

ing low-cost, a sensor error of 10% was stated and the performance of the instrumented crutch system was not reported. Additionally, these types of sensors need periodic calibration which may be a limitation for non-hospital environments.

Chen et al. used strain gauges in their *Smart Crutches* to measure force and an IMU to keep track of crutch orientation [20]. Results are promising, however, machine learning regression was used to calibrate the system. This could suggest forces could only be accurately measured for the specific tasks they were trained on. Seylan and Saranlı equipped forearm crutches with pressure sensors. A quadratic model was used to map pressure measurements to GRFs, based on the angle. Additionally, the pressure sensors had to be covered with a protective soft silicon cap. Delays were introduced because of this and had to be compensated. A study performed by Sardini et al. investigated using a crutch design with a strain gauge for sensors and an accelerometer for orientation [21]. It was stated that an accelerometer is sufficient in case walking slowly is assumed. An accuracy of 8N was found, which is said to be useable in a rehabilitation setting. In summary, it is feasible to accurately measure GRFs required for the BRAFO project using instrumented crutches. An IMU can be used to track orientation. No additional machine learning or mapping function is required when using strain gauges. Despite being more expensive, industrial strain gauge-based sensors offer accurate measurements and reliability in the setup.

This chapter presents a method and validation of measuring ground reaction forces of the instrumented crutches in a dynamic setting. Three trials are executed where swinging motions are performed with the crutches standing on force plates as force reference. All forces are expressed into the same reference system in order to compare them. Data of the 3D force measurements from the instrumented crutches and force plates are compared and errors are determined. Additionally, non-linearity due to the dynamic trial is discussed. The calibration of the ATI Mini 45 FT (Force/Torque) sensor used in the crutches can be found in chapter 2.

3.2 Background

A crutch user uses crutches for weight bearing thereby reducing stress on an injured lower limb. The crutches are placed in front of the user and continuously change their orientation with respect to the ground during gait. Figure 3.1 shows this with respect to the reference system of a force plate.

Crutch to Trial frame Rotation
A reference system called trial frame (ψ_{trial}) is defined before every trial. It is defined such that the axes align with the axes of the force plates in the floor. Transformations from the reference system of the crutch ψ_{crutch} to the reference system of the trial ψ_{trial} are done using the quaternion crutch to trial $\boldsymbol{q_{cr}^{tr}}$ and the inverse of that quaterion $(\boldsymbol{q_{cr}^{tr}})^{-1}$, as seen in equation 3.1. The quaternion multiplication operation is indicated by $\otimes$.

$$\psi_{trial} = \boldsymbol{q_{cr}^{tr}} \otimes \psi_{crutch} \otimes (\boldsymbol{q_{cr}^{tr}})^{-1} \tag{3.1}$$

Quaternions are a four-dimensional system to describe 3D transformations, as seen in equation 3.2. With $\boldsymbol{w}$ the scalar part indicating the rotation and $\boldsymbol{xi\ yj\ zk}$ the vector part.

$$\boldsymbol{q = w + xi + yj + zk} \tag{3.2}$$

A 3D force vector can be described as a quaternion by setting w to 0. A vector F_1 =[2 3 4] for example, will be written as quaternion q = [0 + $2i$+$3j$+$4k$]. The forces of the crutches undergo this transformation process. Forces F_{crutch} are within the crutch's reference system, while forces F_{trial} are within the trial's reference system, aligned with the force plates. The force transformation is described in equation 3.3.

$$F_{trial} = q_{cr}^{tr} \otimes F_{crutch} \otimes (q_{cr}^{tr})^{-1} \tag{3.3}$$

To define a reference system before a trial, the crutch is placed upright with the handle pointing in the x-direction of the force plate in the ground.

Sensor to Crutch Calibration
Orientation of the crutches is tracked using an Xsens Awinda IMU, measuring 3D acceleration and angular velocity. The IMU sensors were placed under the handle of both crutches. These measure in their respective sensor frame denoted by ψ_s. This has to be transformed to the ψ_{crutch} before measurement.

$$\psi_{crutch} = R_s^{cr} * \psi_{sensor} \tag{3.4}$$

Where R_s^{cr} denotes the single rotation from sensor to crutch. This matrix is estimated using inclination and swing data. The crutch is first placed on the ground standing still, during which the 3D accelerometer is expected to measure gravity only. The Y Axis of the crutch is estimated by performing a swinging motion with the crutch by letting it swing in the plane of the handle. The rotation matrix R_s^{cr} was determined by the method presented by Bonnet et al. [22]. Principal Component Analysis (PCA) was applied to the gyroscope measurement to determine the axis with the largest angular rotation. The X Axis is determined by taking the cross-product of the Y and Z axis. Finally, the Y Axis is updated to be the cross product of the Z and X Axis to ensure an orthogonal coordinate system. Equations 3.5 to 3.11 describe this.

$$\vec{z}_s^{\,cr} = Mean\,(\vec{a}_s) \tag{3.5}$$

$$\vec{y}_s^{\,cr} = PCA1\,(\vec{\omega}_s) \tag{3.6}$$

$$\vec{z}_s^{\,cr} = \frac{\vec{z}_s^{\,cr}}{\|\vec{z}_s^{\,cr}\|} \tag{3.7}$$

$$\vec{y}_s^{\,cr} = \frac{\vec{y}_s^{\,cr}}{\|\vec{y}_s^{\,cr}\|} \tag{3.8}$$

$$\vec{x}_s^{\,cr} = \vec{y}_s^{\,cr} \times \vec{z}_s^{\,cr} \tag{3.9}$$

$$\vec{y}_s^{\,cr} = \vec{z}_s^{\,cr} \times \vec{x}_s^{\,cr} \tag{3.10}$$

$$R_s^{cr} = \left[\frac{\vec{x}_s^{\,cr}}{\|\vec{x}_s^{\,cr}\|}; \frac{\vec{y}_s^{\,cr}}{\|\vec{y}_s^{\,cr}\|}; \frac{\vec{z}_s^{\,cr}}{\|\vec{z}_s^{\,cr}\|} \right] \tag{3.11}$$

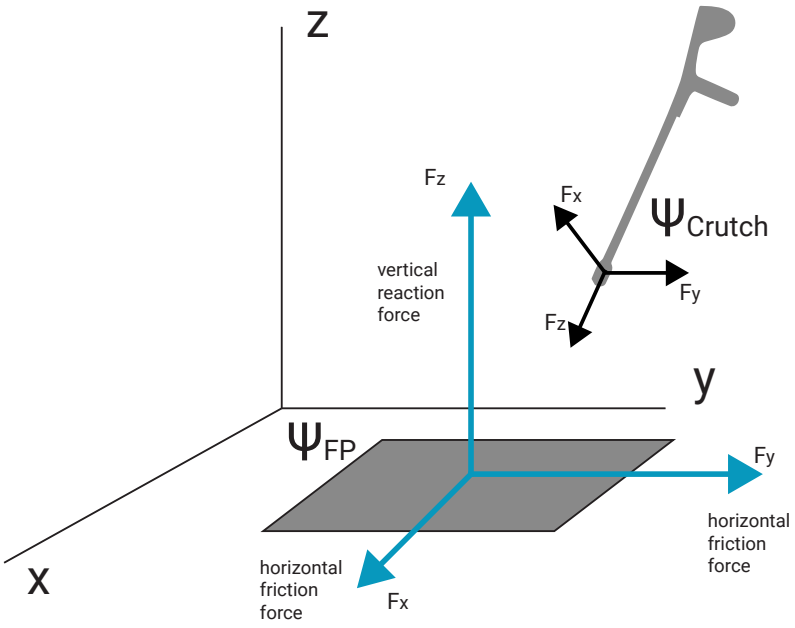

Figure 3.1: Reference system of the force plate (ψ_{FP}) and crutch (ψ_{crutch}).

3.3 Method

The aim of this chapter was to 1) work out the steps to measure GRFs with the instrumented crutches in a dynamic setting, i.e. walking, and 2) validate measured GRFs with the golden standard force plates. This was assessed by performing a series of three trials. Both crutches were placed on an individual force plate and a person was swinging back and forth while exerting force on the crutches. Figure 3.2 shows a top view of how the trials looked like.

Data Collection
The collection of data was done in a clinical walking lab setting. Each crutch was equipped with an Xsens MTw Awinda™ IMU that was placed on the shaft of the crutches right under the handle. MT Manager (version 4.8) software was used to transfer the IMU data wirelessly to a laptop at 100 Hz. Ground reaction forces were recorded at 1 kHz using two force plates (OR6 series, AMTI, Canada) in combination with Vicon Nexus software. The instrumented crutches were equipped with ATI Mini 45 (SI-580-20, Schunk, Arnhem, NL) FT sensors that measured forces at their tip. Crutches had a variable output rate and non-equidistant data points. A built-in first-order low pass filter of f_c = 234 Hz was used to prevent aliasing. A custom-made Python script was used to connect the crutches via Bluetooth and transfer data.

Trials
Trials in this chapter consist of swinging back and forth with the instrumented crutches placed on force plates. Before every trial, a new reference frame is created called trial frame (ψ_{trial}). This reference frame is defined such that it is aligned with the reference system of the force plates on the floor. Forces measured by the force sensors were transformed into this reference system.

Three trials were conducted using individual force plates for each crutch. In each trial, the subject started by standing in front of the force plates with the crutches positioned on them. Subsequently, the subject swung both legs in the air and landed on the opposite side of the

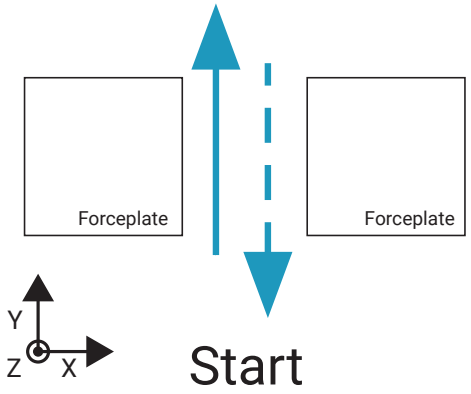

Figure 3.2: Top view of stepping on force plates. Each trial consisted of placing a crutch on either force plate and swinging forward. The person then swung backward along the dashed line. This was repeated 14-20 times per trial.

force plates while exerting force on the crutches. This process was then repeated but with a jump back to the starting position. The back-and-forth motion was repeated 14-20 times in each trial. Figure 3.2 provides a top view of what the trials looked like.

The crutches move and rotate during the trials and orientation is tracked and expressed in the predefined trial frame (ψ_{trial}). Acceleration and angular velocity of the crutches are measured using IMUs. Measurements are used as input for an Error-State Kalman Filter (ESKF), where measurements are fused with a physical model and estimates are improved based on their joint probability. The dynamic nature of this trials potentially introduces non-linearity. For example, due to hysteresis or the rubber tip on the crutch. Force plates in the ground are used as reference values. As a force plate can act as a spring element, rapid movements may show differences between crutch measurements and force plate measurements.

Sensor-to-crutch calibration
Before each trial, the crutch was placed in an upright position and left standing freely for a few seconds. This was followed by swinging the crutch in the plane defined by its shaft and handle. The sensor-to-crutch orientation calibration was done as seen in figure 3.3 and section 3.2.

Analysis
Data of both instrumented crutches was made equidistant and resampled to 100 Hz. An anti-aliasing filter was used and phase delays were compensated. Voltage readings from the FT sensors in the crutches were converted to forces according to $\boldsymbol{F} = \boldsymbol{R\alpha CV}$, as seen in Chapter 2. Where $\boldsymbol{R}$ denotes a rotation around the shaft of the crutch, $\boldsymbol{\alpha}$ denotes a scaling matrix, C denotes a calibration matrix provided by the manufacturer, and $\boldsymbol{V}$ the voltage readings from the sensors in volts. This way the forces $\boldsymbol{F}$ in $\psi_{\boldsymbol{crutch}}$ are obtained.

Readings from both force plates were resampled to 100 Hz. Signals from the IMUs, crutches, and force plates were synchronised using the cross-correlation function. Sensor to crutch orientation $\boldsymbol{R}_{\boldsymbol{s}}^{\boldsymbol{cr}}$ was determined per trial according to steps seen in *Sensor to Crutch Calibration* in section 3.2. Magnitude of the accelerometer signal was taken when the crutches were standing freely to determine the Z Axis. The Y Axis is determined by taking the first principle component of the gyroscope during the swinging motion performed before each trial. The X Axis

resulted from the cross product of both axes.

Validation
Firstly, 3D IMU accelerometer and gyroscope data was transformed from sensor to crutch frame using $\psi_{crutch} = \boldsymbol{R}_s^{crutch} * \psi_{sensor}$. Crutch orientation with respect to ψ_{trial} was tracked using an Error State Kalman Filter. The ESKF tracked the error in orientation, gyroscope offset, and linear acceleration to output the final orientation and angular velocity. The error process consisted of $\boldsymbol{x_k} = (\boldsymbol{\theta_k}\ \boldsymbol{b_k}\ \boldsymbol{a_k})^{\boldsymbol{T}}$, where $\boldsymbol{\theta_k}$ is the orientation error, $\boldsymbol{b_k}$ the gyroscope bias error and $\boldsymbol{a_k}$ the acceleration error. The advantage of tracking the error rather than the orientation itself is that the inertial processes can be considered linear processes in case errors are considered small [23]. The forces in ψ_{trial} are determined using quaternion multiplication of the output of the ESKF and forces in ψ_{crutch}. Figure 3.3 shows the design of the processing pipeline.

Error Metrics
The measurements of force plates and crutches were compared using the Root Mean Square Error (RMSE) in accordance with Chen et al. and Sesar et al. [16, 20]. Additionally, the method of Seylan et al. is used, where the percentage root mean square error is calculated [24]. The percentage RMSE for 1D is calculated using the RMSE and scaling it to the *max* GRF magnitude found in the measurement. Calculating the percentage RMSE for the X Axis is as follows.

$$\boldsymbol{E_x} := \frac{\mathbf{100}}{\mathbf{max}_j \|\mathbf{F}_j\|} \sqrt{\frac{\mathbf{1}}{\boldsymbol{N}} \sum_{\boldsymbol{j=1}}^{\boldsymbol{N}} \left(\hat{\boldsymbol{F}}_{\boldsymbol{j,x}} - \boldsymbol{F}_{\boldsymbol{j,x}}\right)^{\mathbf{2}}} \tag{3.12}$$

Where $\hat{\boldsymbol{F}}_{\boldsymbol{x}}$ denotes the force from the force plate in x direction, $\boldsymbol{F_x}$ is the force from the crutch in x direction and $\|\mathbf{F}_j\|$ is the maximum GRF magnitude observed in the experiment. This is similar for y, and z axes. The percentage RMSE for 3D force is calculated in the same way.

$$\boldsymbol{E_{overall}} := \frac{\mathbf{100}}{\mathbf{max}_j \|\mathbf{F}_j\|} \sqrt{\frac{\mathbf{1}}{\boldsymbol{N}} \sum_{\boldsymbol{j=1}}^{\boldsymbol{N}} \left(\left\|\hat{\mathbf{F}}_j\right\| - \|\mathbf{F}_j\|\right)^{\mathbf{2}}} \tag{3.13}$$

Where instead of a single force dimension, 3D forces are taken. All data was analysed using *MATLAB R2020b* (Mathworks, Natick, Massachusetts, USA).

3.4 Results

Figure 3.4 shows the 3D forces of trial 3 in ψ_{crutch} before rotation to ψ_{trial}. It can be seen that the forces in the X and Y Axis of the crutches and force plates do not overlap. After the rotation, the forces of the crutch and force plate have more overlap, as in figure 3.5. The error in the Y Axis, however, still appears to be quite large.

Forces rotated to ψ_{trial} are seen in figure 3.5. The right crutch of trial 3 is shown again. Peaks of every back-and-forth motion are distinguishable. Forces in the X Axis can be interpreted as pushing the plate sideways in the positive x direction. Forces in the y direction can be interpreted as pushing the plate forwards and backward, while forces in the z direction represent pushing the plate into the floor. Figure 3.6 is a zoomed-in version of figure 3.5. The time between 10s and 20s is shown. The crutch force in the Z Axis appears to lag behind the force plate for short amounts of time. In the Y Axis, the crutch measured larger forces at peak moments than the force plate.

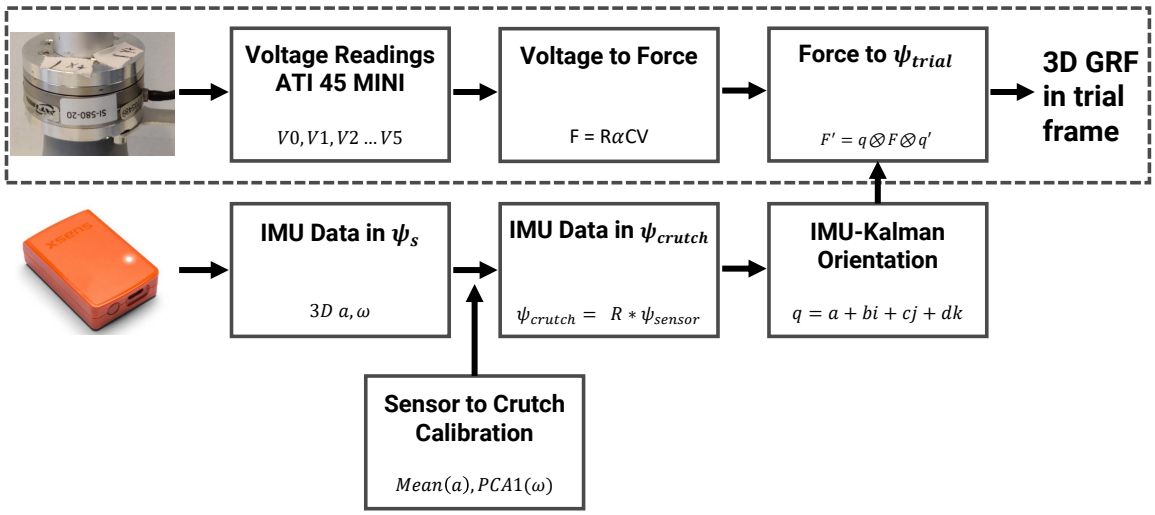

Figure 3.3: Processing steps from ATI 45 Mini FT sensors and IMUs to 3D GRFs in trial frame.

Table 3.1: Average, minimum, and maximum RMS errors across three dynamic trials in three dimensions. Forces in ψ_{trial}.

	Left crutch			Right Crutch		
	Avg. ± SD	**Min**	**Max**	**Avg. ± SD**	**Min**	**Max**
RMSE$_x$ (N)	9.85 ± 3.35	6.85	13.47	5.47 ± 0.69	5.05	6.28
RMSE$_y$ (N)	22.06 ± 2.62	19.17	24.28	22.04 ± 3.23	19.25	25.57
RMSE$_z$ (N)	16.55 ± 1.00	15.61	17.60	18.21 ± 1.43	16.87	19.71

Table 3.1 shows the Root Mean Square Error (RMSE) between GRFs of the crutches and force plates. The largest error is found in the Y Axis with an average error of 22.06 ± 2.62 N for the left crutch and 22.04 ± 3.23 N for the right crutch. Errors in the X direction are lower, being 9.85 ± 3.35 N left and 5.47 ± 0.69 N right. In the vertical direction, errors are smaller than the Y Axis, being 16.55 ± 1.00 left and 18.21 ± 1.43 right.

Table 3.2 shows the percentage RMSE of the reference GRFs and crutch GRFs. The errors are shown for the x, y, and z directions and the overall error. Compared to table 3.1, the values are scaled by the maximum magnitude of forces found in each trial. The error was found to be < 4.54% for all trials in a single direction. The overall average error was 3.35% for the left crutch and 3.44% for the right crutch.

Table 3.2: Average, minimum, and maximum percentage RMS errors across three dynamic trials in three dimensions. Forces in ψ_{trial}.

	Left Crutch			Right Crutch		
	Avg. ± SD	**Min**	**Max**	**Avg. ± SD**	**Min**	**Max**
E_x **(%)**	1.94 ± 0.65	1.37	2.65	1.00 ± 0.09	0.95	1.11
E_y **(%)**	4.14 ± 0.44	3.67	4.54	3.60 ± 0.41	3.22	4.03
E_z **(%)**	3.39 ± 0.28	3.23	3.71	3.42 ± 0.17	3.26	3.59
$E_{overall}$ **(%)**	3.35 ± 0.31	3.17	3.72	3.44 ± 0.15	3.30	3.60

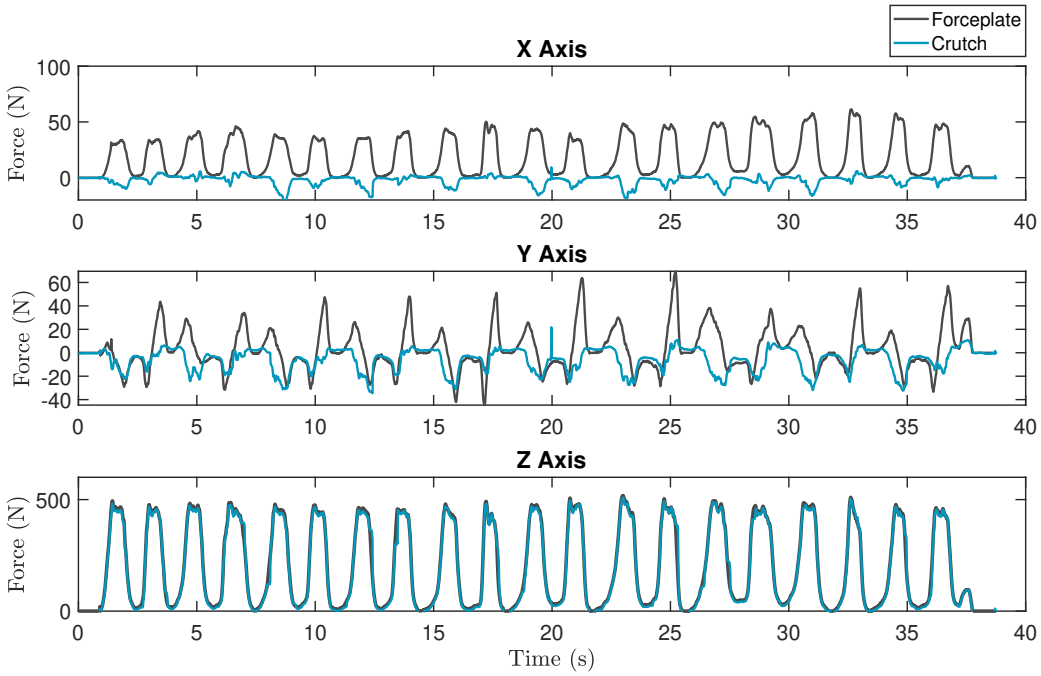

Figure 3.4: Forces of right crutch in ψ_{crutch} of trial 3 i.e. before rotation to trial frame. A total of 21 swings can be distinguished. Dark grey lines indicate the measurements of the force plate and light blue indicates the measurements of the crutch. Each row corresponds to an axis in ψ_{crutch}. Note the difference in force range between the X, Y, and Z Axes.

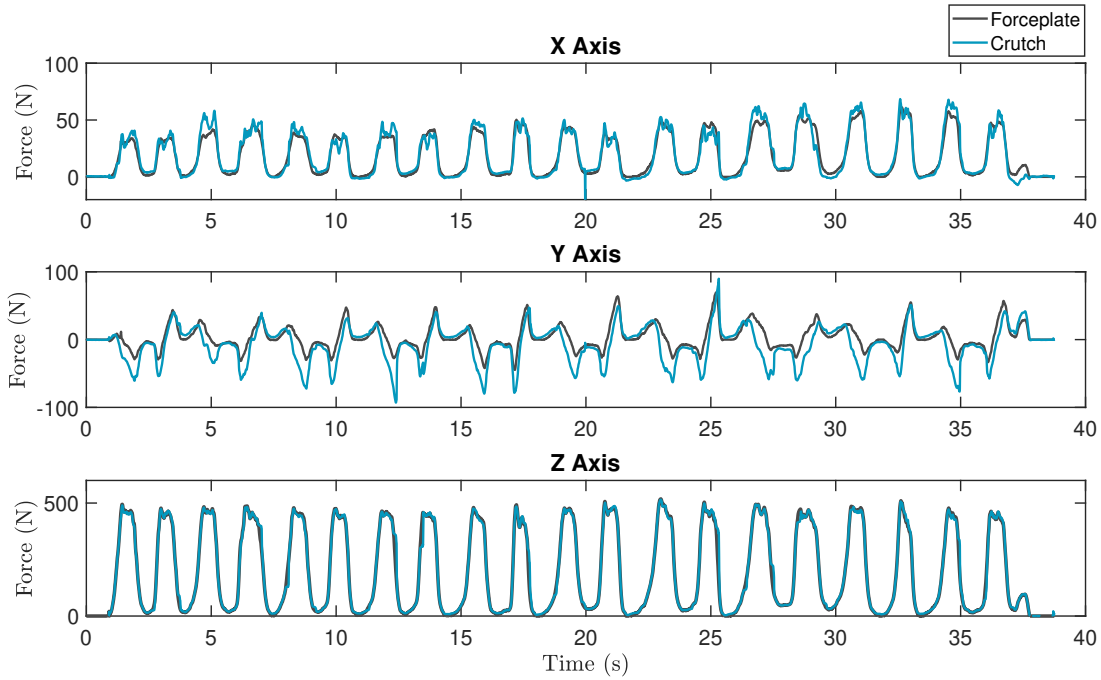

Figure 3.5: Forces of right crutch in ψ_{trial} of trial 3. A total of 21 swings can be distinguished, i.e. 10 complete swings back and forth. Dark grey lines indicate the measurements of the force plate and light blue indicates the measurements of the crutch. Each row corresponds to an Axis in ψ_{trial}. Note the difference in force range between the X, Y, and Z Axes.

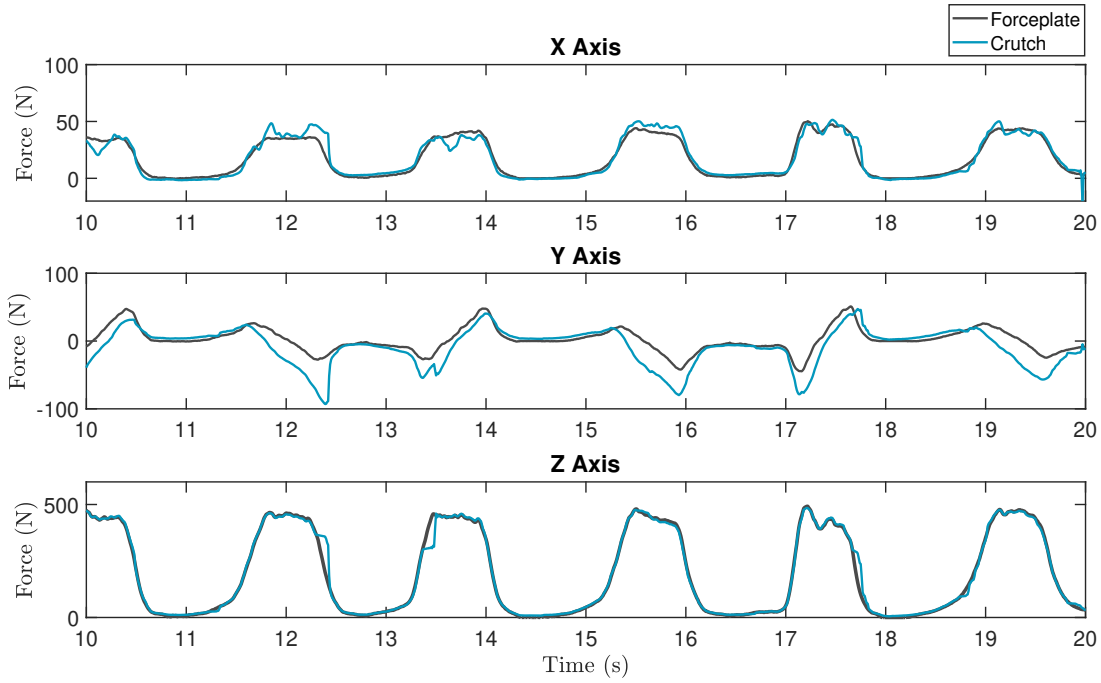

Figure 3.6: Zoomed in version of figure 3.5, where the time frame of 10 to 20 seconds is taken. Six back-and-forth motions are shown. Forces in ψ_{trial}.

3.5 Discussion

This study aimed to design instrumented crutches for the BRAFO project and compare 3D ground reaction forces (GRFs) of these crutches against force plates. This was achieved by using an inertial measurement unit (IMU) to determine the crutches' orientation. The investigation was conducted in a dynamic environment, with forces ranging from 0 to 520N per crutch. With this setup, it is possible to estimate crutch orientation and measure GRFs of crutch gait in a dynamic setting. Using an IMU has the advantage of the instrumented crutches system being portable. Once the sensor-to-crutch calibration is done, the crutches can be used to walk around freely. This allows for usage outside of a gait lab where optical orientation tracking is not available and force plates are not present.

Both the accelerometer and gyroscope measurements of the IMU are used in this research. Combined with an ESKF, the errors are tracked along the trial and expected to remain small [23]. In previous work, the orientation of the crutch is tracked using accelerometer readings only and comparing these to gravity to obtain an angle. This is only expected to give the right angles in a static environment or when walking with a maximum of 0.7 steps per second [19,21,24].

Table 3.1 shows the Root Mean Square Error (RMSE) between GRFs of the crutches and force plates. The largest error is found in the Y Axis with an average error of 22.06 ± 2.62 N for the left crutch and 22.04 ± 3.23 N for the right crutch. Seylan and Saranlı discovered that estimating sideways GRFs results in the highest relative errors within instrumented crutches. This occurs because the soft rubber crutch tip introduces interference between the GRFs and sensors [24]. Chen et al. found an RMSE of 15.9 N for the Y Axis [20]. The X Axis had an RMSE of 10.4 N and the Z Axis 14.1 N. The reference study also performed dynamic tasks with a similar force range and used an IMU to track crutch orientation. RMSEs between the reference study and

this study are similar, however, the error in the Y Axis in this study was larger. On the other hand, the reference study used their measurement trials to calibrate the sensor for their specific situation. In this thesis, calibration of the sensor was performed in a static environment first, as can be found in Chapter 2.

The average percentage RMSE and errors in all three directions are presented in Table 3.2. The obtained errors are notably low, with the largest being 4.14 ± 0.44% for the Y direction. The overall error for the left crutch was 3.35 ± 0.31% and 3.44 ± 0.15% for the right crutch. This is better than the findings of Seylan and Saranlı, who found a percentage RMSE of 7.62 ± 1.33% in the Y direction [24]. Additionally, their combined error across all three directions was 5.95 ± 1.08%. However, it is important to note that Seylan and Saranlı's study had limitations, as they used pressure sensors and a mapping function to estimate forces, with crutch orientation based solely on accelerometer readings. In contrast, this study used ATI sensors, which offer high accuracy but are more expensive compared to the low-cost pressure sensors used in Seylan and Saranlı.

The differences found in Figure 3.6 are mainly seen in the Y Axis. The crutch occasionally lags behind for a fraction of a second compared to the force plate in the Z Axis. This may be caused by several reasons. One of the reasons for this could be the rubber cap at the tip of the crutch. This could work as a damper and introduce non-linearity between the force sensor in the crutch and the floor. These non-linearities could be assessed as seen in Sardini et al, where hysteresis, non-linearity, drift, and resolution are assessed individually using a custom-made setup [21].

Limitations and future work
The trials conducted in this study are designed to replicate the dynamic gait pattern of walking with crutches. It would be interesting to conduct future studies that involve real walking trials to validate these forces. Walking around involves movements of the crutches in all directions, rather than rotations in a single plane. Furthermore, it should be noted the current method assumes a flat surface floor. In case the floor is inclined, the sensor-to-crutch calibration has to be compensated for the angle to measure GRFs correctly. Additionally, the data of the force plates is post-processed with steps defined by the manufacturer. On the contrary, the crutch's data undergoes lowpass filtering and resampling, resulting in dissimilar signal processing methods. For future research, ensuring uniform signal processing techniques would be advisable.

One effect of using strain gauge-based FT sensors is their temperature dependence. Keeping the sensors turned on for a prolonged time will cause drift in the measured voltages. The investigation in Appendix C reveals that drift is indeed present for the used ATI sensors, resulting in a measured change of 20N per hour in the Z Axis and 5N per hour in the X and Y Axes. The most pronounced effects were observed within the initial 20 minutes after activation, however never fully disappeared during the 7 hours the drift was investigated. To mitigate this effect, the crutches are turned on before each measurement session to allow the sensors to warm up. After each trial, the crutches are turned off and on again, and each crutch is placed in a free-standing position. This process allows calibrating the sensors to zero each time. Furthermore, the weight of the crutch is subsequently added back to match the ground reaction forces measured by the force plates. If longer measurement trials are planned, it is advisable to investigate the drift issue more thoroughly. However, for measurement trials lasting several minutes, the drift effect is minimal. For an overview of the drift over time, please refer to Appendix C.

Orientation estimations from the ESKF are verified in previous work by Roetenberg et al. [23]. In case IMUs are unavailable or unwanted, an optical method of orientation tracking could be used instead. Appendix D presents a method to track the orientation of the crutches with a VICON system in a laboratory setting. Furthermore, information about the velocity and positions of the crutches could be added using IMU strapdown as done by Brescianini et al. [25]. This would give additional gait information useful for the BRAFO project.

The internal MEMS IMU of the crutches could be used for tracking orientation instead the Xsens Awinda. This would mean it is no longer necessary to rely on an additional IMU system. If the internal IMUs would be used, a calibration procedure would be necessary [26]. Specifications of the internal IMUs can be found in Appendix B.

Lastly, it is important to mention that this study solely focuses on forces and does not consider torques. Although the FT sensors do have the capability to measure torques, they are not calibrated for that purpose as discussed in Chapter 2. Furthermore, validating torques with force plates presents challenges due to the influence of the precise placement of the crutch on the plate. In future studies, it would be interesting to add torque information. In an ambulatory sensing setup, this provides information about the distance of the crutch with respect to the user. Refai et al. used the forces and torques of the feet to estimate the center of mass (CoM) [1]. The forces and torques of the crutches could be added to this to estimate the CoM of a crutch user.

3.6 Conclusion

This chapter shows the feasibility of using strain gauge-based force sensors and IMUs on instrumented crutches to track 3D GRFs in a dynamic setting. An overall percentage root mean square error was found of 3.35 ± 0.31% for the left crutch and 3.44 ± 0.15% for the right crutch. These findings are comparable with literature and indicate that the crutches could be used to measure forces during walking trials. Further research should be done on the impact of the rubber crutch tip acting as a damper and the validation of forces in real walking scenarios.

III. Comparing 3D Ankle Force and Moment to Partial Weight Bearing

Chapter 4

Comparing Net 3D Force and Moment to PWB in Ankle Fracture Patients Walking With Instrumented Crutches

This chapter compared 3D net ankle force and moments to the current clinical rehabilitation measure of partial weight-bearing (PWB). A method was presented to determine 3D net force and moments on both an impaired and non-impaired ankle joint. PWB was compared to this 3D load in a population of four healthy subjects and two patients. The crutch system designed and validated in the previous chapters is used in the measurements in the context of the BRAFO research. Ethical approval was granted by the local hospital, the CMO Arnhem-Nijmegen, and the local ethical committee of the university.

4.1 Introduction

Early weight-bearing and active mobilisation after an ankle surgery result in an earlier return to work and sports compared to immobilisation [4, 27–30]. Weight-bearing is traditionally instructed by a physiotherapist using a regular body scale and only considering forces in a single direction [31,32]. Weight-bearing is enabled by using walking support such as forearm crutches to transfer part of the weight [6]. Partial Weight Bearing (PWB) however, does not give a full image of the actual ankle load, potentially leading to an inaccurate assessment of load during early weight-bearing activities. To get a comprehensive understanding of the net (external) force and moment on the ankle during rehabilitation outside of the clinic, an ambulatory measurement system needs to be developed.

PWB is a measure that is often used in the rehabilitation practice of lower limb injuries [6]. It describes the partial body weight a patient is allowed to place on the affected limb. During rehabilitation, the allowed weight-bearing ranges from non to partial to full weight-bearing. 25% PWB means 25% of body weight is transmitted to the impaired side, while the crutches carry the remainder. However, Warren and Lehmann found subjects not to be reliable in a specified weight-bearing instruction [33]. In the study by Winstein et al., the consistency of achieving 30% weight bearing was investigated in a cohort of sixty healthy participants. During training, augmented feedback on PWB was given. The group that received feedback after each training trial exhibited the lowest errors, with 10% discrepancies observed during a 2-day retention test [34]. Li et al. studied the variability in ground reaction force (GRF) during PWB [14]. A 3-point PWB gait type was studied, where the impaired side is placed on the ground simultaneously with both crutches. This is followed by a step from the non-impaired

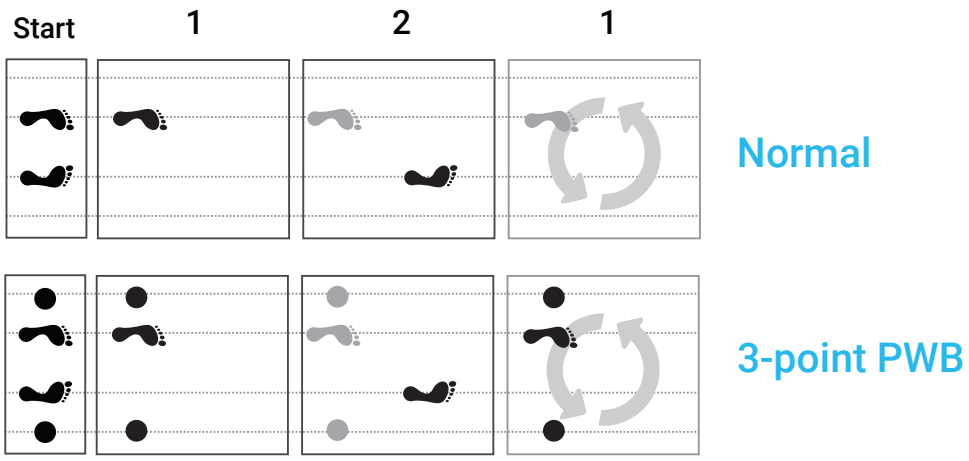

Figure 4.1: Normal gait on top. 3-point partial weight-bearing gait on the bottom. Part of the body weight is transferred to the crutches when placing the injured side on the floor. Adapted from Rasouli [6].

side. Figure 4.1 shows normal and 3-point PWB gait. Li et al. showed the twelve subjects were unable to execute PWB at the appointed levels defined for them. Specifically, 10% and 90% showed large variations, with mean peak vertical GRFs of 36% and 62% respectively. Stallard et al. investigated the GRFs of crutch walking. However, a swing-through gait was used and forces were not studied in all three directions [35, 36]. In summary, utilising Partial Weight Bearing as a metric falls short in providing a comprehensive assessment of the stress placed on the ankle joint. PWB is frequently reproduced incorrectly and exclusively considers vertical forces. Anteroposterior and mediolateral forces are not taken into consideration, nor does it consider pivotal moments around the ankle joint. Assessing moments is a significant aspect when determining actual load and is therefore important during rehabilitation [37, 38]. Showing the need for more elaborate information than PWB, could change rehabilitation guidance. Protocols could be improved, patient outcomes enhanced and risks due to inadequate assessment minimised. Consequently, it becomes crucial to determine the combined net 3D forces and moments (F&M) that affect the ankle joint.

Forearm crutches are often used in lower limb injuries including ankle fractures to allow reduced weight bearing [6]. Merrett et al. equipped a forearm crutch with a force-sensitive resistor and accelerometer to determine PWB in the vertical direction in a small pilot group [19]. Sesar et al. developed an instrumented crutch tip that could be connected to any crutch. A force sensor and an inclinometer were used to determine vertical ground reaction force (vGRF) [16]. Seylan et al. created a forearm crutch using an accelerometer for orientation and low-cost pressure sensors with a mapping function to measure force. A machine learning method was used to map pressure and inclination information to force with good estimates [24].

Sardini et al. constructed and analysed two wireless instrumented crutches to monitor gait. Axial and shear forces and anteroposterior and mediolaterial angles are monitored and data was transmitted wirelessly over Bluetooth. Clinical evaluation showed the crutches can be used for quantitive gait analysis, 3D crutch force, and instruct patients to correct use in early-stage rehabilitation. Additionally, the importance of a minimally invasive setup is mentioned to be used in clinical training and long-term home monitoring [21, 39]. The reviewed studies describe the development of instrumented crutches to determine vGRF or 3D forces at the

crutch tip or PWB on the affected extremity. Merrett et al. estimated PWB using the formula $\boldsymbol{PWB = 100\% - F_{crutches}}$, indicating the biomechanical coupling between forces measured by the crutches and foot GRFs [40]. However, literature is lacking on the direct correlation between crutch GRFs and 3D net ankle forces and moments. Crutches are therefore expected to fall short of meeting this objective. It becomes therefore interesting to explore alternative methods to measure ankle joint force and moments during ambulatory crutch-assisted walking.

An assumption commonly made is to assume the foot to be a triangle with a rotational point at the ankle joint [41]. Schepers et al. studied the forces and moments at the ankle joint using an ambulatory system with ForceShoes^{TM}(Xsens Technologies B.V.,Enschede). They are equipped with two force and moment sensors on each foot. Using the equations of motion and neglecting the inertial terms, the GRFs and Center of Pressure (CoP) provide the ankle moments [42, 43]. ForceShoes^{TM} present a minimalist ambulatory setup that has been validated against optical marker data of VICON and force plate data.

The primary objective of this chapter is to compare partial weight bearing (PWB) with the actual net 3D force and moments (F&M) at the ankle joint. This involves a comprehensive exploration of the 3D forces and moments acting at the ankle joint. The comparison aims to thoroughly evaluate the ankle load experienced by ankle fracture patients, intending to determine whether relying solely on PWB overlooks crucial information. Two instrumented crutches were used as walking support. These were equipped with force and moment sensors and an inertial measurement unit (IMU) to keep track of their orientation. Subjects walked 10-meter walking tests (10MWT) wearing ForceShoes^{TM} as reference.

While it might seem like comparing distinct metrics, this comparison is essential for a comprehensive understanding of ankle fracture rehabilitation. With the aim of BRAFO in mind of developing an ambulatory system, this information is important for instructions and monitoring during early-weight-bearing. The comprehensive system of both crutches and ForceShoes^{TM} offers a complete view of ankle loading and crutch utilisation during rehabilitation, exceeding PWB information. Thereby forming the groundwork for subsequent assumptions within the BRAFO project. In the BRAFO project, a user-friendly system for monitoring ankle load, gait patterns, and balance is investigated and developed. Comprehensive load information serves as a foundation for determining what specific force and moment directions to include when estimating ankle load through crutches and sensor inputs and potential assumptions that could be made in models applied in BRAFO. Ankle force and moments were calculated using foot GRF and CoP. 3D force and moments were compared to PWB. The 3D force measurements from the crutches were used to get a full understanding of the present forces during crutch gait.

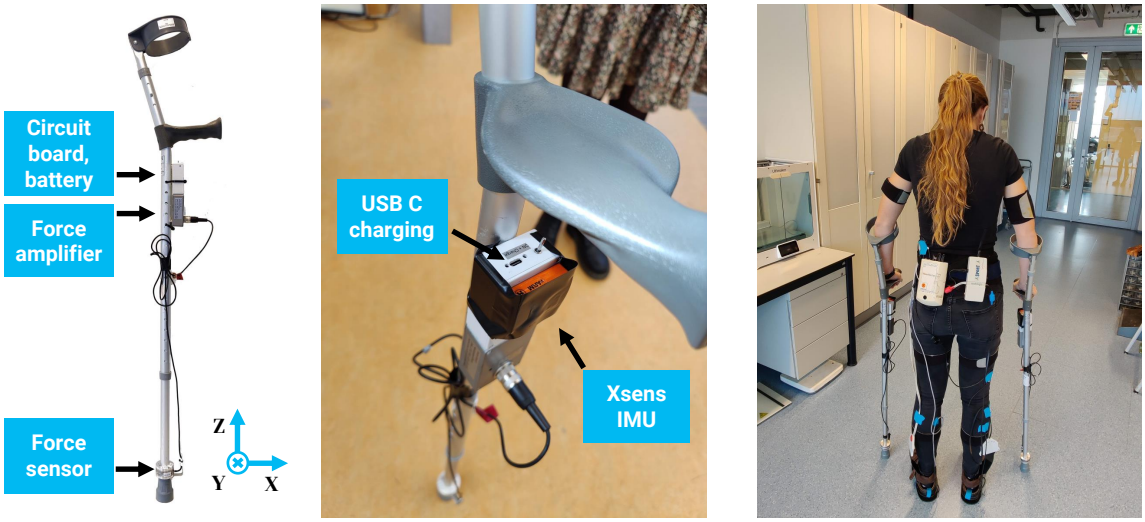

Figure 4.2: **Left:** Side view of an instrumented crutch. Regular forearm crutches were cut in half directly above the crutch tip and equipped with a force sensor above the rubber crutch tip. Additional hardware was used to give the crutch wireless data transfer capabilities over Bluetooth. **Middle:** An external Xsens Awinda IMU was attached to the crutch in measurements. **Right:** Participant using the instrumented crutches in a measurement session, wearing the full setup.

4.2 Methods

4.2.1 Measurement System

Instrumented Crutches

Figure 4.2 shows an image of the instrumented crutches and their components. Custom-made instrumented crutches were used in this study, made from regular forearm crutches. Each instrumented crutch consists of: 1) A 6 DOF Force/Torque strain-gauge-based sensor (ATI MINI 45 SI-580-20, Schunk, Arnhem, NL) measuring axial and shear forces; 2) a force amplifier, amplifying each individual channel; 3) a circuit board with microprocessor and wireless Bluetooth data transfer capabilities; and 4) a battery for power supply. Data from the crutches was sent wirelessly to a PC. Connection was made using a custom-made Python script running on the PC. The total weight of an instrumented crutch equals 1.1 kg.

Each crutch was equipped with an Xsens MTw Awinda^{TM} IMU that was placed on the casing of the circuit board. MT Manager (version 4.8) software was used to transfer the IMU data wirelessly to a laptop at 40 Hz. IMU data was then upsampled at 100 Hz. Data from the crutches was made equidistant and resampled at 100 Hz. Data was synchronised and an Error State Kalman Filter (ESKF) was used to track the orientation of the IMU on the crutches. Forces at the crutch tip were then transformed into trial frame ψ_{tr}, which is defined before every walking trial. This is a right-handed coordinate system with the X Axis along the walking direction and the Z Axis pointing up. Data was subsequently filtered using a double low-pass filtering process with a second-order Butterworth filter operating at a cutoff frequency of 10 Hz, designed to eliminate phase lag. Calibration of the force sensors is described in Chapter 2. The design and validation of the instrumented crutch system for measuring GRFs is described in chapter 3.

Table 4.1: Overview of included healthy subjects simulating an ankle fracture. Mean and standard deviation are presented.

Parameter	Age (year)	Length (cm)	Weight (kg)	Shoesize (EUR)	Impaired Foot	IMU Height Pelvis (cm)	Insole (EUR)
Outcome	23.5 ± 4.20	173.0 ± 5.35	67.3 ± 8.61	40.3 ± 2.06	R-4	108 ± 5.89	41-42

Table 4.2: Overview of included patients 7-12 weeks after an ankle fracture. Mean and standard deviation are presented.

Parameter	Age (year)	Length (cm)	Weight (kg)	Shoesize (EUR)	Impaired Foot	IMU Height Pelvis (cm)	Insole (EUR)
Outcome	49.5 ± 6.36	183.0 ± 9.90	78.9 ± 1.84	42.0 ± 2.83	L-1, R-1	117 ± 3.53	41-42/ 45-46

Pressure insoles and reference

Figure 4.2 shows the ForceShoes™ worn by a subject on the right. These contain two 3D F&M sensors, both on the forefoot and heel, and two IMUs. An Xbus placed on the participant's hip was used to transfer 3D F&M sensor data wirelessly to a PC. Plantar pressure insoles (medilogic©, T&T medilogic Medizientechniek GmbH, Germany) were placed inside the ForceShoes™ using tape. The soles have 151 resistive sensors that register pressure and come with a wireless transmitter that is worn around the participant's hip. The insoles remain unused in this chapter, however, contain information for future research in the BRAFO project. The internal IMU of the ForceShoes™ was used to synchronise crutches, IMUs, ForceShoes™, and insoles. Data of the ForceShoes™ was sampled at 100 Hz and data of the Medilogic Insoles at 60 Hz. Data was subsequently filtered using a double low-pass filtering process with a second-order Butterworth filter operating at a cutoff frequency of 10 Hz, designed to eliminate phase lag.

4.2.2 Participants and Ethics

Four healthy participants (3 female, 1 male) participated in this study. None of the participants reported a previous record of difficulty in walking that could affect the study. They were directed to consider their right ankle as the affected side, which entailed selecting a weight-bearing percentage freely for this particular side. Before the experiment started, all participants signed an informed consent, which had been approved by the faculty's Ethical Committee. Two ankle fracture patients (one male, one female) participated and were allowed 25% and 50% weight bearing respectively. Both patients signed an informed consent and conducted consultation with a surgeon. Ethical approval was granted by the CMO Arnhem-Nijmegen (2022-13165) and the ethical department of the local hospital (ZGT22-30). Measurements on the patients were executed between 7 to 12 weeks after ankle fracture. Additional inclusion criteria included an age range of 18-55, no condition affecting gait other than the ankle fracture, and the cognitive capacity to speak Dutch. Table 4.1 and 4.2 show the average and standard deviation of age, length, weight and shoesize (European Size Chart) of the healthy participants and patients.

4.2.3 Data Collection

The ForceShoes™ system and pressure insoles were calibrated before each measurement. Sensor-to-crutch calibration was performed with the crutches before each measurement, defining a reference system for expressing crutch forces. The reference system named ψ_{trial} was defined such that the X Axis was aligned with the walking direction and the Z Axis pointed upwards. Additionally, the crutches' force sensors were zeroed before each measurement. During the measurement sessions, a set of 11 IMUs were strategically positioned on various anatomical segments of the participants. It is worth noting this IMU configuration had broader applications in the BRAFO project but did not directly relate to the present study. Participants were instructed to perform a 10-meter walking test (10-MWT) three times at their self-selected walking speed. To facilitate this, healthy participants were provided with practice time before the measurements, allowing them to acclimate to walking with crutches. A synchronisation step was performed as part of the protocol in every measurement to align data. Measurements on the patients were performed under the guidance of a hospital-based physiotherapist.

4.2.4 3D Ankle Joint Force and Moment

The net, or external, moment on a joint was calculated using the equation of motion [44]. This method is called inverse dynamics (ID) and is often used in clinical analysis [45]. External forces applied to the body are considered, as well as the distance between the force vector and center of the joint, kinematics of the joint, and moments of inertia. The moment of an ankle joint is described with equation 4.1 according to Schepers et al. [42, 43].

$$\boldsymbol{M}^{\boldsymbol{g}}_{\boldsymbol{ank}} = -\left(\boldsymbol{x}^{\boldsymbol{g}}_{\boldsymbol{CoP}} - \boldsymbol{x}^{\boldsymbol{g}}_{\boldsymbol{ank}}\right) \times \boldsymbol{F}^{\boldsymbol{g}}_{\mathbf{GRF}} + \left(\boldsymbol{x}^{\boldsymbol{g}}_{\boldsymbol{ft}} - \boldsymbol{x}^{\boldsymbol{g}}_{\boldsymbol{ank}}\right) \times \boldsymbol{m}_{\boldsymbol{ft}}\boldsymbol{s}^{\boldsymbol{g}}_{\boldsymbol{ft}} + \boldsymbol{R}^{\boldsymbol{g}}_{\boldsymbol{s}}\frac{\boldsymbol{d}}{\boldsymbol{dt}}\left(\boldsymbol{I}_{\boldsymbol{ft}}\boldsymbol{\omega}^{\boldsymbol{s}}_{\boldsymbol{ft}}\right) \quad (4.1)$$

With $\boldsymbol{M}^{\boldsymbol{g}}_{\boldsymbol{ank}}$ the moment in the ankle and $\boldsymbol{F}^{\boldsymbol{g}}_{\boldsymbol{GRF}}$ the ground reaction forces. $\boldsymbol{m}_{\boldsymbol{ft}}$ describes the mass of the foot, $\boldsymbol{s}^{\boldsymbol{g}}_{\boldsymbol{ft}}$ the acceleration of the foot including gravity and $\boldsymbol{R}^{\boldsymbol{g}}_{\boldsymbol{s}}$ the rotationmatrix from sensor frame to global frame. $\boldsymbol{I}_{\boldsymbol{ft}}$ is the moment of inertia of the foot and $\boldsymbol{w}^{\boldsymbol{s}}_{\boldsymbol{ft}}$ the angular velocity of the foot. The position of the ankle, the CoP, and the center of mass of the foot are respectively described by $\boldsymbol{x}^{\boldsymbol{g}}_{\boldsymbol{ank}}$, $\boldsymbol{x}^{\boldsymbol{g}}_{\boldsymbol{CoP}}$ and $\boldsymbol{x}^{\boldsymbol{g}}_{\boldsymbol{ft}}$. As contributions of inertial terms are neglectable, equation 4.1 reduces to equation 4.2 [44].

$$\boldsymbol{M}^{\boldsymbol{g}}_{\boldsymbol{ank}} = -\left(\boldsymbol{x}^{\boldsymbol{g}}_{\boldsymbol{CoP}} - \boldsymbol{x}^{\boldsymbol{g}}_{\boldsymbol{ank}}\right) \times \boldsymbol{F}^{\boldsymbol{g}}_{\mathbf{GRF}}. \quad (4.2)$$

Distance $\boldsymbol{x}_{\boldsymbol{CoP}} - \boldsymbol{x}_{\boldsymbol{ank}}$ is based on the point of reference of the CoP. As point of reference, the heel of the foot is taken. Distance from the heel of the foot to the ankle joint is taken as 20% of the length of the foot, as found by an In Vivo study by Hashizume et al. [46]. The CoP under the foot $\boldsymbol{x}^{\boldsymbol{g}}_{\boldsymbol{CoP}}$ is calculated using equation 4.3 according to Schepers et al. It requires the combined moment of both the heel and forefoot sensor. Combining the moment of both sensors of the ForceShoes™ is done according to equation 4.4.

$$\mathbf{x}_{\boldsymbol{CoP,foot}} = \begin{pmatrix} \frac{-\boldsymbol{M}_{\boldsymbol{y}}}{\boldsymbol{F}_{\boldsymbol{z}}} \\ \frac{\boldsymbol{M}_{\boldsymbol{x}}}{\boldsymbol{F}_{\boldsymbol{z}}} \\ \mathbf{0} \end{pmatrix} \quad (4.3)$$

Combining the moments of the sensor on the heel and on the forefoot is done according to equation 4.4. $\boldsymbol{M}_{\boldsymbol{h}}$ and $\boldsymbol{M}_{\boldsymbol{f}}$ indicate the moments measured by the heel and forefoot sensor respectively. $\boldsymbol{F}_{\boldsymbol{h}}$ and $\boldsymbol{F}_{\boldsymbol{f}}$ are the forces measured by the heel and forefoot. $\boldsymbol{x}_{\boldsymbol{f}} - \boldsymbol{x}$ is the distance between the forefoot sensor and a reference point $\boldsymbol{x}$.

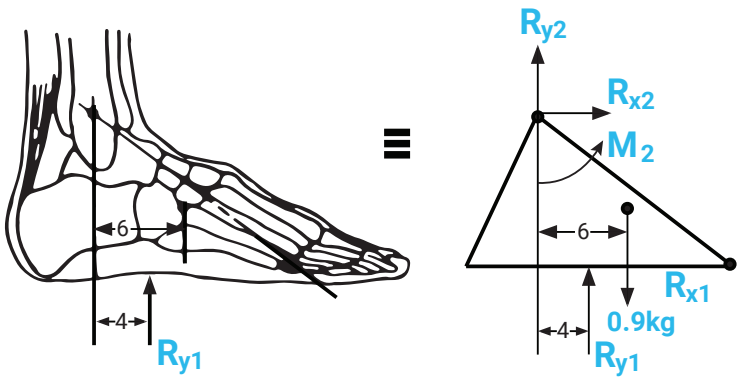

Figure 4.3: Free body diagram of the foot and ankle. The ankle joint and foot are typically modeled as a triangle with forces and moments acting on it. R represents horizontal and vertical forces, M represents moments working on the foot and ankle. Adapted from Winter [41].

$$ {}^{S}\vec{M}(\vec{x}) = {}^{S}\vec{M}_h + {}^{S}\vec{M}_f + (-{}^{S}\vec{x}) \times {}^{S}\vec{F}_h + ({}^{S}\vec{x}_f - {}^{S}\vec{x}) \times {}^{S}\vec{F}_f \tag{4.4} $$

Winter states the foot can be modeled as a triangle when researching forces and moments in the ankle joint [41]. This means the internal forces and moments inside the foot are not taken into consideration. This is in line with the equation provided by Schepers et al. [42, 43]. Figure 4.3 shows the comparison of the anatomy of the foot and its model.

4.2.5 Comparing Ankle F&M to PWB

3D Ankle forces and moments and 3D crutch forces of both a healthy participant and patient 1 are shown in a single trial. Average gait cycles during trials are shown afterwards, for a healthy subject and both patients. All forces are normalised to Body Weight (%BW) and moments to Body Weight Height (%BWH). Individual gait cycles are time normalised to 100 data points, using cubic spline data interpolation function. Initial ground contact and toe-off were used as the start and end point of the gait cycle.

Correlation Crutches with Ankle Moment
As described in the introduction, a coupling between force measurements of the crutches and 3D F&M on the ankle joint is expected. To assess the capacity of the crutches for directly determining ankle moments, an analysis was performed to examine the correlation between vertical crutch force and 3D ankle moments. The objective was to determine the relationship between these variables. If this correlation is found to be inadequate, it emphasises the need to include the ForceShoes™ for accurate ankle moment measurements in this chapter.

To accomplish this, the ratio between ankle moments and vertical crutch force was calculated for each step taken by both patients. The ratio of plantar, inversion, and abduction ankle moments was compared to the step duration. A ratio that varies per step, without a prominent change in step duration, indicates these moments should be measured during patients' walking trials. The ratio was defined as in equation 4.5. Equal calculations are done for the inversion and abduction ankle moment. Notably, dividing a moment by a force yields the unit meter (m). The step duration was calculated using floor contact data based on the vertical force measured by the ForceShoes™.

Table 4.3: Meaning of average and maximum forces/moments found during measurements and the gait stage.

Measure	Explanation
Average	Average force or moment in single direction during gait. Forces in % BW and moments in % BWH.
Max	Maximum force or moment in single direction during gait. Forces in % BW and moments in % BWH.
Gait stage	Part in gait cycle where maximum force or moment is found.

$$\boldsymbol{Ratio_{plantar}} = \frac{\boldsymbol{M_{ankle,plantar}}}{\boldsymbol{F_{z,crutch}}} \tag{4.5}$$

Analysing 3D F&M and PWB
The direct comparison between 3D F&M and PWB proves challenging due to their difference. While PWB accounts for the vertical component of 3D F&M, it missing crucial information concerning shear forces and moments. Therefore, the comparison requires the use of two distinct metrics: vector magnitudes and their impact on the resultant force/moment. Evaluating both aspects is fundamental for a comprehensive understanding of the force and moment impact on the ankle joint and comparison to PWB.

The magnitude provides the quantitative measure of the forces and moments, giving insight into the overall net load experienced by the ankle. On the other hand, the contribution to the resulting vector gives information about how individual directions contribute to the result experienced at the ankle joint. The contribution highlights the components missing when only considering PWB. The assessment with both metrics provides an overall view of the net ankle load as well as an effective method to compare 3D F&M to PWB.

Force and moment magnitudes
The analysis involved the calculation of both average and maximum forces and moments magnitudes for every trial. Analysing both average and peak values during steps offers a nuanced view of ankle load. The average reflects the consistent load experienced by the ankle during walking. In contrast, the maximum force shows critical points during gait. PWB is typically reported as the maximum force on the impaired side during a gait cycle [19]. This, however, does not provide information on whether this is a constant load or an exceptional peak. Therefore, including both average and maximum values offers a deep understanding of 3D ankle loading and highlights the limitations of relying on PWB as a metric only.

To specifically assess actual steps, a Z Axis threshold of 0.1 times an individual's body weight (BW) is applied. Additionally, the gait stage where the maximum value was observed was identified and reported. Defined times in the gait cycle according to Winter are initial contact, foot flat, mid-stance, heel off, and toe-off [41]. An overview of the used measures is given in Table 4.3. A comparison between 3D F&M and PWB is made by comparing force in the vertical direction to moments and lateral forces.

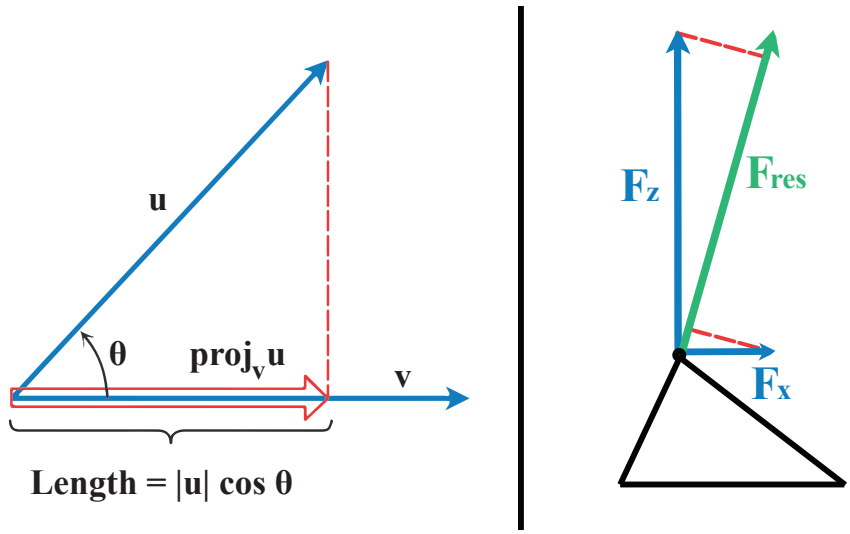

Figure 4.4: **Left:** Overview of vector projection of vector **u** on vector **v**. The length of the vector projection is determined by Length = $|\mathbf{u}|\cos\theta$. Adapted from Thomas' Calculus [47].
Right: Free body diagram of a foot and ankle joint with forces F_x and F_z working on it. The resulting force F_{res} is determined by the **norm** of both vectors. The length of the vector projection of F_z on F_{res} is significantly larger than F_x.

Contribution to resulting force and moment
PWB only considers the vertical force and overlooks the resultant force vector. For a better understanding of ankle load, the resulting 3D force vector is calculated based on F_x, F_y, and F_z. Contributions of individual force directions on this resultant force highlight the difference with PWB. While F_z aligns with what PWB considers, F_x and F_y reveal the aspects overlooked by PWB. Additionally, this analysis includes 3D moments, revealing other dimensions that PWB does not take into consideration.

The contribution of individual force directions F_x F_y and F_z to the resulting force F_{res} was assessed using the length of the vector projection. The resulting force was calculated using the **vecnorm** of the 3D force. Vector projection $proj_{Fx}$ F_{res} represents the effective force of F_x in the direction of F_{res}. The length of this vector projection, i.e. scalar component, is the magnitude of the effective force. Equations 4.6 and 4.7 describe the calculation of the vector projection and vector projection length [47]. Image 4.4 shows a graphical representation of the vector projection and vector length. The identical approach is taken for the moments M_x, M_y and M_z.

$$proj_v \mathbf{u} = \left(\frac{\mathbf{u}\cdot\mathbf{v}}{|\mathbf{v}|^2}\right)\mathbf{v} \tag{4.6}$$

$$Length = |\mathbf{u}|\cos\theta = \frac{\mathbf{u}\cdot\mathbf{v}}{|\mathbf{v}|} = \mathbf{u}\cdot\frac{\mathbf{v}}{|\mathbf{v}|} \tag{4.7}$$

4.3 Results

Two trials of healthy participants were excluded from the analysis due to issues with the Xsens Awinda setup. A total of 10 trials of healthy participants and 6 trials of patients were included. Duration of the 10-MWT trials varied between 8-30 seconds, depending on the self-chosen walking speed of the participants.

4.3.1 Correlation Crutches with Ankle Moment

Figure 4.5 shows the relationship between vertical crutch force and ankle moments. In the first row, a bar chart illustrates the ratio between the plantar ankle moment and vertical crutch force. For patient 1, the ratio between these remains relatively constant at around 0.5, although a slight fluctuation per step is seen. Patient 2 displays more variability between steps. Mind the plantar ankle moment is measured in Newton meters, while the crutch force is measured in Newton. Rows 2 to 5 demonstrate the ratio in all three moment directions ranging between 0.5 to 1.5m. The ratio alters from step to step, even when the step duration remains constant. This shows the vertical force measured by the crutches is not directly correlated to moments on the ankle joint. Additional measurement equipment is required to obtain accurate measurements of the ankle moments.

4.3.2 3D Ankle Force

Figure 4.6 and 4.7 show the net forces present at the ankle joints of a healthy participant and patient 1. Forces are displayed in anteroposterior, mediolateral, and vertical directions. The healthy participant chose a walking speed of 1.5 steps/s and the patient chose a walking speed of 0.83 steps/s. Forces are normalised to % BW. Weight-bearing had been left a free choice for the healthy participant. Based on judgment of the physiotherapist, the patient was allowed 25% weight-bearing.

Vertical force at the impaired ankle corresponds to partial weight-bearing information. Both the healthy participant and patient 1 showed peaks of 50% BW in vertical direction. The patient showed to consistently exceed the allowed weight-bearing of 25% BW. The shape of the peaks, however, is different, as the healthy participant has a clear peak early in step progression. Patient 1 has flat peaks during the steps. Both PWB and 3D F&M measurements showed to include the difference in step characteristics.

Additional information in the other force directions is gained from the ForceShoes^{TM}. Force in the anteroposterior direction of the healthy participant peaked at 20% BW for the non-impaired and 5% BW for the impaired side. Anteroposterior force of patient 1 peaked at 10% BW non-impaired and 5% BW impaired. Mediolateral forces of both the healthy participant and patient 1 peaked at -8% BW of the non-impaired side. On the impaired side of patient 1 lateral force is visible at every step. The healthy participant showed forces of 4% BW in both medial and lateral directions. Additionally, the vertical force of the non-impaired ankle is M-shaped for the healthy participant, while it is more flat for patient 1. The exclusion of information beyond PWB would have been a limitation, overlooking gait characteristic aspects. These aspects include anteroposterior force, mediolateral information, and vertical force characteristics in understanding the comprehensive functionality of the non-impaired ankle.

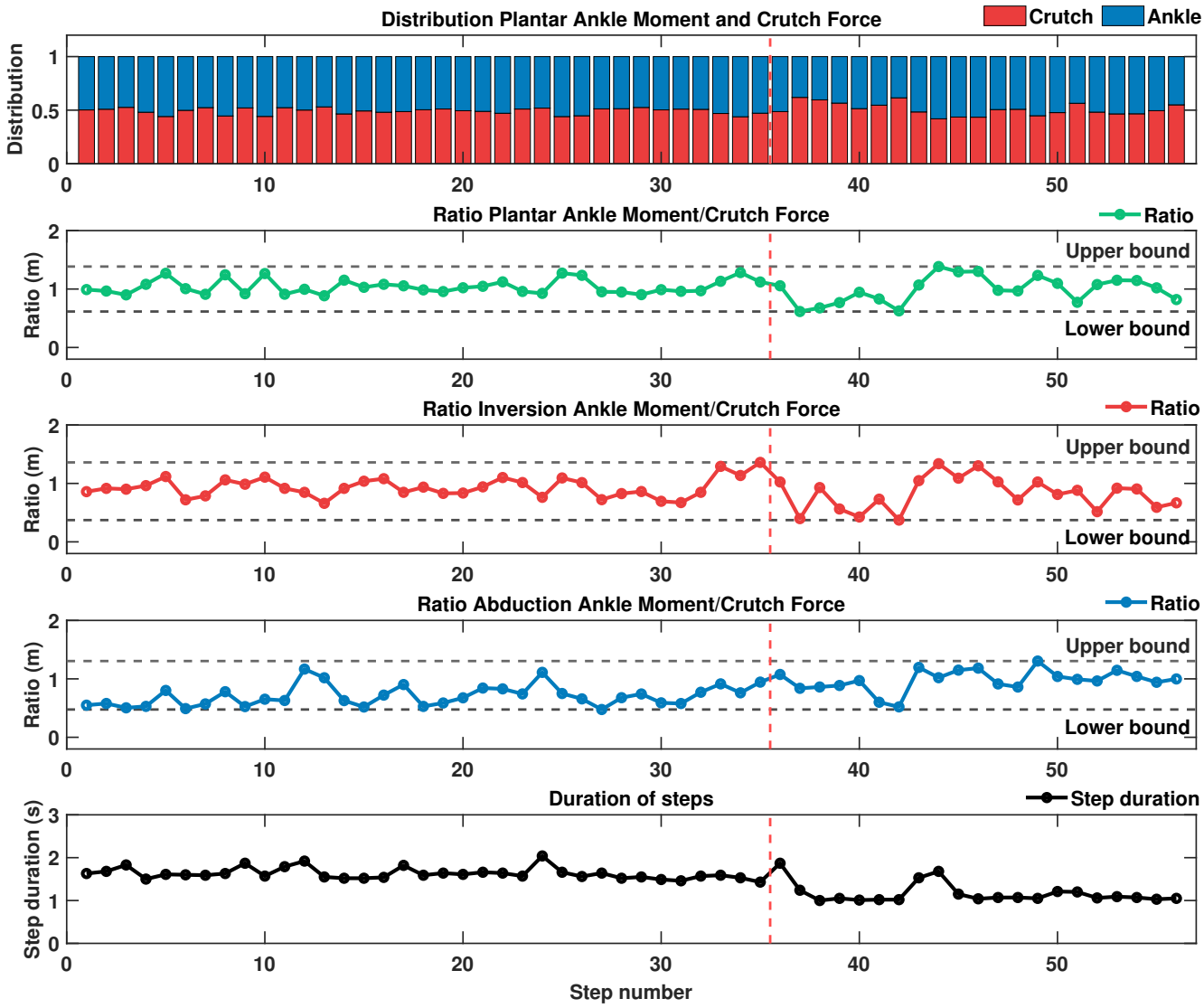

Figure 4.5: Ratio between plantar ankle moments and vertical crutch force. Patient 1's measurements precede the red dotted line; patient 2's follow after. **Row 1:** Distribution between plantar moment on the ankle and vertical force on the crutch. Both are normalised and the distribution is around 0.5. **Row 2 to 4:** Ratio between ankle moment and crutch force. **Row 5:** Duration of steps in seconds.

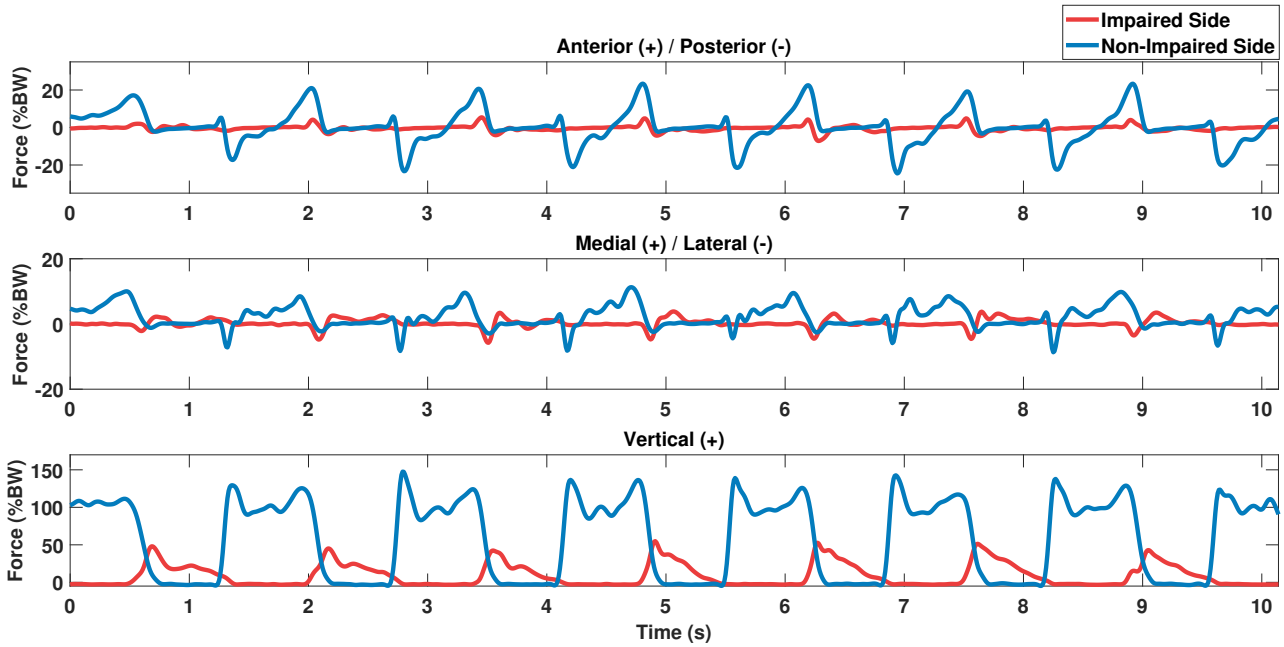

Figure 4.6: **Healthy participant**. Forces of a healthy person, imitating an impaired right ankle. The 10-MWT took about 10 seconds to finish.

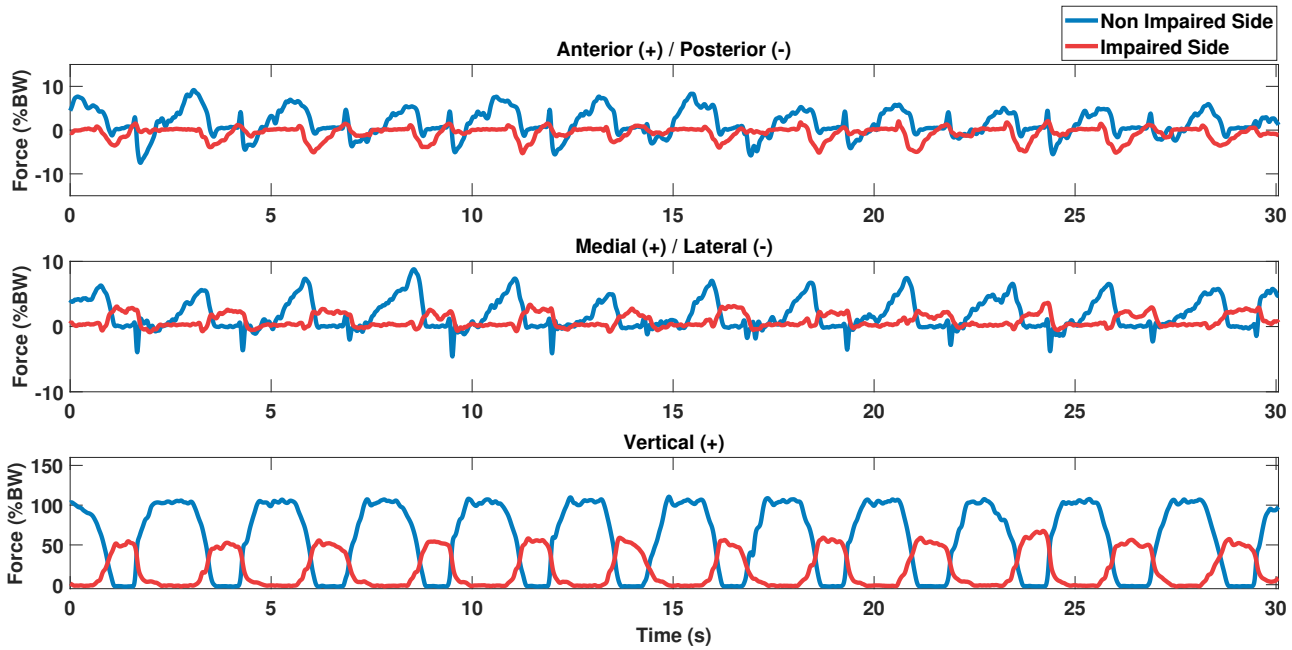

Figure 4.7: **Patient 1**. Forces of a patient that was allowed 25% weight-bearing. The 10MWT took about 30 seconds to finish.

4.3.3 3D Ankle Moments

Figure 4.8 and 4.9 show the net moments around the ankle joints of the healthy participant and patient 1. Moments are displayed in plantar/dorsiflexion, inversion/eversion, and abduction/adduction directions. Moments were normalised to % Body Weight Height (BWH).

Partial weight bearing does not consider moments, which is additional information acquired by the use of ForceShoes^{TM}. Both the healthy participant and patient 1 showed noticeable, brief flexion moment peaks on the non-impaired side: around 10% BWH for the former and 8% BWH for the latter. However, patient 1 exhibited a distinct pattern in flexion moment peaks on their impaired side compared to the healthy participant. Inversion moments were minimal for both individuals, yet patient 1 alternated between inversion and eversion when stepping on the non-impaired ankle. Abduction/adduction moments were less than 1% BWH on the non-impaired side and less than 0.4% on the impaired side.

Flexionmoments during crutch gait appeared to be significant in the 10-MWT, primarily on the non-impaired side. Timing of peak moment differed between the two individuals. Magnitude and timing of moments on both the impaired and non-impaired side are rehabilitation characteristics that would be overlooked by using PWB exclusively.

4.3.4 3D Crutch Force

The previous paragraphs threw light on the importance of measuring 3D ankle F&M and the limitations of PWB. Next, the contribution of the instrumented crutches is studied. Figures 4.10 and 4.11 show crutch forces in the trial reference system (ψ_{trial}). The crutch Y Axis forces oppose each other, unlike the ankle joint's mediolateral forces. Both participants had longer crutch loading phases than impaired-side step duration. Patient 1 consistently exerted more force on the crutch opposite the impairment, unlike the healthy participant. Z Axis forces ranged between 30% BW and 40% BW, while X and Y Axis forces remained small, except for the healthy participant's X Axis forces peaking at 20% BW during propulsion.

The instrumented crutches give insight into crutch use. Differences between left and right crutch vertical loads are visible, as well as crutch ground contact time. Together with propulsion and mediolateral forces, this gives information about the balance of a crutch user. PWB as a measure itself does not consider 3D crutch force. Figure 4.10 and 4.11 however show the useful information the instrumented crutches contain for rehabilitation.

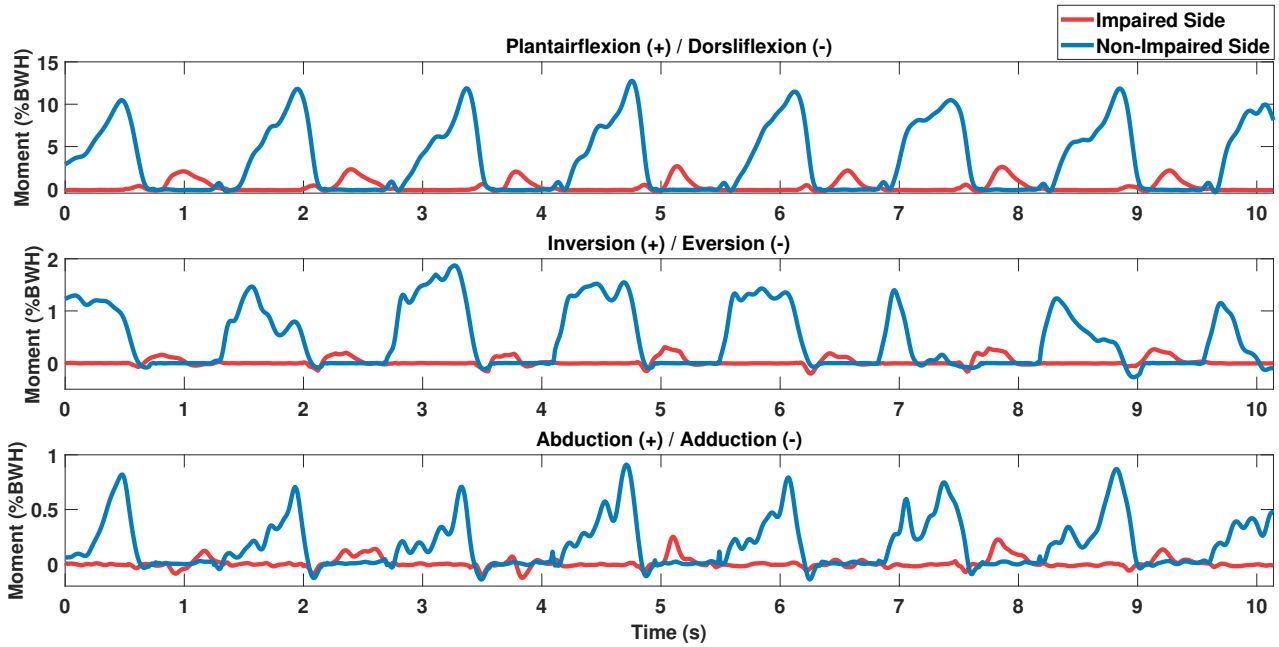

Figure 4.8: **Healthy participant.** Moments of a healthy person, imitating an impaired right ankle. The 10-MWT took about 10 seconds to finish.

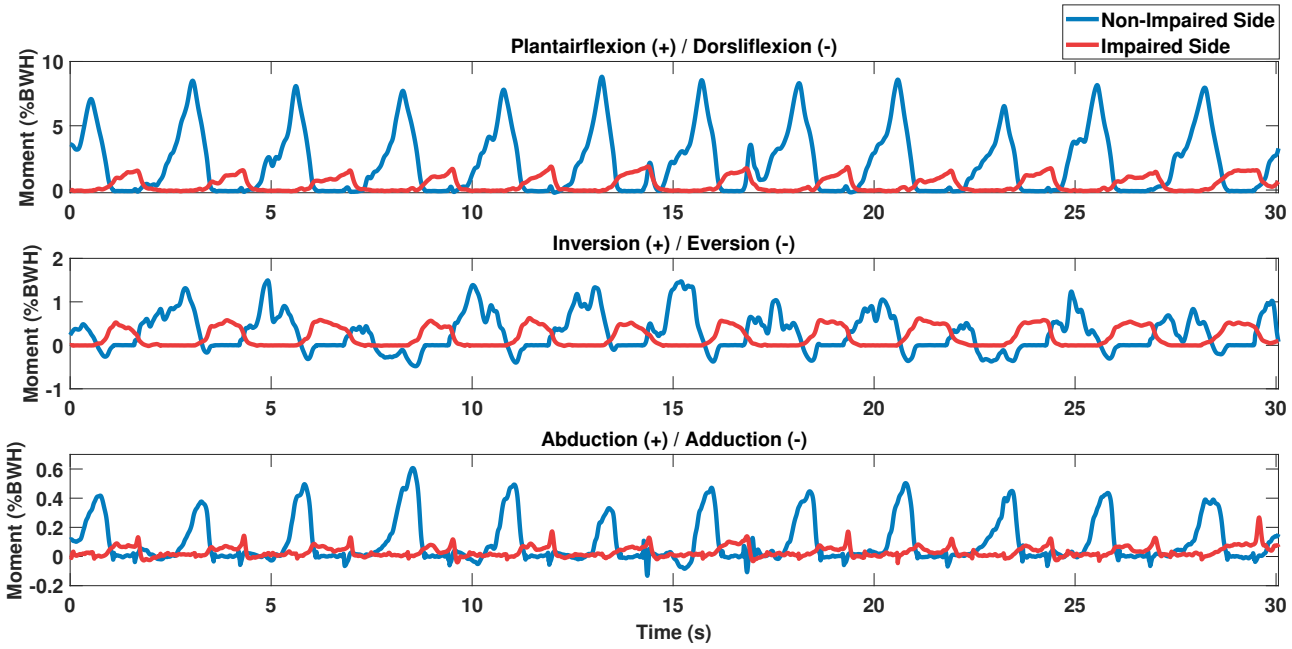

Figure 4.9: **Patient 1.** Moments of patient 1, who was allowed 25% weight-bearing.. The 10-MWT took about 30 seconds to finish.

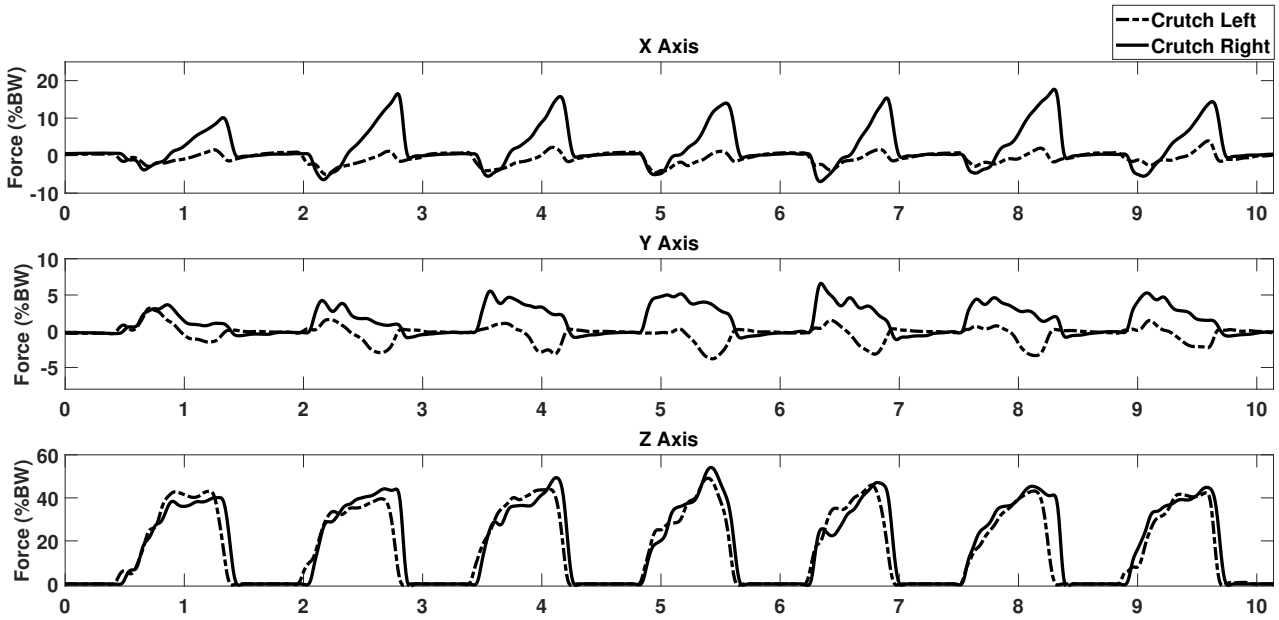

Figure 4.10: Forces of the crutches of the healthy participant. Forces are in ψ_{trial}. Forces in the Y Axis are therefore opposing. The 10-MWT took about 10 seconds to finish.

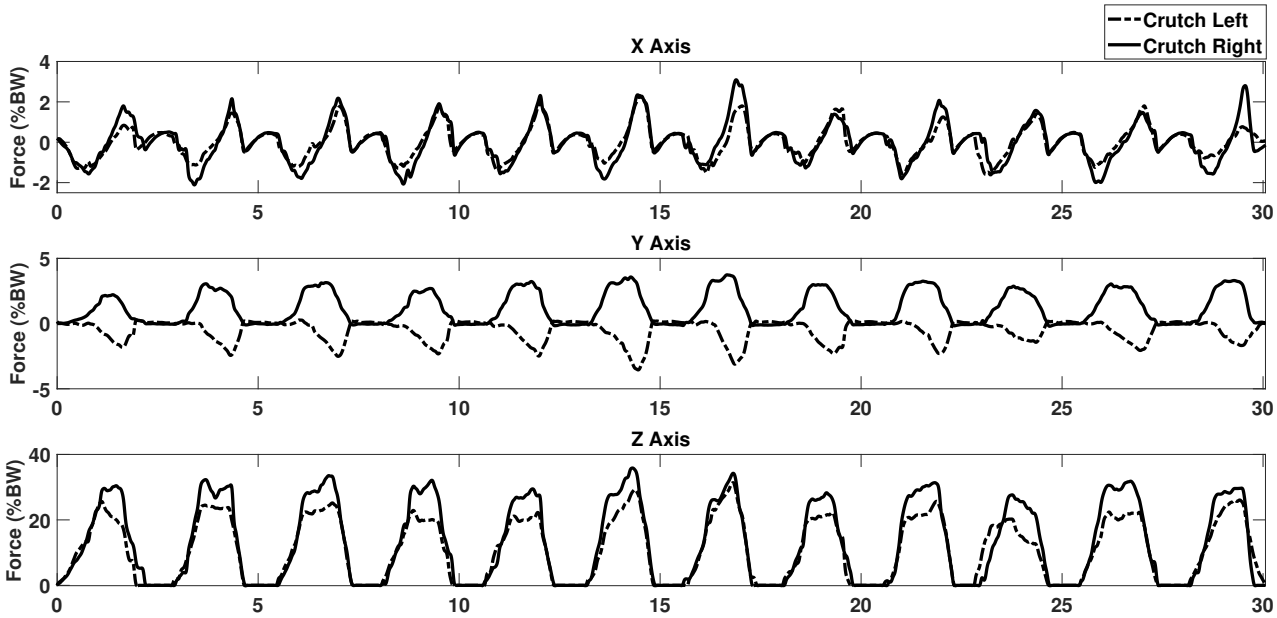

Figure 4.11: Forces of the crutches of patient 1. Forces are in ψ_{trial}. Forces in the Y Axis are therefore opposing. The 10-MWT took about 30 seconds to finish.

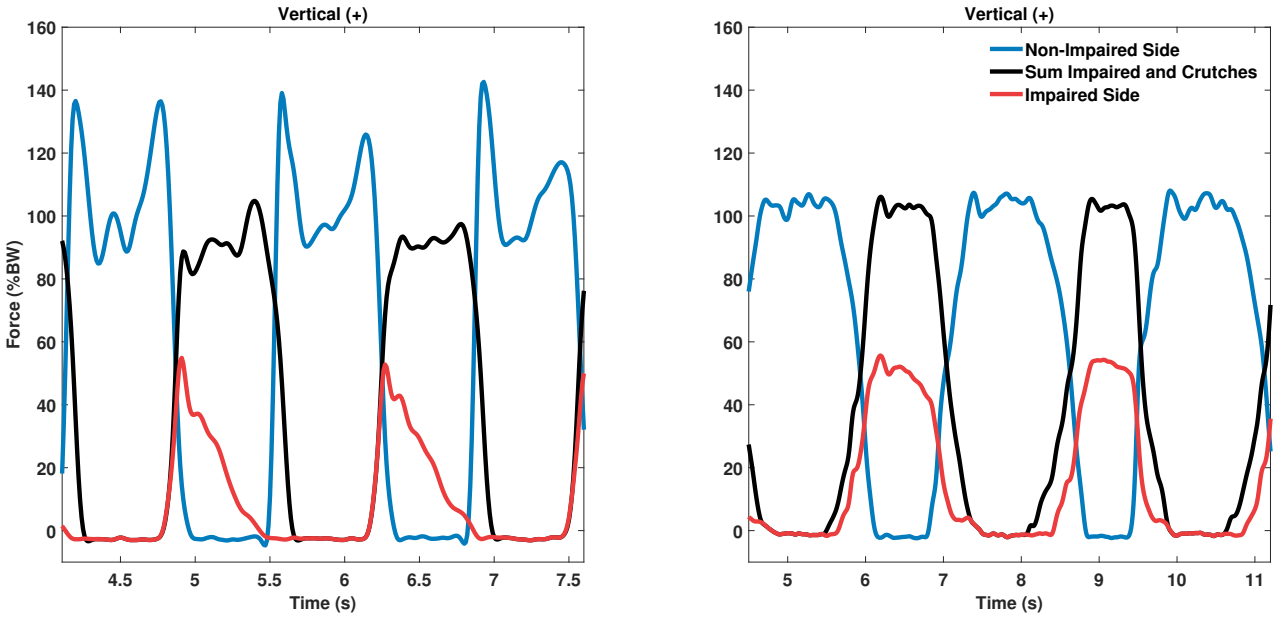

Figure 4.12: **Left:** Healthy participant. **Right:** Patient 1. Zoomed in plot. The black line indicates the sum of both crutches and the vertical force on the impaired ankle.

4.3.5 PWB from crutches

Figure 4.12 shows a zoomed-in version of forces on the ankle joints in the vertical direction. Summing force of both left and right crutch and the impaired ankle gives a total of 100% BW during stance. This translates to the possibility of the instrumented crutches to estimate PWB in a 10-MWT with a basic model. Previously, the limitations of the crutches in directly estimating ankle moments were established. Nonetheless, it is shown here they could play a role in scenarios where only the vertical force on the ankle needs to be known and ankle moments cannot be directly measured. As described earlier, however, PWB proved to be inadequate for accurate assessment of a 10-MWT, and there is a need for accurate 3D ankle F&M estimation.

4.3.6 Averaged Forces and Moments

Figures 4.13 to 4.15 show the averaged gait cycles of the healthy participant, patient 1 and patient 2. These illustrate the 3D forces and moments affecting the ankle, both in magnitude and timing. These visuals offer a comprehensive overview of the aspects overlooked when only considering PWB. Standard deviation is omitted from the plots for clarity. Anteroposterior, mediolateral, and vertical forces are plotted in red, green, and blue respectively. Inversion/eversion, plantarflexion/dorsiflexion, and abduction/adduction moments are named inversion, plantarflexion, and abduction in the plots for clarity. Self-chosen walking speeds of the healthy participant, patient 1 and patient 2 were 1.5, 0.83, and 1.25 steps/s.

Notable is the difference in shape between vertical forces on the non-impaired ankle. Patient 1 displayed minimal distinctions between forces at foot-flat, midstance, and heel-off, a contrast that becomes more visible in the case of patient 2 and even more so in the case of the healthy participant. Both patients performed 50% PWB, despite patient 1 only being allowed 25%. Patient 2 however, was allowed 50% PWB and loaded the impaired ankle more during every step. Anteroposterior and mediolateral forces scaled with the size of vertical force. This shows the

measurement setup is capable of revealing interpersonal differences. If only PWB was available, these differences would not be discovered.

Plantarflexion moments of the non-impaired ankle of both patients peaked at the relatively large value of 8% BWH and 12% BWH of the healthy participant. This sheds light on possible increased moments on the non-impaired side due to the nature of crutch gait. What is also revealed using 3D F&M rather than PWB, is the notable difference of the peak on the impaired side. Patient 1 and 2 had their peaks at 75% of stance with heights of 2% and 4% BWH respectively. A peak was found at 50% stance of 2% BWH in the averaged cycle of the healthy participant. PWB as a measure for rehabilitation would not have given insights into the difference between impaired and non-impaired moments and possible compensatory mechanisms of the non-impaired side in crutch walking.

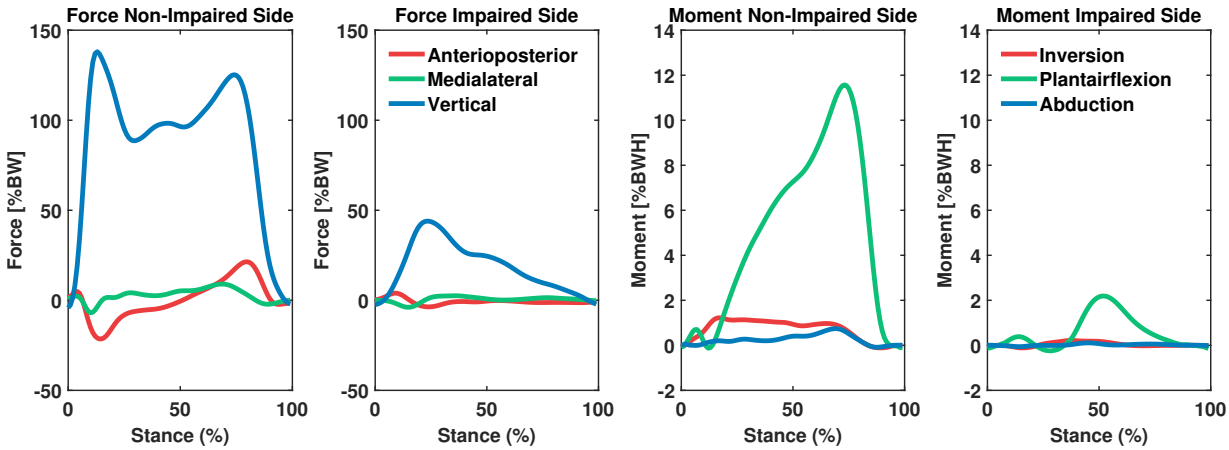

Figure 4.13: **Healthy participant.** Averaged gait cycles of healthy participant. The right ankle was the impaired side. The task was a 10-MWT. The two left images are forces and the two right are moments.

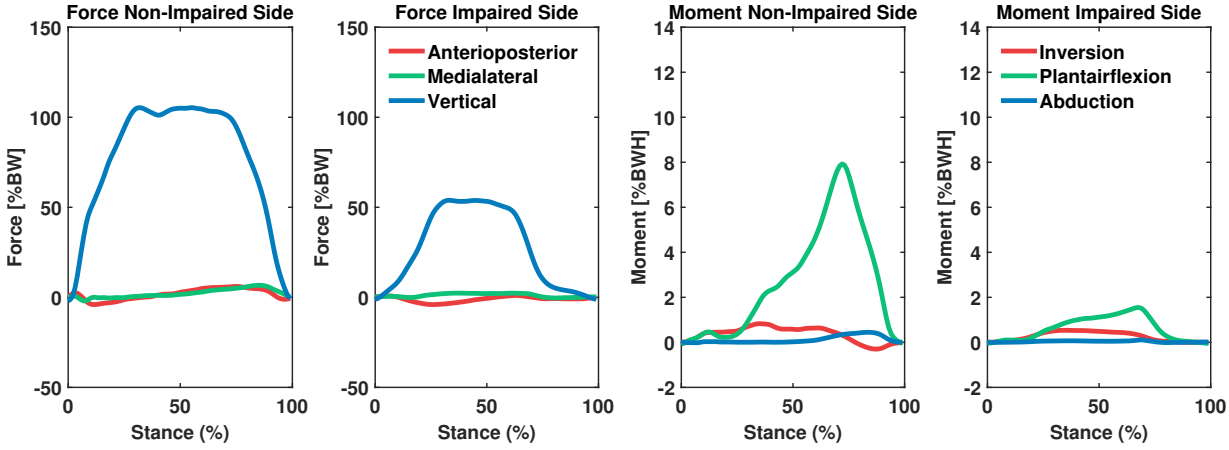

Figure 4.14: **Patient 1 - 25% weight-bearing allowed.** Averaged gait cycles of patient 1. The right ankle was the impaired side. The task was a 10-MWT.

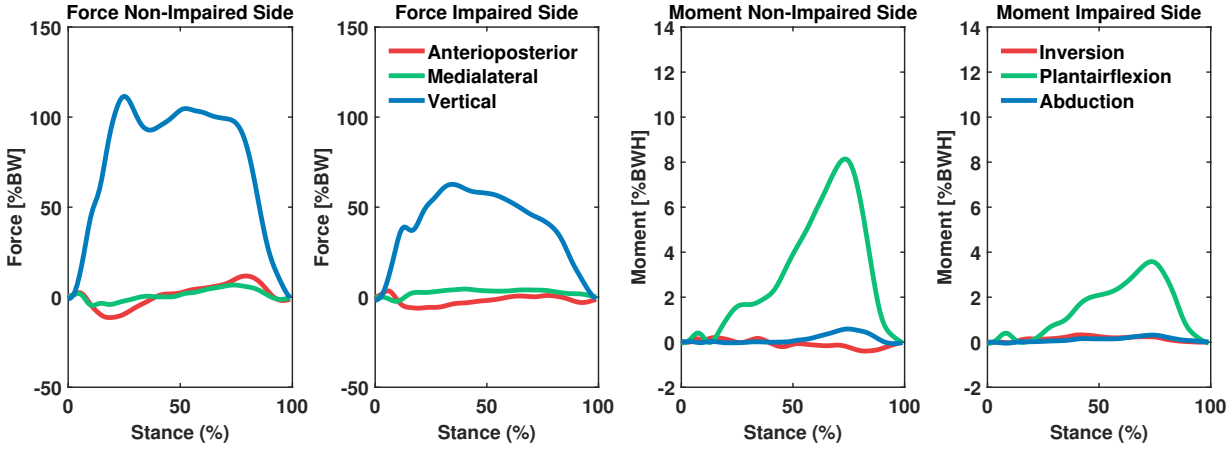

Figure 4.15: **Patient 2 - 50% weight-bearing allowed.** Averaged gait cycles of patient 2. The right ankle was the impaired side. The task was a 10-MWT.

4.3.7 Scores

Table 4.4 to 4.6 present data on both the average and maximum forces and moments observed during 10-MWT trials. 'AP' denotes the anteroposterior direction, while 'ML' represents the mediolateral direction. The tables provide both mean and standard deviations. Table 4.4 presents data from four healthy participants, with a total of 10 trials. On the other hand, table 4.5 and 4.6 present data specifically from patient 1 and 2 respectively. These patient-specific tables are based on three trials each. The presented values were normalised to percentage body weight (%BW) for forces and percentage body weight times height (%BWH) for moments.

The largest averages and maxima were found in the vertical force direction, corresponding to PWB. The four healthy participants reproduced the impaired ankle with an average vertical force of 25.3 $\pm$ 5.3% BW. Notable is the large standard deviation in the maximum vertical force of 56.7 $\pm$ 23.4% BW. The non-impaired ankle was on average loaded with less than body weight, while maximally the force exceeded body weight in all cases.

Additional information about anteroposterior force, mediolateral force, and 3D moments is gained from the 3D F&M measurement system. A relatively large anteroposterior force on the impaired ankle of 10.80 $\pm$ 1.02% BW is seen in patient 2. An even larger force of 16.65 $\pm$ 0.4% BW was present on the non-impaired ankle of patient 2. Forces in the mediolateral direction were smaller. Again, forces on the non-impaired ankle exceeded those on the impaired ankle.

Largest moments were found in the plantair/dorsalflexion moment direction. Maximum flexion moments on the impaired ankle were 2.99 $\pm$ 0.7% BWH for the healthy participant, 1.82 $\pm$ 0.07% BWH for patient 1, and 4.24 $\pm$ 0.56% BWH for patient 2. As expected, larger moments were found on the non-impaired ankle. Inversion moments on the impaired ankle remained below 1% BWH. Both average and maximum abduction moments were consistently below 1% BWH across all cases. The variations in quantities across moment directions offer valuable biomechanical insights into crutch walking, made possible by the elaborate analysis using 3D F&M.

This analysis also revealed patients 1 and 2 showed agreement in the phase of gait where maxima of anteroposterior, mediolateral, and vertical forces were found. The same was found to be true of the moments, except for the maximum inversion moment. This was during the "foot flat" phase for patient 1, while for patient 2, these were observed during "mid-stance" for the impaired ankle. The healthy participants consistently showed to be unable to reproduce agreement in moment maxima gait stages. This section offers insight into the magnitude of crutch walking gait following an ankle fracture, emphasising the necessity of including actual ankle fracture patients and a more comprehensive analysis beyond PWB.

Table 4.4: Average and maximum force and moment found in 10-MWT trials of healthy participants. Average of 4 participants with a total of 10 trials.

		Force (%BW)			Moment (% BWH)		
Foot	**Mean ± std**	**AP**	**ML**	**Vertical**	**Flexion**	**Inversion**	**Abduction**
Impaired	**Average**	2.08 ± 0.54	2.20 ± 0.52	**25.3 ± 5.3**	**1.31 ± 0.43**	0.15 ± 0.06	0.12 ± 0.05
	Max	6.34 ± 1.6	5.84 ± 1.1	**56.7 ± 23.4**	**2.99 ± 0.7**	0.45 ± 0.25	0.33 ± 0.12
	Gait stage	Foot flat	Foot flat	Foot flat	Mid-stance	Mid-stance	Mid-stance
Non-Impaired	**Average**	7.76 ± 1.3	2.6 ± 0.94	**90.24 ± 4.3**	**5.08 ± 0.48**	0.52 ± 0.17	0.17 ± 0.07
	Max	22.9 ± 3.9	7.7 ± 2.1	**128.0 ± 13.7**	**10.1 ± 1.54**	1.52 ± 0.27	0.59 ± 0.18
	Gait stage	Foot flat	Heel off	Foot flat	Heel off	Foot flat	Heel off

Table 4.5: Average and maximum force and moment found in 10-MWT trials of patient 1.

		Force (%BW)			Moment (% BWH)		
Foot	**Mean ± std**	**AP**	**ML**	**Vertical**	**Flexion**	**Inversion**	**Abduction**
Impaired	**Average**	1.83 ± 0.02	1.77 ± 0.04	**41.75 ± 0.99**	**0.88 ± 0.04**	0.39 ± 0.08	0.06 ± 0.003
	Max	5.30 ± 0.27	3.74 ± 0.32	**66.88 ± 5.15**	**1.82 ± 0.07**	0.66 ± 0.06	0.25 ± 0.02
	Gait stage	Foot flat	Mid-stance	Foot flat	Heel off	Foot flat	Heel off
Non-Impaired	**Average**	3.38 ± 0.05	2.81 ± 0.11	**83.9 ± 0.59**	**3.09 ± 0.15**	0.47 ± 0.05	0.14 ±0.004
	Max	9.97 ± 0.82	8.74 ± 0..38	**109.1 ± 1.31**	**8.70 ± 0.13**	1.53 ± 0.1	0.61 ± 0.02
	Gait stage	Heel off	Heel off	Foot flat	Heel off	Foot flat	Heel off

Table 4.6: Average and maximum force and moment found in 10-MWT trials of patient 2.

		Force (%BW)			Moment (% BWH)		
Foot	**Mean ± std**	**AP**	**ML**	**Vertical**	**Flexion**	**Inversion**	**Abduction**
Impaired	**Average**	3.08 ± 0.34	3.21 ± 0.04	**45.27 ± 2.33**	**1.51 ± 0.18**	0.18 ± 0.05	0.12 ± 0.01
	Max	10.80 ± 1.02	6.38 ± 0.58	**74.29 ± 3.28**	**4.24 ± 0.56**	0.49 ± 0.05	0.38 ± 0.03
	Gait stage	Foot flat	Mid-stance	Foot flat	Heel off	Mid-stance	Heel off
Non-Impaired	**Average**	6.48 ± 0.40	2.93 ± 0.45	**79.31 ± 0.65**	**3.36 ± 0.16**	0.39 ± 0.09	0.17 ± 0.03
	Max	16.65 ± 1.18	9.78 ± 1.36	**114.38 ± 3.34**	**8.97 ± 0.32**	1.35 ± 0.21	0.85 ± 0.11
	Gait stage	Heel off	Heel off	Foot flat	Heel off	Heel off	Heel off

Table 4.7 - 4.9 illustrate the contribution of individual force and moments directions on the resulting force and moment $\boldsymbol{F_{res}}$ and $\boldsymbol{M_{res}}$. This sheds light on the aspect overlooked when only considering partial weight-bearing. The force components include anteroposterior 'AP', mediolateral 'ML', and vertical forces, expressed as a percentage of body weight (% BW). The moment components are categorised in plantarflexion/dorsiflexion 'flexion', inversion/eversion 'inversion', and abduction/adduction 'abduction'.

In the first table, based on measurements of healthy participants, the vertical force contributes the highest percentage to the resultant force. Values are typically close to or exceeding 97% BW, showing PWB does include most of the resulting vertical force. In Table 4.8 and 4.9 concerning patients, a similar trend is visible, where vertical force was dominant to the resultant force, with values higher than 98% BW.

Looking at information beyond PWB gives new insights. The maximum value in the anteroposterior direction, reaching 12.8 $\pm$ 4.7% BW on the impaired side, is also notable. In the impaired ankle of patient 2 a maximum of 15.59 $\pm$ 1.21% BW was found in the anteroposterior direction. Regarding the resultant moment, the flexion and inversion moments had a substantial role. In average values, the flexion moments were most significant, with values of 90.9% BWH or above. In the maximum values, both the flexion and inversion moment appear as important contributors to the resultant moment. The maximum inversion moment of 57.0 $\pm$ 44.9% BWH on the impaired side of the healthy participants however is smaller than on the non-impaired side and shows a large variation.

Flexion moments remain substantial in shaping average and maximum resultant moments for both patients. Both the flexion and inversion moments were relevant for the maximum resultant moments, with values of larger than 98% BWH. This gives insights into the importance of flexion and inversion moments for the biomechanics of crutch gait and the need for 3D F&M for a comprehensive understanding.

Table 4.7: Contribution to resultant force and moment using vector method of healthy participants.

		Contribution to F_{res} (%)			**Contribution to M_{res} (%)**		
	Mean ± std	**AP**	**ML**	**Vertical**	**Flexion**	**Inversion**	**Abduction**
Impaired	**Average**	1.60 ± 0.9	1.20 ± 0.5	**97.3 ± 1.3**	**91.9 ± 5.6**	6.7 ± 5.6	1.4 ± 0.9
	Max	12.8 ± 4.7	7.6 ± 2.4	**99.9 ± 0.1**	**99.86 ± 0.3**	**57.0 ± 44.9**	8.6 ± 4.0
Non-	**Average**	1.1 ± 0.25	0.2 ± 0.1	**98.7 ± 0.3**	**90.9 ± 4.8**	8.7 ± 4.7	0.33 ± 0.1
Impaired	**Max**	11.1 ± 5.2	5.56 ± 2.6	**99.9 ± 0.02**	**100 ± 0.0**	**96.8 ± 4.3**	5.9 ± 2.3

Table 4.8: Contribution to resultant force and moment using vector method of patient 1.

		Contribution to F_{res} (%)			**Contribution to M_{res} (%)**		
	Mean ± std	**AP**	**ML**	**Vertical**	**Flexion**	**Inversion**	**Abduction**
Impaired	**Average**	0.38 ± 0.01	0.24 ± 0.02	**99.37 ± 0.03**	**71.63 ± 1.24**	27.91 ± 1.21	0.47 ± 0.04
	Max	3.40 ± 1.63	3.0 ± 0.77	**99.99 ± 0.0**	**99.18 ± 0.16**	**99.14 ± 0.07**	3.56 ± 0.78
Non-	**Average**	0.33 ± 0.02	0.44 ± 0.03	**99.23 ± 0.03**	**76.66 ± 0.85**	22.85 ± 0.84	0.49 ± 0.27
Impaired	**Max**	14.52 ± 4.11	7.45 ± 0.81	**100.0 ± 0.0**	**99.98 ± 0.02**	**99.98 ± 0.03**	6.89 ± 0.01

Table 4.9: Contribution to resultant force and moment using vector method of patient 2.

		Contribution to F_{res} (%)			Contribution to M_{res} (%)		
	Mean ± std	**AP**	**ML**	**Vertical**	**Flexion**	**Inversion**	**Abduction**
Impaired	**Average**	0.98 ± 0.22	0.63 ± 0.07	**98.39 ± 0.29**	**91.04 ± 0.43**	8.19 ± 0.35	0.78 ± 0.10
	Max	15.59 ± 1.21	5.87 ± 0.42	**99.93 ± 0.06**	**99.94 ± 0.04**	**98.69 ± 0.15**	6.08 ± 0.87
Non-	**Average**	1.10 ± 0.15	0.28 ± 0.08	**98.62 ± 0.19**	**90.28 ± 1.89**	9.31 ± 1.85	0.41 ± 0.10
Impaired	**Max**	11.47 ± 6.35	3.83 ± 1.45	**99.99 ± 0.01**	**99.99 ± 0.003**	**97.92 ± 0.62**	4.67 ± 1.38

4.4 Discussion

In this chapter, a methodology for the estimation of 3D forces and moments in the ankle joint during the gait of patients using instrumented crutches was introduced. This approach represents an advancement beyond current clinical practice, which primarily examines force in the Z Axis, known as Partial Weight Bearing. The study involved a comprehensive investigation and comparison of 3D forces and moments in the ankles of four healthy participants and two patients, together with an analysis of the 3D forces exerted on the crutch tip. The research included an assessment of both average and maximum 3D F&M. Furthermore, contributions of each individual force and moment direction on $\boldsymbol{F_{res}}$ and $\boldsymbol{M_{res}}$ have been analysed. The clinically validated ForceShoes™ system served as golden standard reference for the calculation of 3D forces and moments, giving precision to the study [48].

Figure 4.5 illustrates the relationship between vertical crutch force and 3D ankle moments. The ratio varied between 0.5 to 1.5m, with the largest variations in patient 2. Ratio changes in one specific moment direction do not consistently align with ratio changes in another moment direction. Furthermore, these fluctuations do not coincide with step duration changes. Consequently, it suggests that the force measured by the crutches does not directly correspond to the overall moments at the ankle joint. This underscores the requirement of using ForceShoes™ for measuring 3D ankle force and moments, in addition to the instrumented crutches.

Figures 4.6 to 4.9 and 4.13 to 4.15 illustrate 3D ankle F&M of 10-MWT trials as well as averaged gait cycles. These figures revealed significant differences between the impaired and non-impaired ankles. Particularly, the 3D forces and moments on the non-impaired ankle closely resemble a standard walking pattern, as has been previously observed using ForceShoes™, as reported by Schepers et al. and Veltink et al. [42, 49]. This similarity includes the characteristic M-shaped curve in the vertical force direction, as well as the distinct peaks in anteroposterior direction corresponding to breaking and propulsion. Furthermore, the typical shape of the peak in mediolateral direction and the relatively large distinct shape of the plantar ankle moment peak were clearly visible. This suggests the non-impaired ankle shows a close-to-normal walking pattern. However, to investigate how the non-impaired side compensates, PWB is not sufficient, and 3D F&M measurements are needed.

On the contrary, the impaired ankle displayed a distinct pattern in both force and moment, with neither patient showing the typical M-curve in vertical force. While anteroposterior and mediolateral forces had similar shapes to the non-impaired side, they were weaker. The plantarflexion moments also differed, lacking the usual skewed summit and dip. Moreover, patient 1, despite being explicitly instructed and shown the allowed force on a scale, performed 50% weight-bearing instead of the prescribed 25%. This corresponds with prior research by Lie, Warren, and Winstein, and which highlighted the difficulty of reproducing partial weight-

bearing other than 50% [14, 33, 34]. The force and moment profiles of the simulated impaired ankle in the healthy participant differed significantly from those observed in both patients. This underscores a timing discrepancy in the way the foot transitioned during weight-bearing, in contrast to patients with actual ankle fractures. **Appendix A** displays the time-averaged forces and moments of the other three healthy participants in Figure A.2 to A.4. Once more, this reveals that the simulated ankles do not accurately replicate the characteristics of an actual fractured ankle. The ambulatory measurement system in this chapter allows for understanding the ankle biomechanics during crutch walking and interpersonal variations, which is not possible using PWB only.

Figures 4.10 and 4.11 provide 3D forces measured at the crutch tip. **Chapter 3** discussed errors of 3.35 $\pm$ 0.31 % for the left crutch and 3.44 $\pm$ 0.15% for the right crutch. Both the healthy subject and patient 1 exhibited patterns similar to those observed in previous research and the trials conducted in **Chapter 3**. Notably, there are recognisable breaking and propulsion forces in the $\boldsymbol{F_x}$ dimension, and sideways forces in $\boldsymbol{F_y}$, "pushing the crutches outward." The vertical loading phase in $\boldsymbol{F_z}$ is also clearly evident. Sardini et al. conducted 10-MWTs with a group of 10 participants using instrumented crutches for 3-point PWB [21]. Their findings closely resemble the results of this study, with patterns in $\boldsymbol{F_x}$, $\boldsymbol{F_y}$, and $\boldsymbol{F_z}$ showing remarkable similarities. However, it is important to highlight that their study exclusively focused on healthy participants following specific instructions to maintain 10% PWB. Furthermore, their instrumented crutches relied solely on accelerometer-based orientation estimations. Considering the low errors observed with the instrumented crutches and the notable resemblance in force patterns to the study by Sardini et al., it is reasonable to conclude that these instrumented crutches hold promise for accurately measuring ground reaction forces in an ambulatory setting and are a valuable addition in combination with 3D ankle F&M information.

Figure 4.12 and **Appendix A** Figure A.1 illustrate an interesting finding in this study. The visualisations reveal that the cumulative vertical force acting on the impaired ankle and both crutches collectively approach 100% of the participant's body weight during gait. Notably, this phenomenon remained consistent across a diverse range of self-selected walking speeds, which varied from 0.83 steps/s for patient 1 to 1.5 steps/s for a healthy participant. This finding holds great promise for real-time monitoring of PWB when utilising instrumented crutches. These results align with those reported by Merrett et al., who used the formula $\boldsymbol{PWB_{\%} = 100\% - F_{crutches}}$ with normalised forces, and observed a similar trend for 0%, 50%, and 75% PWB conditions [40]. Figure 4.5 however showed no direct correlation between 3D ankle moments and vertical crutch force, and this relationship could be further investigated. In an ambulatory setting, a simple feedback mechanism, such as an audible beep or LED indicator, could be used to inform patients when they exceed a prescribed level of PWB, as determined by their physiotherapist. This would empower patients and the hospital in optimising rehabilitation outcomes after an ankle fracture and maintain the prescribed weight-bearing restrictions.

Table 4.4 to 4.6 have provided valuable insights into the average and maximum forces and moments observed in a 10-MWT. Thereby revealing differences between the impaired and non-impaired ankles in both simulated and actual ankle fractures. Additionally, differences between 3D forces and moments, and PWB were made insightful. Of particular significance is the difference between the average vertical force on the impaired side of 43.51% BW compared to 81.61% BW on the non-impaired side in both patients. This distinction highlights the essential role of crutches in redistributing the weight, relieving the burden on the fractured ankle. Notable are the observed maximum forces in anteroposterior and vertical direction and

moments of flexion. The added value of 3D F&M compared to PWB appeared here in both understanding the large anteroposterior force contribution as well as insights into the non-impaired side during a 10-MWT.

Patient 2 showed a maximum anteroposterior force of 10.80% BW, a vertical force of 74.29% BW, and a flexion moment of 4.24% BWH on the impaired side. Despite patient 1 loading the impaired ankle with 50% PWB instead of the allowed 25% PWB, flexion moments of an average of 0.88% BWH and 1.82% BWH maximum were found, which is half of patient 2. This observation suggests that patients might instinctively manage weight-bearing by limiting their moments, rather than controlling vertical forces. Current clinical practice primarily examines force in the vertical direction, meaning the significant maximum contribution of the anteroposterior direction and flexion moment are not taken into consideration.

Table 4.7 to 4.9 compared the average and maximum contribution of individual force and moment directions to the resulting force and moments. It is evident the vertical force direction with a contribution exceeding 98% is the most important component of $\boldsymbol{F_{res}}$, which will be included when only PWB is considered. Notably, on the impaired side of patient 2, the maximum contribution of the anteroposterior force reached 15.59% BW, a factor that is often overlooked when focusing solely on PWB. Furthermore, the analysis highlights the substantial significance of flexion and inversion moments. In all cases, both average and maximum flexion moments exceeded 71.63% BWH, indicating their crucial role in gait dynamics. Maximum inversion moments accounted for over 98% BWH of $\boldsymbol{M_{res}}$ in both patients. However, as mentioned previously, Table 4.4 to 4.6 consistently show these inversion moments to be below 1.53% BWH, emphasising their limited clinical significance. These insights reveal the complexities of force and moment contributions in assessing gait and the implications for rehabilitation strategies.

Calculating Individual Forces

In order to provide a more comprehensive understanding and intuition of the forces and moments investigated, normalised values are calculated back to the original values and compared. Due to ethical considerations and the ethical agreement with the hospital, specific measurements of the patients involved are not disclosed. Instead, representative approximations for patients' weight and length are used. Calculating force is done using formula 4.8.

$$\boldsymbol{F = \%BW/100 * m * g} \tag{4.8}$$

With $\boldsymbol{m}$ the mass of the person and $\boldsymbol{g}$ the gravitational acceleration. Similarly, the moment is calculated using 4.9.

$$\boldsymbol{M = \%BWH/100 * m * g * h} \tag{4.9}$$

Where $\boldsymbol{h}$ is the length of a person. For the calculations, it is assumed patient 1 has a mass of 80 kg and a height of 1.75 m, while patient 2 is assumed to have a mass of 80 kg and a height of 1.90 m. The Tables 4.10 and 4.11 provide the calculated forces and moments for patients 1 and 2 in units of Newtons (N) and Newton meters (Nm), respectively.

A notable observation is the similarity in the magnitudes of vertical forces in both patients, which can be attributed to their comparable body weights. However, patient 1 exhibits approximately half the anteroposterior force in both the impaired and non-impaired sides compared to patient 2.

When examining each patient individually, a clear contrast emerges. Patient 2 displays forces

and moments on the impaired side that are approximately half of those on the non-impaired side. In contrast, for patient 1, while anteroposterior and vertical forces on the impaired side are roughly half of those on the non-impaired side, the moments are only a quarter of the non-impaired side. This discrepancy aligns with the literature, which indicates that patient 1 was unable to achieve the prescribed 25% partial weight-bearing [14,33,34].

It appears that patient 1 was able to maintain flexion moments within the recommended weight-bearing range when assuming that the impaired side was allowed one-fourth of the non-impaired side's load. It is worth noting that there was a discrepancy in walking speeds between the two patients, with patient 1 taking 0.83 steps per second and patient 2 taking 1.5 steps per second. This variance explains the differences in anteroposterior force magnitudes between the two patients. Intriguingly, despite their self-selected walking speeds, both patients managed to maintain flexion moments within the prescribed weight-bearing range, with patient 1 at 25% and patient 2 at 50%. It shows to further research this finding, 3D ankle F&M information is needed in future research.

Table 4.10: Anteroposterior force, vertical force, and flexion moments of patient 1.

		Force (N)		Moment (Nm)
Foot	**Mean**	**AP**	**Vertical**	**Flexion**
Impaired	**Average**	14.4	327.7	12.1
	Max	41.6	524.9	25.0
Non-Impaired	**Average**	26.5	658.4	42.4
	Max	78.2	856.2	119.5

Table 4.11: Anteroposterior force, vertical force, and flexion moments of patient 2.

		Force (N)		Moment (Nm)
Foot	**Mean**	**AP**	**Vertical**	**Flexion**
Impaired	**Average**	24.2	355.3	22.5
	Max	84.8	583.0	63.2
Non-Impaired	**Average**	50.9	622.4	50.1
	Max	130.7	897.0	133.8

Limitations and Future Work

The 3D ankle forces and moments calculated in this chapter are specifically for a 10 Meter Walking Test when using 3-point Partial Weight-bearing gait. If other gait types, such as swing-through gait are studied, as done by Stallard et al. forces on the non-impaired side would be increased as a result of the increased swing-speed [35,36]. However, for rehabilitation purposes, the 3-point Partial Weight Bearing gait remains common because it allows for partial loading of an impaired ankle. Furthermore, while a 10 Meter Walking Test provides a standardised task applicable to all participants, it offers a simplified reality. Real-life walking includes a wider range of activities, including turns, walking stairs, and engagement in activities of daily living that subject the ankle to more varied loading patterns.

The current system making use of instrumented crutches and ForceShoes^{TM} presents practical challenges in real-life scenarios. Firstly, the ForceShoes^{TM} are relatively bulky, and their force sensors require zeroing before each measurement session. The instrumented crutches require sensor-to-crutch calibration of the IMU, as well as zeroing before each measurement session. This process cannot be done independently by patients, as it requires the crutches to be stand-

ing freely. Additionally, the initial orientation of the crutches must be known before applying the filter. Furthermore, it is essential to note that measurements from the ForceShoes™ are not transformed to the same reference system as defined for the crutches. Consequently, forces and moments are considered from the perspective of the ankle joint itself, rather than from a unified reference frame aligned with the crutch force. This can be a limitation, especially when participants perform more complex walking patterns, such as figure-eight shapes.

Only two patients and four healthy participants were included in this study. Healthy participants were unable to reproduce the gait of an actual ankle fracture patient. Specifically in the timing and loading pattern on the impaired side. As the patient cohort was restricted to N = 2, the outcomes of this study may not be generalised to a larger population. Included patients were measured 7-12 weeks after fracture indicating a stable fracture. Other findings may occur when doing measurements outside of this 7-12 weeks range or when patients are included that are allowed 75% PWB. In future research, it would therefore be valuable to expand the population and diversify the data set. This would give a more comprehensive understanding of gait patterns in various clinical contexts.

Current research simplified the foot and ankle as a triangle with a rotation point. Previous research by Schepers and Veltink, and Winter used this model to calculate forces and moments at the ankle joint [41,42]. However, Winter typically used this model in static situations. Schepers and Veltink did use this model for walking, however only reported on the flexion moments at the ankle joint. Additionally, the distance from the heel to the rotational point is based on a ratio found in In Vivo studies. A study by Sado et al. [50] suggested the actual geometric centre of rotation of the ankle should be considered instead. Their research revealed that the current method underestimates peak dorsiflexion and inversion moments during walking. Consequently, it is interesting to explore the effects of adopting a more comprehensive model in following research.

Furthermore, in this chapter, a comparison was made between the current clinical measure of Partial Weight Bearing and forces in the Z direction. It should be noted these are in fact not directly comparable. As PWB is a measure typically used for Ground Reaction Forces while this chapter focuses on forces on the ankle. It is worth noting that the mass of the foot should ideally be subtracted from the calculations; however, this value amounts to only 1.4% of body weight on average [51]. Given the small magnitude of this difference (1.4%), this adjustment has not been made.

Only net, or external, forces and moments were researched in this chapter. Adding internal forces, moments and angles could give a more comprehensive understanding of the total load placed on the ankle. Internal forces and moments describe the contraction of muscles and visco-eleastric properties of the joint, as researched by Siegler et al. [52]. In doing so, rehabilitation progress could be assessed even more intensively. Parameters such as Range of Motion, joint stiffness and force placed on surrounding muscles could be investigated. Chesworth and Vandervoort suggested these factors play an important role in ankle fracture rehabilitation [53].

As a next step, 3D net ankle forces and moments could be estimated from available sensor data. As part of the BRAFO research, all participants were equipped with 1D plantar pressure insoles, a set of 12 IMUs on crucial body parts, instrumented crutches and ForceShoes™ during measurements. Modelling force and moments would make the bulky ForceShoes™, which are not available in an ambulatory rehabilitation setting, obsolete. For a 10-MWT specifically, this chapter showed anteroposterior and vertical force, as well as flexion moments, were most

significant. Vertical force could be estimated using the method of Merrett et al, who subtracted the vertical force of both crutches from the expected force [40]. Flexion moments could be estimated using this vertical force and the centre of pressure obtained from the plantar pressure insoles, as done by DeBerardinis et al. [2].

Finally, tasks could be modelled that are more advanced than walking straight. For example, walking in a figure-eight shape or activities of daily living. In these activities, it is expected shear forces and other moment directions become more important. Mohamed Refai et al. achieved positive outcomes using subject-specific regression models [1]. They constructed 3D force and moment models based on pressure data collected from pressure sensors within the soles, provided by Medilogic®. Additionally, alternative approaches for modelling ankle force and moments were presented by Lee and Park, and Grzesiak et al., who utilised Artificial Neural Networks with IMU data as input. Notably, Long Short-Term Memory (LSTM) networks were introduced as a promising method for gait parameter modeling.

4.5 Conclusion

In this chapter, a novel method for estimating 3D forces and moments in the ankle joint during crutch gait was introduced. This method represents a significant improvement compared to current clinical practices, which typically focus on Z Axis force, known as Partial Weight Bearing. The study involved a comprehensive investigation and comparison of 3D forces and moments in the ankles of four healthy participants and two patients, providing a detailed analysis of both average and maximum values. Moreover, contributions of individual force and moment direction on the resulting force ($\boldsymbol{F_{res}}$) and moment ($\boldsymbol{M_{res}}$) were examined.

The clinically validated ForceShoes™ system acted as the golden standard for precise 3D force and moment measurements. Significant differences in walking patterns between the impaired and non-impaired ankles were revealed. Anteroposterior and vertical force as well as flexion moments appeared to be most important both in magnitude and contribution $\boldsymbol{F_{res}}$ and $\boldsymbol{M_{res}}$ in a 10-MWT. Inversion moments significantly influenced the resulting moment ($\boldsymbol{M_{res}}$), emphasising their importance in the biomechanics of crutch walking. Nonetheless, the vector magnitude remained minimal. The extensive analysis of 3D forces and moments revealed this interplay and clearly demonstrated the added value compared to focussing on PWB only.

Healthy subjects were unable to reproduce the walking pattern of an actual ankle fracture. While patient 1 failed to comply with the vertical force PWB prescription, both patients kept their plantarflexion moment in the allowed range. Despite PWB as a clinical measure missing crucial information on anteroposterior force and flexion moment, it remains a practical measure in a rehabilitation setting. Future research should focus on investigating and modelling 3D force and moments in more varied tasks.

IV. General Discussion

Chapter 5

Discussion And Conclusion

The first objective of the study was to design and validate an ambulatory 3D net force measurement setup to be used on ankle fracture patients. The second objective was to use this system to compare 3D force and moment on impaired and non-impaired ankles with the current clinical practice of partial weight bearing (PWB). Measurements were performed on four healthy subjects and two ankle fracture patients.

The proposed system gives more information than currently used methods for patients walking with crutches [19, 20, 39, 40]. In these approaches only Ground Reaction Forces (GRFs) on the crutch in known, however, measuring force on the ankle joint is dependent on force plates or inaccurate estimations. Additionally, moments on the foot were not considered at all. The system developed in this study allows for accurate measurements of crutch GRFs and net ankle joint force and moment in an ambulatory setting. This makes it possible to monitor load and gait patterns during rehabilitation after an ankle fracture.

Smeeing and colleagues emphasised the need for close monitoring of ankle loading in case of early weight-bearing [4, 27]. Earlier return to work and sports was found when performing weight-bearing earlier than the currently used six-week immobilisation period. Rehabilitation after an ankle fracture mainly takes place at home, giving challenges for close monitoring. The BRAFO (Balanced Rehabilitation after an Ankle Fracture Operation) project focuses on developing such a measurement system. Its primary objective is to develop and validate a durable and user-friendly system for monitoring load, gait patterns, and balance in patients throughout their daily activities. The system developed and validated in this thesis allows for load monitoring as well as gait patterns, and has the potential to measure balance parameters throughout daily activities.

The current system was verified using force plates and used ForceShoes^{TM} that have been validated in previous research by Van Den Noort and colleagues [48]. Results from the experiments indicated the system's capability to capture force and moment gait patterns in both healthy subjects replicating an ankle fracture and actual ankle fracture patients. It provides an objective method to control the amount of weight-bearing. However, the system still has limitations and cannot be directly employed in real-life home rehabilitation. Nevertheless, new developments could improve the system, potentially allowing people with ankle fractures to return to work and sport at an earlier stage.

5.1 Research Questions

The main goal of this research was to design and validate an ambulatory measurement setup to be used on ankle fracture patients. This system was used to study force and moment characteristics on both the impaired and non-impaired ankles. The current clinical practice of partial weight bearing was compared to the actual 3D force and moment on the ankle. Three research questions were defined to support the goal.

What is the relationship between measurement from the instrumented crutches and presented forces?
The calibration steps outlined in Chapter 2 demonstrated accurate measurements with the ATI 3D Force sensors (ATI Mini 45 SI-580-20, Schunk, Arnhem, NL) in the range of 0 - 260N. The procedure involved converting sensor voltage readings to force by multiplication by a calibration matrix $\boldsymbol{C}$, introducing a scaling factor for each force direction $\boldsymbol{\alpha}$, and applying a rotation to align crutch axes with sensor axes $\boldsymbol{R}$. The force calculation was expressed using the formula $\boldsymbol{F = R\alpha CV}$.

Vertical direction force showed strong correlations with $\boldsymbol{R^2}$-values of 1 Root Mean Square Errors (RMSE) all under 0.5N. Shear force RMSEs were below 2N with $\boldsymbol{R^2}$-values of 1. Offsets were applied to the crutches' amplifiers to prevent clipping of the Analog-to-digital converter. It was found the amplifier remained linear when applying different amplifier offsets, indicating the relationship found remains valid when offsets change. In addition, a rotation angle of 43° was found for the left crutch sensor, and a rotation -22° for the right crutch sensor. Comparable research by Chamorro-Moriana and colleagues reported a comparable $\boldsymbol{R^2}$-value of 0.993 for the force sensor in their forearm crutch [17]. Chamorro-Moriana and colleagues additionally emphasised the mechanical error should remain smaller than 9.81N for the system to be suitable in a patient setting. The sensors with the presented calibration steps met this request. It must be noted, however, that calibration is performed in a static environment, and torque measurements were not calibrated.

How can 3D GRFs be measured using instrumented crutches in combination with an IMU?
The results in Chapter 3 showed the steps involved in the design and validation of instrumented crutches for tracking 3D GRFs in a dynamic setting. The forces measured locally at the crutch tip were converted to a reference system that was defined before every trial. Outcomes were compared to two calibrated force plates (OR6 series, AMTI, Canada) in a gait lab. The presented design used Xsens Awinda IMUs to measure the linear acceleration and angular velocity of the crutches. Before every trial, a sensor-to-segment calibration was performed to make measurements independent of the precise IMU placement. An Error State Kalman Filter (ESKF) was used to track the orientation of both crutches. Sensor calibration as presented in Chapter 2 was used. Finally, the output of the ESKF was used to transform local 3D force measurements to a reference system defined before every trial.

From three dynamic trials, an overall force percentage RMSE of $3.35 \pm 0.31\%$ for the left crutch and $3.44 \pm 0.15\%$ for the right crutch was determined in comparison to force plates. Comparable research by Seylan and Saranlı, who utilised pressure-sensitive sensors, reported an overall force percentage RMSE of $7.62 \pm 1.33\%$ for their instrumented crutch [24]. Notably, this current study made use of industrial force sensors, contributing to its strengths. The low errors in combination with the portable setup allow ambulatory measurements with this system. There are certain limitations to the presented system, however. A level walking surface is required during measurements, and relative errors in the forward-backward direction may originate from

the non-linear behaviour introduced by the rubber crutch tip. Extended measurements exceeding an hour may experience errors of 20N due to temperature drift, as described in Appendix C. The testing range covers 0 - 520N, focusing on a walking scenario. Future research could explore the system's performance in diverse tasks such as walking in a figure-eight shape or engaging in activities of daily living.

What information does 3D net ankle force and moment contain compared to PWB?
A novel method for estimating net 3D forces and moments in the ankle joint during crutch gait was presented in Chapter 4. The instrumented crutches were used in combination with the ForceShoes™ system for measurements on four healthy participants simulating an ankle fracture and two ankle fracture patients. Information provided by the comprehensive 3D measurements was compared to the current clinical measure Partial Weight Bearing (PWB), which only contains information about vertical force. 3D force and moment directions of 10-meter-walking-tests were investigated both in quantity and in contribution to the resulting force ($\boldsymbol{F_{res}}$) and moment ($\boldsymbol{M_{res}}$).

It was concluded vertical forces were the most important component of $\boldsymbol{F_{res}}$, contributing 98% on both the impaired and non-impaired ankles. The plantarflexion and inversion moment accounted for 98% of $\boldsymbol{M_{res}}$ on both ankles during part of the gait, indicating their importance in walking biomechanics. However, the inversion moment remained below 1.53% of body weight height, highlighting the plantarflexion moment as the most crucial information. Anteroposterior force peaked at 15.6% of body weight. While PWB captures vertical force data, it overlooks critical aspects such as the plantarflexion moment and anteroposterior force during 10-meter walking tests.

Furthermore, it was concluded that healthy subjects were unable to replicate the gait observed in actual ankle fracture patients. This includes both quantities of force and moments, as well as timing of peak load during stance. Notably, the patient permitted 25% PWB consistently executed 50% PWB, aligning with previous studies [14,33,34]. Interestingly, both patients managed to maintain their plantarflexion moment within the permitted range. Investigating the connection between exceeding prescribed partial weight-bearing while staying within the accepted plantarflexion moment range would be an interesting topic of future research. Additionally, future research could dive into analysing patterns involving more challenging tasks, such as walking a figure-eight shape or performing activities of daily living. Finally, plantar pressure or IMU-data-based models could be employed to model 3D force and torque, making the bulky ForceShoes™ obsolete.

5.2 Recommendations for Future Work

With the new method proposed for measuring 3D net ankle force and moment, recommendations for future work are discussed.

Potential of Data Set for BRAFO

The protocol and measurements conducted in this thesis were more comprehensive than those examined in the chapters. They contained additional tests involving walking in figure-eight shapes, stepping on a step, and rising from a chair. Furthermore, throughout these measurements, participants and patients wore pressure-sensitive insoles, had IMUs on various body parts, and executed sensor-to-segment calibrations. The inclusion of more patients contributes significantly to the value of this dataset for future research. It serves as a cornerstone for the other BRAFO pillar, focusing on gait characteristics and movement parameters. Additionally, it forms a crucial foundation for estimating 3D ankle forces and moments using biomechanical or data-driven models, making the ForceShoes^{TM} obsolete.

Estimation of 3D Ankle Force and Moment

The thesis did not delve into the estimation of 3D ankle force and moment based on sensor input, despite being thoroughly explored and executed. Two potential approaches exist for this purpose. The biomechanical route involves integrating the crutches into an OpenSim model and using the crutch ground reaction force, with IMUs aiding in estimating segment orientations. Alternatively, the commonly used four-segment model in crutch gait literature could be further explored.

On the data-driven modeling side, the pressure insoles could be leveraged to estimate 3D ankle force and moments. This approach involves employing a linear model that maps the pressure-sensitive areas to the ForceShoes^{TM} data, a method demonstrated by Refai et al. [1]. Neural Networks, specifically Long Short-Term Memory (LSTM) models, are well-suited for direct modeling of 3D force and moments using data from crutches, IMUs, and pressure-sensitive insoles.

Extension of Ankle Models

The ankle model used in this thesis is a simplified representation that considers external forces and moments. More complex ankle models could be used as done in [54] or [55]. Internal forces and moments, as highlighted in [52], could potentially be considerably higher and hold an important role in a comprehensive understanding of recovery. Moreover, enhancing the model by incorporating the metatarsophalangeal joint, situated at the ball of the foot, could be researched to improve its accuracy.

While the BRAFO project primarily focuses on the ankle, future research could consider including the knee and hip in the models. This would make the measurement system applicable to a wider range of fracture types.

Crutch Design

For future research, a redesign of the crutches is advised to guarantee the stability of the system. Moreover, the crutches have the potential to provide more information than is currently the case. 3D moments could be added, as well as 3D velocity and 3D position data using the IMUs. The internal IMU of the crutches could be used, eliminating the need to rely on an external IMU system. Moreover, during revalidation, a patient might transition to using a single crutch, posing new challenges to the system.

5.3 Concluding Remarks

To conclude, this novel approach presents a valuable foundation for novel research in ambulatory crutch gait rehabilitation. The system presented allows for an in-depth analysis of the mechanics of recovery of ankle fracture patients. It is therefore encouraged for future researchers to pursue this direction for studying rehabilitation and early weight-bearing. Hopefully, this thesis will eventually contribute to clinical studies or telemetry practices, aiding patients in achieving faster returns to work, sports, and everyday activities.

Bibliography

[1] Irfan M, Refai M, Van Beijnum BJF, Buurke JH, Veltink PH. Gait and Dynamic Balance Sensing Using Wearable Foot Sensors.

[2] DeBerardinis J, Neilsen C, Lidstone DE, Dufek JS, Trabia MB. A comparison of two techniques for center of pressure
}measurements. Journal of Rehabilitation and Assistive Technologies Engineering. 2020 1;7:205566832092106. Available from: /pmc/articles/PMC7338728//pmc/articles/PMC7338728/?report=abstracthttps://www.ncbi.nlm.nih.gov/pmc/articles/PMC7338728/.

[3] Febrer-Nafría M, Pallarès-López R, Fregly BJ, Font-Llagunes JM. Prediction of three-dimensional crutch walking patterns using a torque-driven model. Multibody System Dynamics. 2021 1;51(1):1-19. Available from: https://link.springer.com/article/10.1007/s11044-020-09751-z.

[4] Smeeing DPJ, Houwert RM, Briet JP, Kelder JC, Segers MJM, Verleisdonk EJMM, et al. Weight-bearing and mobilization in the postoperative care of ankle fractures: a systematic review and meta-analysis of randomized controlled trials and cohort studies. PloS one. 2015 2;10(2). Available from: https://pubmed.ncbi.nlm.nih.gov/25695796/.

[5] Daniel H K Chow M PhD; Chris T K Cheng. Quantitative analysis of the effects of audio biofeedback on weight-bearing characteristics of persons with transtibial amputation during early prosthetic ambulation; 2000. Available from: https://www.rehab.research.va.gov/jour/00/37/3/chow.htm.

[6] Rasouli F, Reed KB. Walking assistance using crutches: A state of the art review. Journal of Biomechanics. 2020 1;98:109489.

[7] Haubert LL, Gutierrez DD, Newsam CJ, Gronley JAK, Mulroy SJ, Perry J. A Comparison of Shoulder Joint Forces During Ambulation With Crutches Versus a Walker in Persons With Incomplete Spinal Cord Injury. Archives of Physical Medicine and Rehabilitation. 2006 1;87(1):63-70.

[8] Daly PJ, Fitzgerald RH, Melton LJ, Llstrup DM. Epidemiology of ankle fractures in Rochester, Minnesota. Acta orthopaedica Scandinavica. 1987;58(5):539-44. Available from: https://pubmed.ncbi.nlm.nih.gov/3425285/.

[9] Jensen SL, Andresen BK, Mencke S, Nielsen PT. Epidemiology of ankle fractures. A prospective population-based study of 212 cases in Aalborg, Denmark. Acta orthopaedica Scandinavica. 1998;69(1):48-50. Available from: https://pubmed.ncbi.nlm.nih.gov/9524518/.

[10] Moseley AM, Beckenkamp PR, Haas M, Herbert RD, Lin CWC, Evans P, et al. Rehabilitation After Immobilization for Ankle Fracture: The EXACT Randomized Clinical

Trial. JAMA. 2015 10;314(13):1376-85. Available from: https://jamanetwork.com/journals/jama/fullarticle/2449186.

[11] Dehghan N, McKee MD, Jenkinson RJ, Schemitsch EH, Stas V, Nauth A, et al. Early weightbearing and range of motion versus non-weightbearing and immobilization after open reduction and internal fixation of unstable ankle fractures: A randomized controlled trial. Journal of Orthopaedic Trauma. 2016 7;30(7):345-52. Available from: https://journals.lww.com/jorthotrauma/Fulltext/2016/07000/Early_Weightbearing_and_Range_of_Motion_Versus.1.aspx.

[12] Schubert J, Lambers KTA, Kimber C, Denk K, Cho M, Doornberg JN, et al. Effect on Overall Health Status With Weightbearing at 2 Weeks vs 6 Weeks After Open Reduction and Internal Fixation of Ankle Fractures. Foot and Ankle International. 2020 6;41(6):658-65. Available from: https://journals.sagepub.com/doi/10.1177/1071100720908853?url_ver=Z39.88-2003&rfr_id=ori%3Arid%3Acrossref.org&rfr_dat=cr_pub++0pubmed.

[13] Gehonoreerde projecten | Technisch Medisch Centrum;. Available from: https://www.utwente.nl/nl/techmed/innovatie/fondsen/pioneers-in-healthcare/gehonoreerde-projecten/#technologie-toepassen-in-de-zorg-vouchers.

[14] Li S, Armstrong CW, Cipriani D. Three-point gait crutch walking: Variability in ground reaction force during weight bearing. Archives of Physical Medicine and Rehabilitation. 2001 1;82(1):86-92.

[15] Utah's Joint Replacement Specialists | Hofmann Arthritis Institute;. Available from: https://hofmannarthritisinstitute.com/.

[16] Sesar I, Zubizarreta A, Cabanes I, Portillo E, Torres-Unda J, Rodriguez-Larrad A. Instrumented Crutch Tip for Monitoring Force and Crutch Pitch Angle. Sensors (Basel, Switzerland). 2019 7;19(13). Available from: /pmc/articles/PMC6650966//pmc/articles/PMC6650966/?report=abstracthttps://www.ncbi.nlm.nih.gov/pmc/articles/PMC6650966/.

[17] Chamorro-Moriana G, Sevillano JL, Ridao-Fernández C. A Compact Forearm Crutch Based on Force Sensors for Aided Gait: Reliability and Validity. Sensors 2016, Vol 16, Page 925. 2016 6;16(6):925. Available from: https://www.mdpi.com/1424-8220/16/6/925/htmhttps://www.mdpi.com/1424-8220/16/6/925.

[18] ATI Industrial Automation: F/T Sensor mini45;. Available from: https://www.ati-ia.com/products/ft/ft_models.aspx?id=mini45.

[19] Merrett GV, Ettabib MA, Peters C, Hallett G, White NM. Augmenting Forearm Crutches with Wireless Sensors for Lower Limb Rehabilitation.

[20] Chen YF, Napoli D, Agrawal SK, Zanotto D. Smart Crutches: Towards Instrumented Crutches for Rehabilitation and Exoskeletons-Assisted Walking. Proceedings of the IEEE RAS and EMBS International Conference on Biomedical Robotics and Biomechatronics. 2018 10;2018-August:193-8.

[21] Sardini E, Serpelloni M, Lancini M. Wireless Instrumented Crutches for Force and Movement Measurements for Gait Monitoring. IEEE Transactions on Instrumentation and Measurement. 2015 12;64(12):3369-79.

[22] Bonnet S, Bassompierre C, Godin C, Lesecq S, Barraud A. Calibration methods for inertial and magnetic sensors. Sensors and Actuators A: Physical. 2009 12;156(2):302-11.

[23] Roetenberg D, Luinge HJ, Baten CTM, Veltink PH. Compensation of magnetic disturbances improves inertial and magnetic sensing of human body segment orientation. IEEE Transactions on Neural Systems and Rehabilitation Engineering. 2005 9;13(3):395-405.

[24] Seylan Saranli U. Estimation of ground reaction forces using low-cost instrumented forearm crutches. IEEE Transactions on Instrumentation and Measurement. 2018 6;67(6):1308-16.

[25] Brescianini D, Jung JY, Jang IH, Park HS, Riener R. INS/EKF-based stride length, height and direction intent detection for walking assistance robots. IEEE International Conference on Rehabilitation Robotics. 2011.

[26] Zhang R, Hoflinger F, Reind LM. Calibration of an IMU using 3-D rotation platform. IEEE Sensors Journal. 2014;14(6):1778-87.

[27] Smeeing DPJ, Houwert RM, Briet JP, Groenwold RHH, Lansink KWW, Leenen LPH, et al. Weight-bearing or non-weight-bearing after surgical treatment of ankle fractures: a multicenter randomized controlled trial. European journal of trauma and emergency surgery : official publication of the European Trauma Society. 2020 2;46(1):121-30. Available from: https://pubmed.ncbi.nlm.nih.gov/30251154/.

[28] Arif GUL, Batra S, Mehmood S, Gillham N. Immediate unprotected weight-bearing of operatively treated ankle fractures. Acta Orthopaedica Belgica. 2007 6;73(3):360-5. Available from: https://europepmc.org/article/med/17715727.

[29] Thomas G, Whalley H, Modi C. Early mobilization of operatively fixed ankle fractures: A systematic review. Foot and Ankle International. 2009 7;30(7):666-74.

[30] Cimino W, Ichtertz D, Slabaugh P. Early mobilization of ankle fractures after open reduction and internal fixation. Clinical orthopaedics and related research. 1991;267:152-6.

[31] Lee JU, Kim MY, Kim JH, Lee JA, Yoon NM, Hwang BY, et al. Analysis of Plantar Foot Pressure during the Non-crutch, Two-point, and Four-point Crutch Gait performed by Healthy Volunteers. Journal of Physical Therapy Science. 2011;23(3):489-93.

[32] Bril AT, David V, Scherer M, Jagos H, Kafka P, Sabo A. Development of a Wearable Live-feedback System to Support Partial Weight-bearing While Recovering From Lower Extremity Injuries. Procedia Engineering. 2016 1;147:157-62.

[33] Warren C, Lehmann J. Training procedures and biofeedback methods to achieve controlled partial weight bearing: an assessment. Archives of physical medicine and rehabilitation. 1975.

[34] Winstein CJ, Pohl PS, Cardinale C, Green A, Scholtz L, Waters CS. Learning a partial-weight-bearing skill: effectiveness of two forms of feedback. Physical therapy. 1996;76(9):985-93. Available from: https://pubmed.ncbi.nlm.nih.gov/8790276/.

[35] Stallard J, Sankarankutty M, Rose GK. Lower-limb vertical groundreaction forces during crutch walking. Journal of Medical Engineering & Technology. 1978;2(4):201-2.

[36] Stallard J, Dounis E, Major RE, Rose GK. One leg swing through gait using two crutches. An analysis of the ground reaction forces and gait phases. Acta orthopaedica Scandinavica. 1980;51(1):71-7. Available from: https://pubmed.ncbi.nlm.nih.gov/7376848/.

[37] Liu J, Lockhart TE. Role of Ankle Joint in Successful Reactive-Recovery: A 3D Joint Moment Analysis. http://dxdoiorg/101177/154193120404801238. 2004 9;48(12):1444-8. Available from: https://journals.sagepub.com/doi/10.1177/154193120404801238?icid=int.sj-abstract.similar-articles.2.

[38] Kim Y, Lee KM, Koo S. Joint moments and contact forces in the foot during walking. Journal of Biomechanics. 2018 6;74:79-85.

[39] Sardini E, Serpelloni M, Lancini M, Pasinetti S. Wireless Instrumented Crutches for Force and Tilt Monitoring in Lower Limb Rehabilitation. Procedia Engineering. 2014 1;87:348-51.

[40] Merrett GV, Peters C, Hallet G, White NM. An instrumented crutch for monitoring patients' weight distribution during orthopaedic rehabilitation. Procedia Chemistry. 2009 9;1(1):714-7.

[41] Winter DA. Biomechanics and Motor Control of Human Movement: Fourth Edition. Biomechanics and Motor Control of Human Movement: Fourth Edition. 2009 9;7:1-370. Available from: https://onlinelibrary.wiley.com/doi/book/10.1002/9780470549148.

[42] Schepers HM, Veltink PH. Estimation of ankle moment using ambulatory measurement of ground reaction force and movement of foot and ankle. Proceedings of the First IEEE/RAS-EMBS International Conference on Biomedical Robotics and Biomechatronics, 2006, BioRob 2006. 2006;2006:399-401.

[43] Schepers HM, Koopman HFJM, Veltink PH. Ambulatory assessment of ankle and foot dynamics. IEEE Transactions on Biomedical Engineering. 2007 5;54(5):895-902.

[44] Hof AL. An explicit expression for the moment in multibody systems. Journal of Biomechanics. 1992 10;25(10):1209-11.

[45] Holder J, Trinler U, Meurer A, Stief F. A Systematic Review of the Associations Between Inverse Dynamics and Musculoskeletal Modeling to Investigate Joint Loading in a Clinical Environment. Frontiers in Bioengineering and Biotechnology. 2020 12;8:603907.

[46] Hashizume S, Iwanuma S, Akagi R, Kanehisa H, Kawakami Y, Yanai T. In vivo determination of the Achilles tendon moment arm in three-dimensions. Available from: www.elsevier.com/locate/jbiomech.

[47] Weir MD, Hass J, Giordano FR, Based on (work): Thomas GB, Updated edition of (work) : Weir MD. Thomas' calculus : early transcendentals. 2008:1. Available from: https://www.worldcat.org/title/71173934.

[48] Van Den Noort J, Van Der Esch M, Steultjens MP, Dekker J, Schepers M, Veltink PH, et al. Influence of the instrumented force shoe on gait pattern in patients with osteoarthritis of the knee. Medical & Biological Engineering & Computing. 2011 12;49(12):1381-92. Available from: https://researchinformation.amsterdamumc.org/en/publications/influence-of-the-instrumented-force-shoe-on-gait-pattern-in-patie.

[49] Veltink PH, Liedtke C, Droog E, Van Der Kooij H. Ambulatory measurement of ground reaction forces. IEEE Transactions on Neural Systems and Rehabilitation Engineering. 2005 9;13(3):423-7.

[50] Sado N, Shiotani H, Saeki J, Kawakami Y. Positional difference of malleoli-midpoint from three-dimensional geometric centre of rotation of ankle and its effect on ankle joint kinetics. Gait & Posture. 2021 1;83:223-9.

[51] Plagenhoef S, Gaynor Evans F, Abdelnour T. Anatomical Data for Analyzing Human Motion. Research Quarterly for Exercise and Sport. 1983;54(2):169-78. Available from: https://www.tandfonline.com/doi/abs/10.1080/02701367.1983.10605290.

[52] Siegler S, Moskowitz GD, Freedman W. Passive and active components of the internal moment developed about the ankle joint during human ambulation. Journal of Biomechanics. 1984 1;17(9):647-52.

[53] Chesworth BM, Vandervoort AA. Comparison of Passive Stiffness Variables and Range of Motion in Uninvolved and Involved Ankle Joints of Patients Following Ankle Fractures. Physical Therapy. 1995 4;75(4):253-61. Available from: https://dx.doi.org/10.1093/ptj/75.4.253.

[54] Leardini A, O'Connor JJ, Catani F, Giannini S. A geometric model of the human ankle joint. Journal of Biomechanics. 1999 6;32(6):585-91.

[55] Sikidar A, Kalyanasundaram D. An open-source OpenSim® ankle-foot musculoskeletal model for assessment of strains and forces in dense connective tissues. Computer Methods and Programs in Biomedicine. 2022 9;224:106994.

[56] Elwenspoek M, Wiegerink R. Mechanical Microsensors. 2001. Available from: http://link.springer.com/10.1007/978-3-662-04321-9.

[57] Faber GS, Chang CC, Kingma I, Martin Schepers H, Herber S, Veltink PH, et al. A force plate based method for the calibration of force/torque sensors. Journal of biomechanics. 2012 4;45(7):1332-8. Available from: https://research.utwente.nl/en/publications/a-force-plate-based-method-for-the-calibration-of-forcetorque-sen.

[58] Russo A, Reginelli A, Zappia M, Rossi C, Fabozzi O, Cerrato M, et al. Ankle fracture: Radiographic approach according to the Lauge-Hansen classification. Musculoskeletal Surgery. 2013 8;97(SUPPL. 2):155-60. Available from: https://link.springer.com/article/10.1007/s12306-013-0284-x.

[59] The Radiology Assistant : Weber and Lauge-Hansen Classification;. Available from: https://radiologyassistant.nl/musculoskeletal/ankle/weber-and-lauge-hansen-classification#short-overview-weber-and-lauge-hansen-summary.

[60] The Radiology Assistant : Algoritm for Ankle Fractures 2.0;. Available from: https://radiologyassistant.nl/musculoskeletal/ankle/fractures-video-lesson-1.

Appendix A

Additional Gait Graphs

A.1 Sum Impaired and Crutches

Force in the vertical direction of three healthy participants and patient 2. Plots are zoomed in on one trial for each participant. The sum of both crutches and the impaired ankle approach 100% BW during a step.

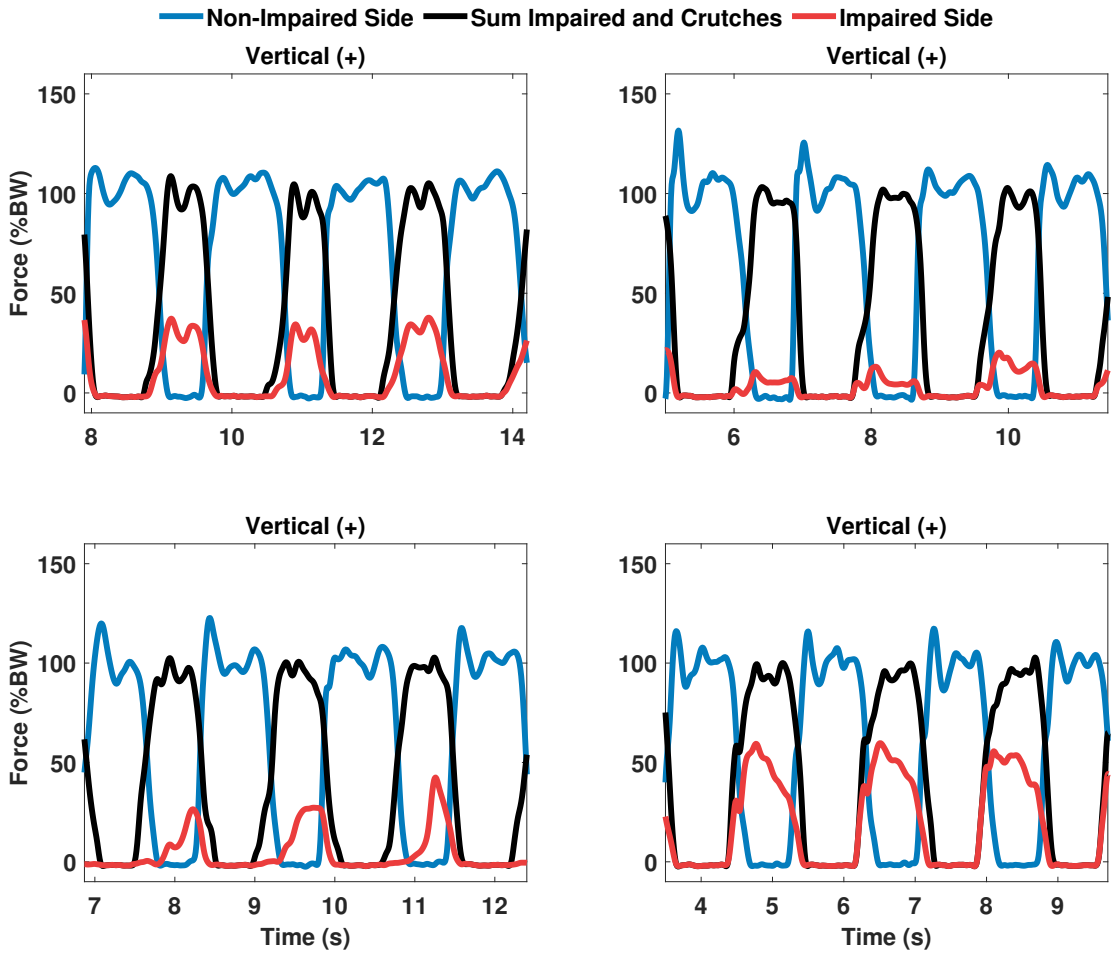

Figure A.1: **Top left:** Healthy person 1. **Top right:** Healthy person 3. **Bottom left:** Healthy person 4. **Bottom right:** Patient 2.

A.2 Averaged Gait Cycles

Figure A.2 to A.4 show time-normalised gait cycles of 3D force and moment at the ankle of three healthy participants.

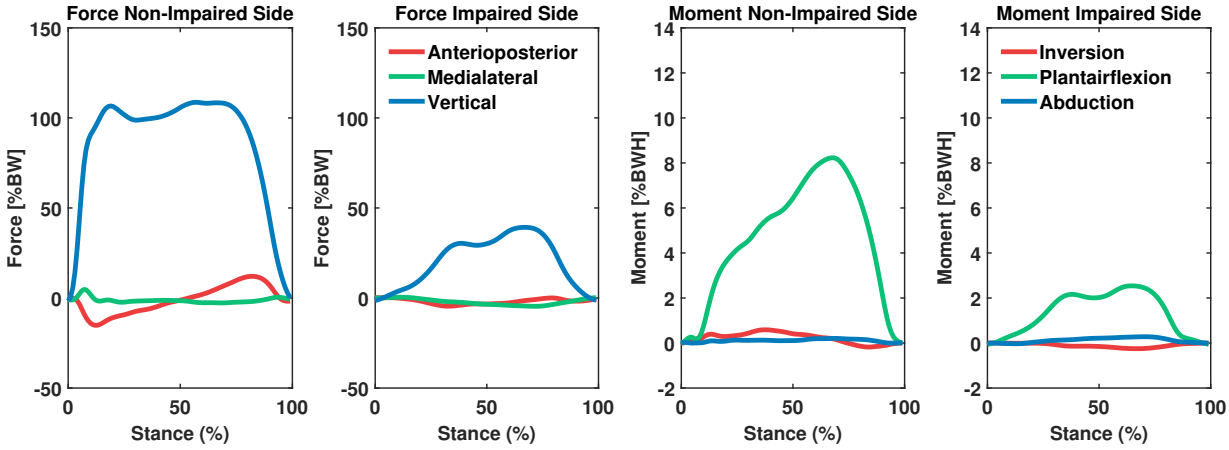

Figure A.2: **Healthy participant.** Averaged gait cycles of healthy participant. The right ankle was the impaired side. The task was a 10-MWT. The two left images are forces and the two right are moments.

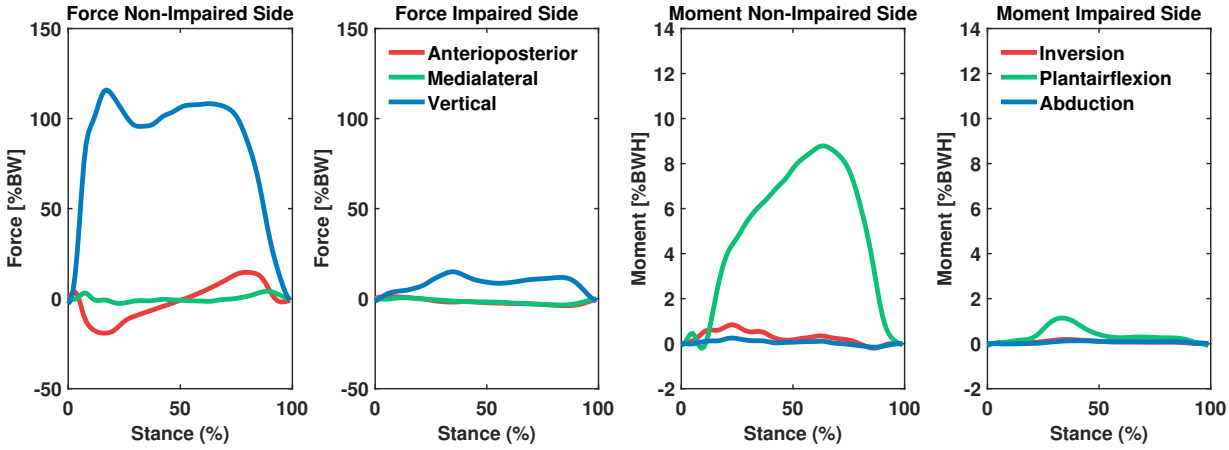

Figure A.3: **Healthy participant.** Averaged gait cycles of healthy participant. The right ankle was the impaired side. The task was a 10-MWT. The two left images are forces and the two right are moments.

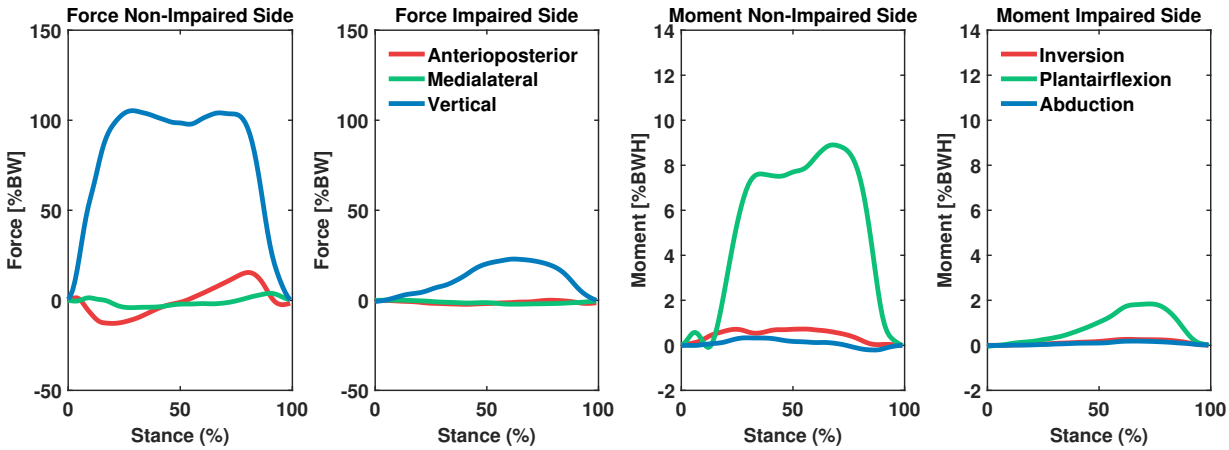

Figure A.4: **Healthy participant.** Averaged gait cycles of healthy participants. The right ankle was the impaired side. The task was a 10-MWT. The two left images are forces and the two right are moments.

A.3 Individual 3D Force and Moments Plots

Figure A.5 to A.8 show the force at the ankle joint during a 10-MWT.

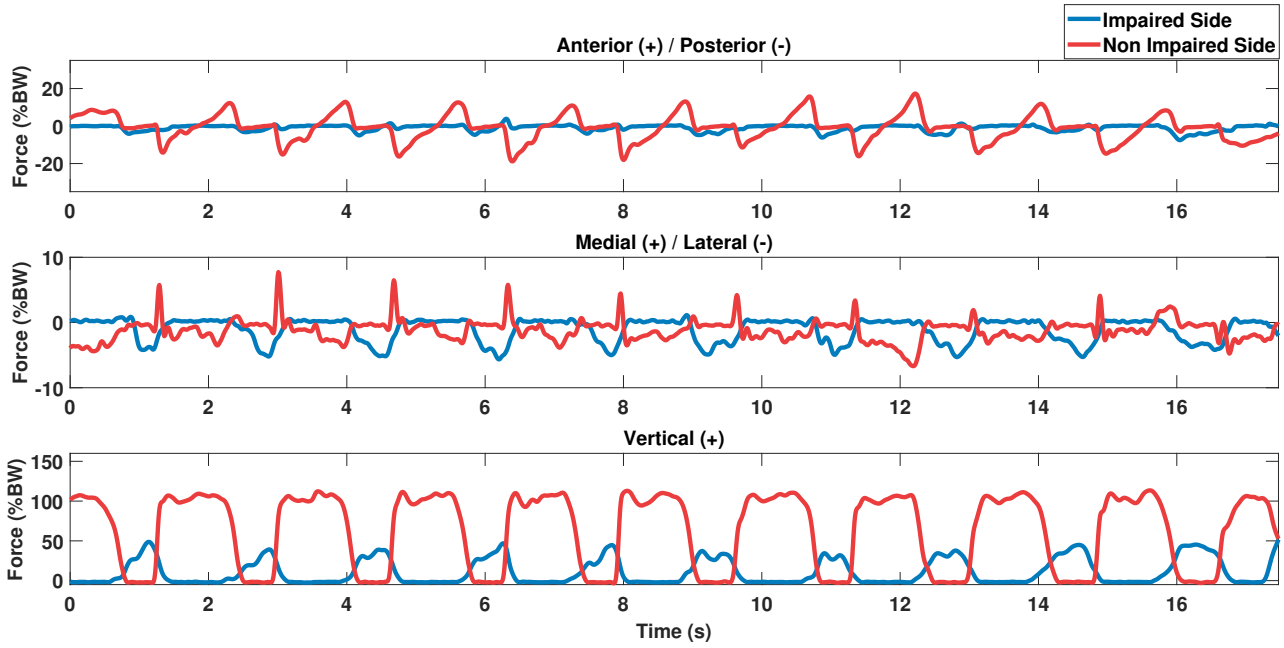

Figure A.5: **Healthy participant 1**. Forces of a healthy person, imitating an impaired right ankle.

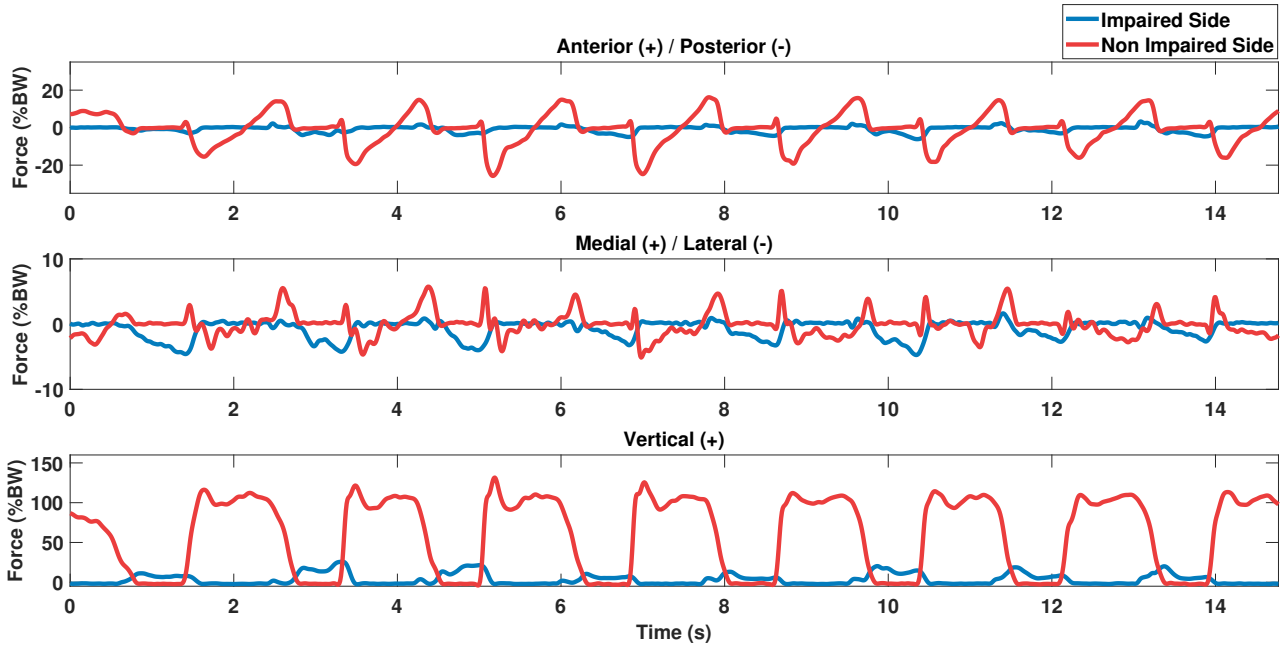

Figure A.6: **Healthy participant 2**. Forces of a healthy person, imitating an impaired right ankle.

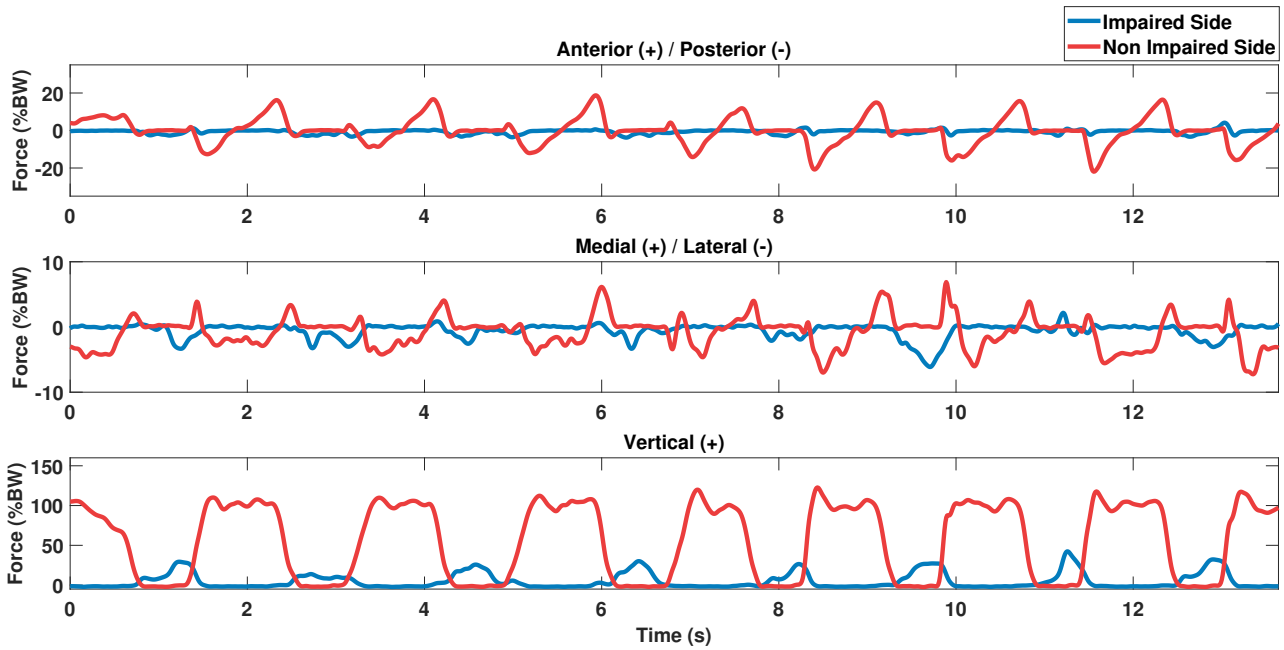

Figure A.7: **Healthy participant 3**. Forces of a healthy person, imitating an impaired right ankle.

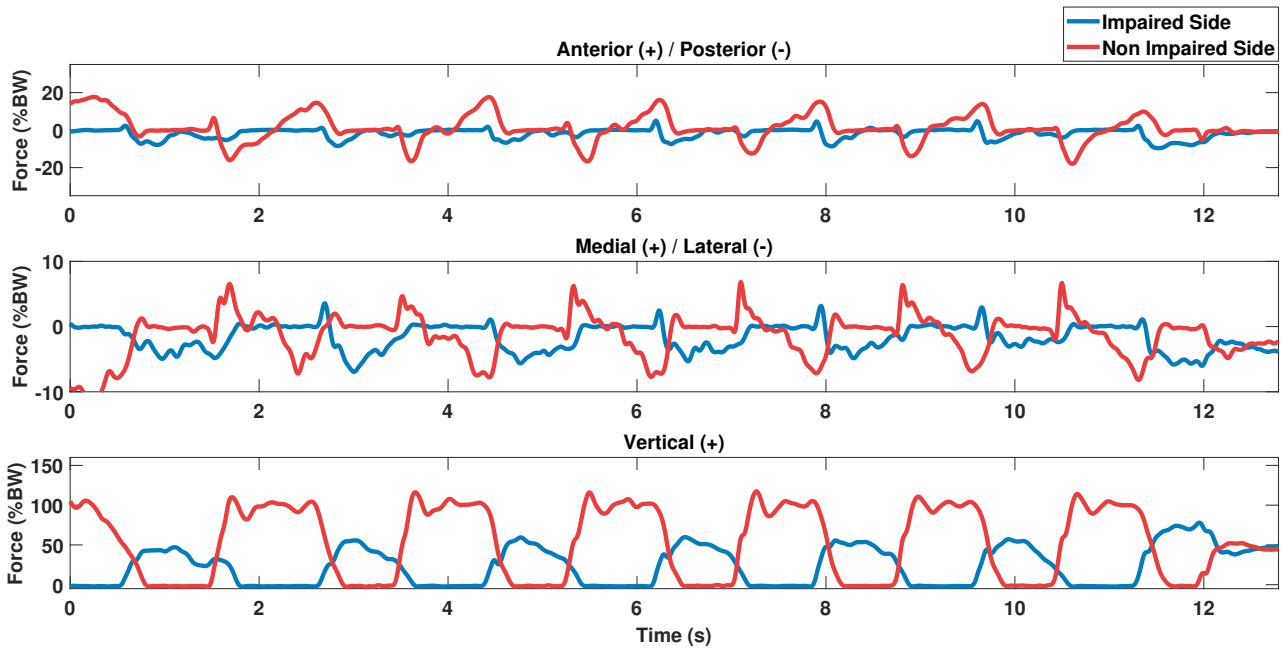

Figure A.8: **Healthy participant 4**. Forces of a healthy person, imitating an impaired right ankle.

Figure A.9 to A.12 show the moments at the ankle joint during a 10-MWT.

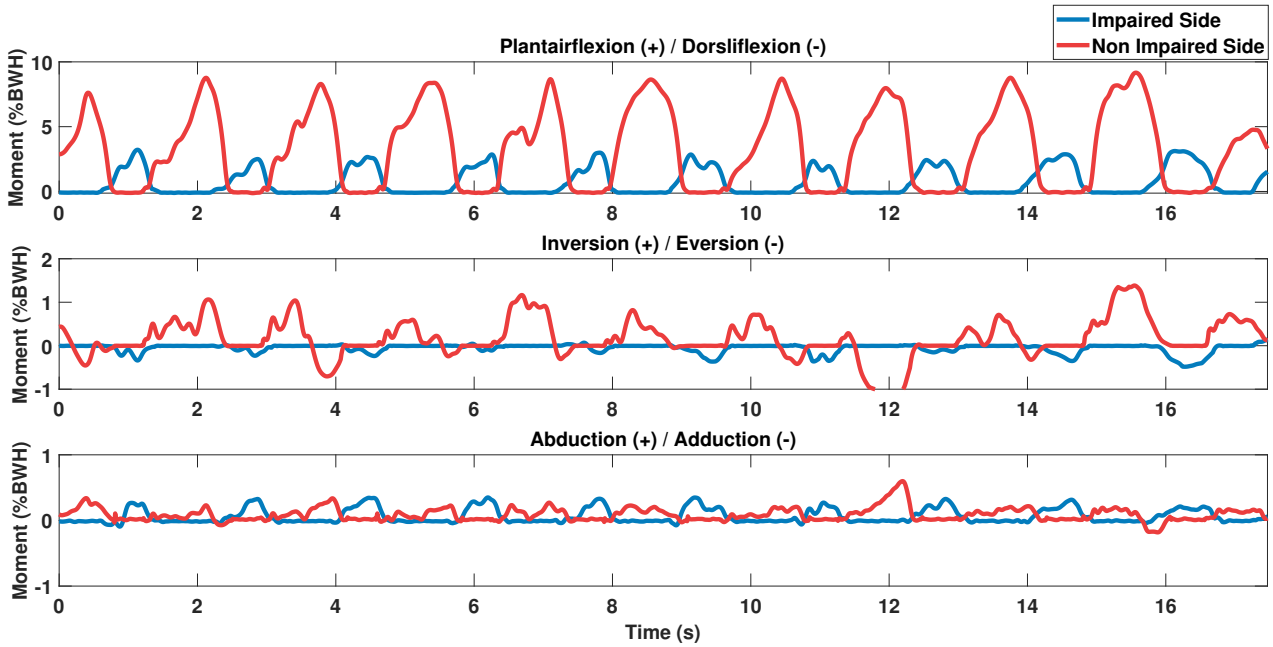

Figure A.9: **Healthy participant 1**. Moments of a healthy person, imitating an impaired right ankle.

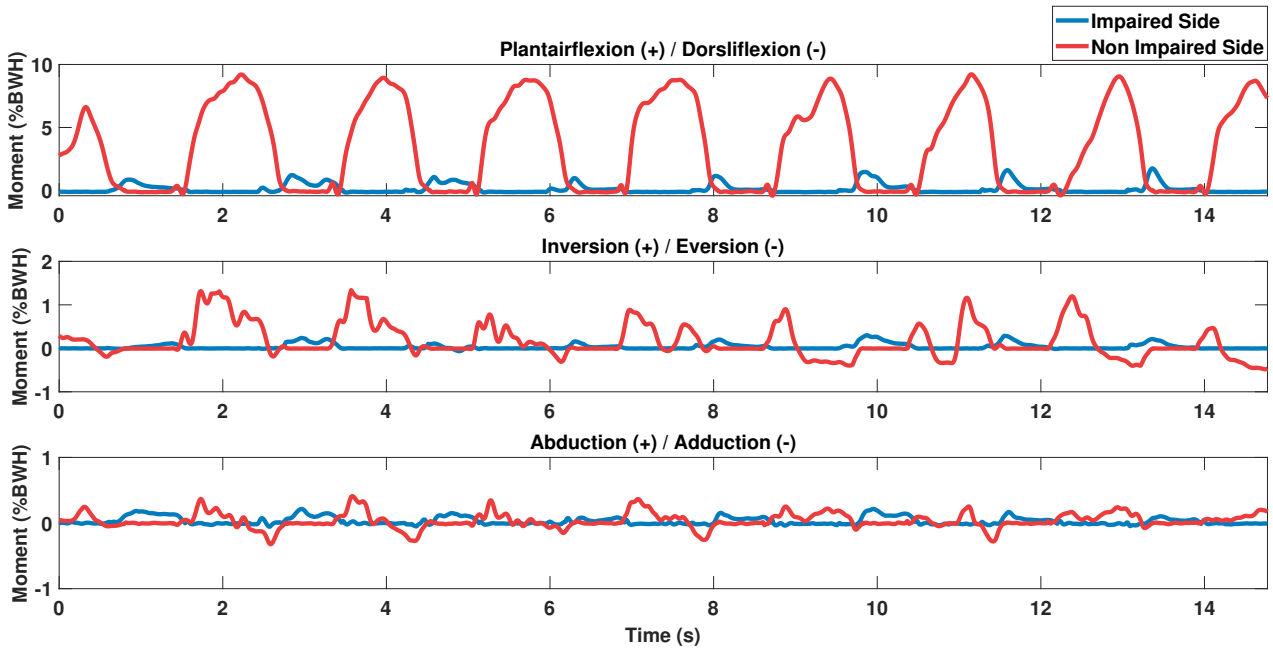

Figure A.10: **Healthy participant 2**. Moments of a healthy person, imitating an impaired right ankle.

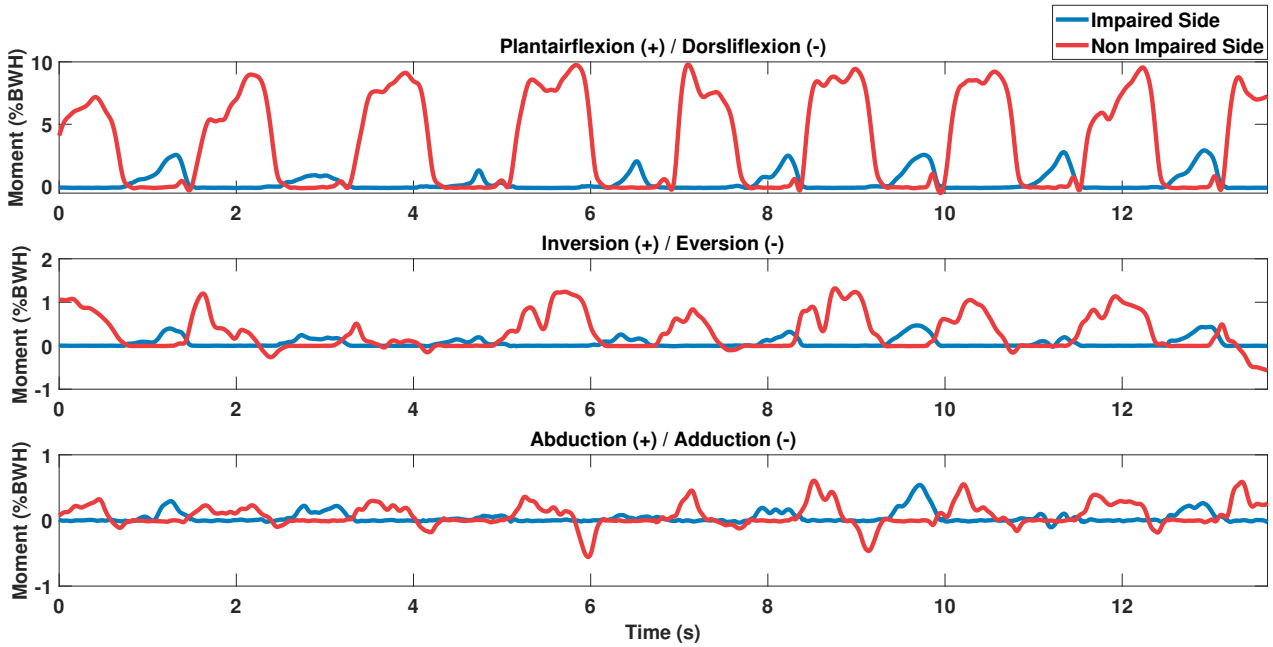

Figure A.11: **Healthy participant 3**. Moments of a healthy person, imitating an impaired right ankle.

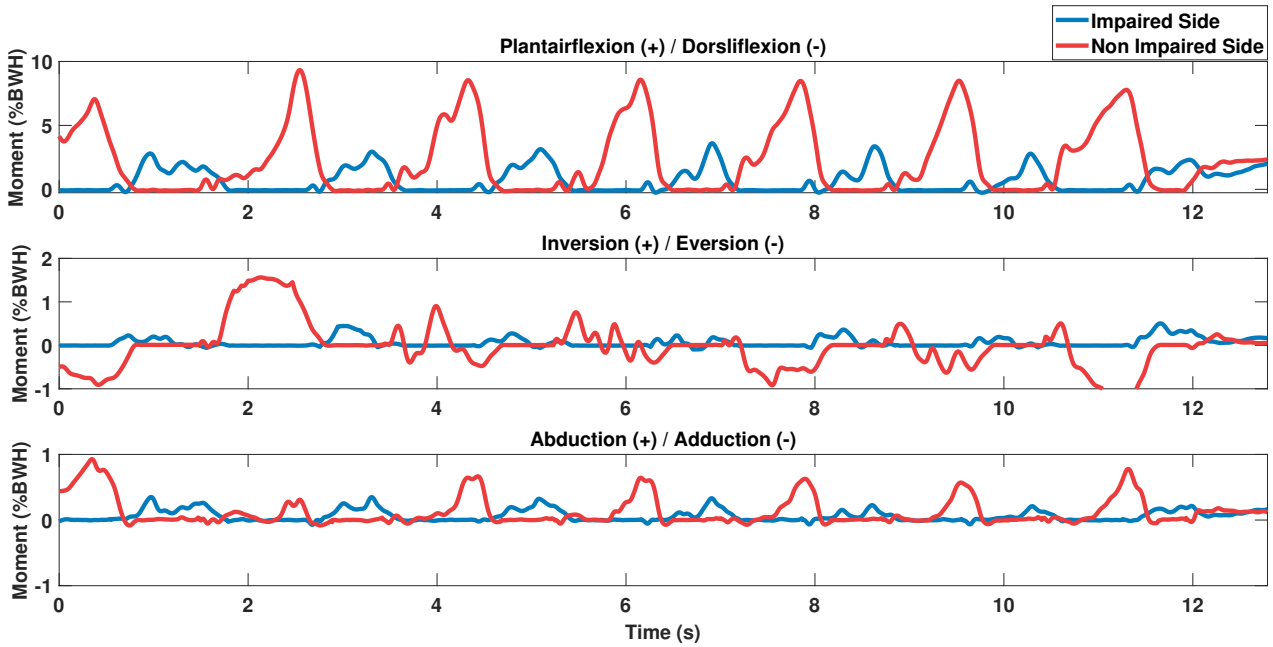

Figure A.12: **Healthy participant 4**. Moments of a healthy person, imitating an impaired right ankle.

Figure A.13 to A.16 show the 3D forces on the crutches of healthy participants during a 10 MWT.

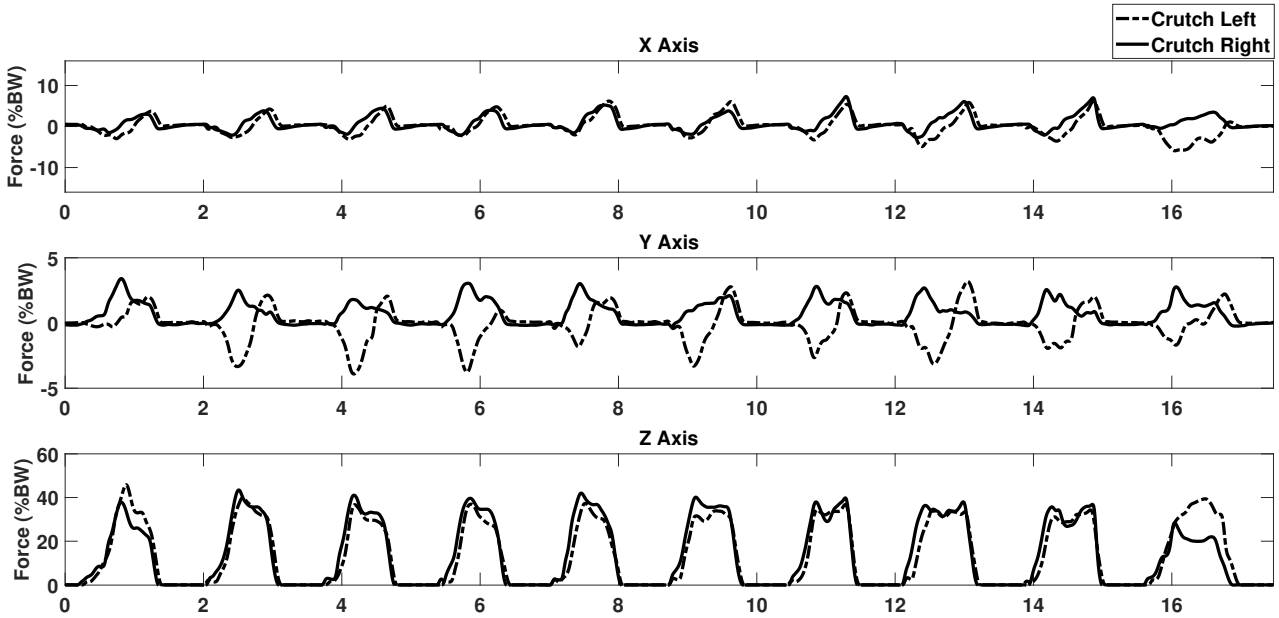

Figure A.13: **Healthy participant 1**. Forces of a healthy person, imitating an impaired right ankle.

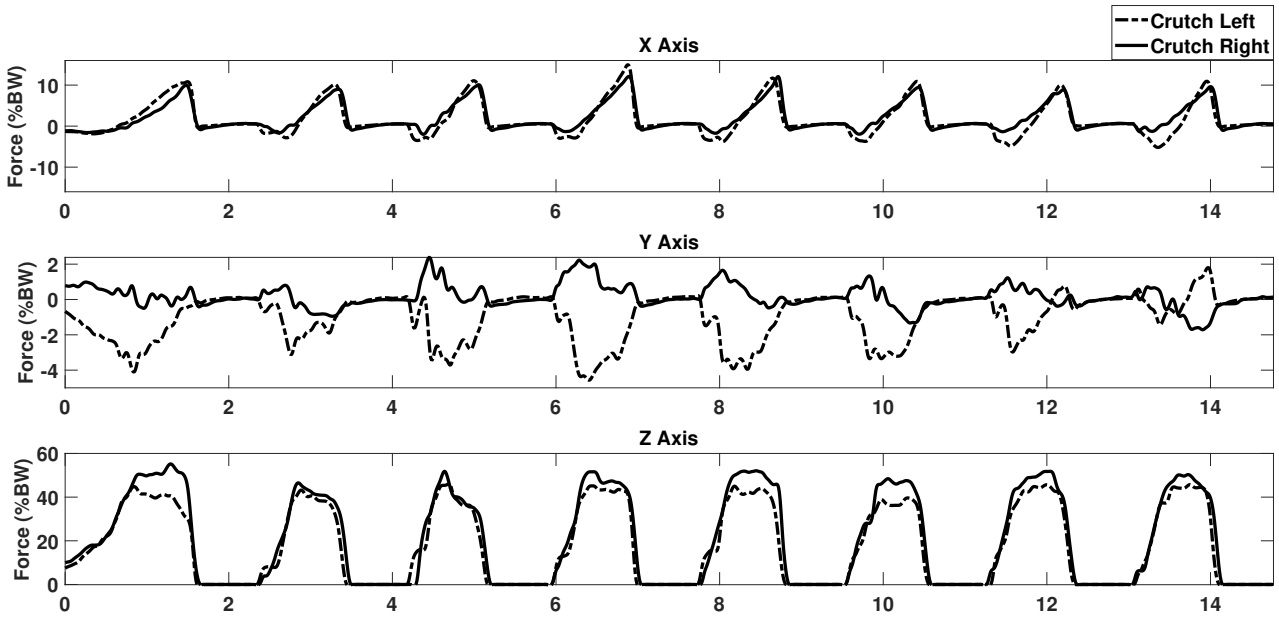

Figure A.14: **Healthy participant 2**. Forces of a healthy person, imitating an impaired right ankle.

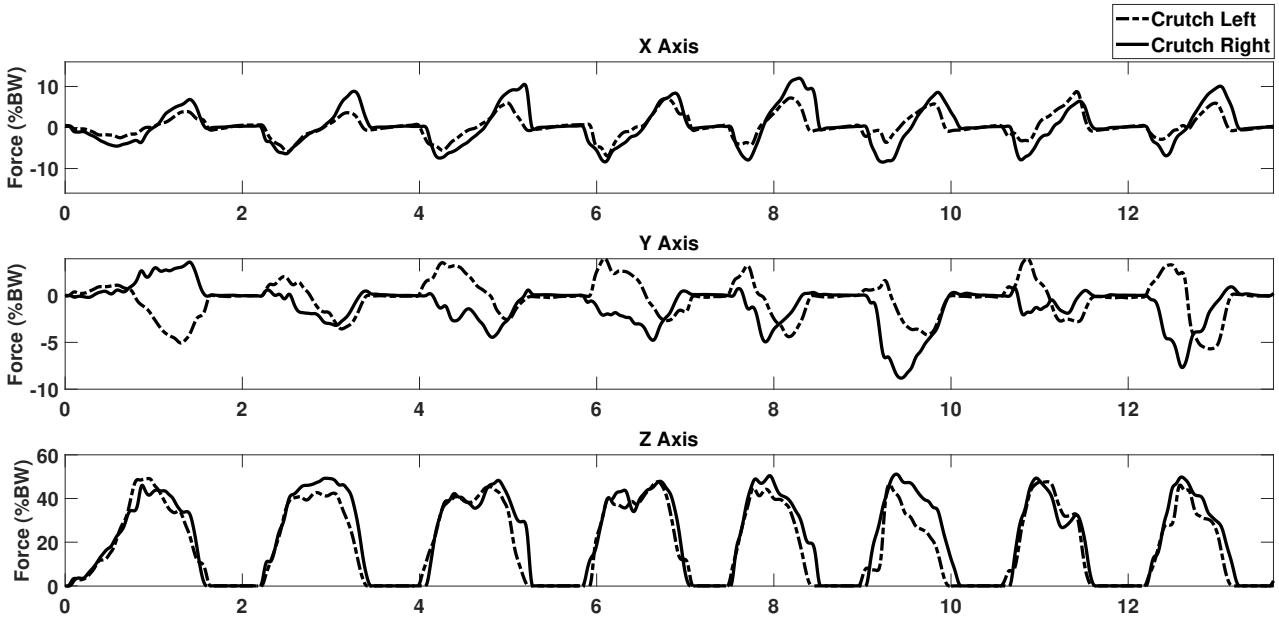

Figure A.15: **Healthy participant 3**. Forces of a healthy person, imitating an impaired right ankle.

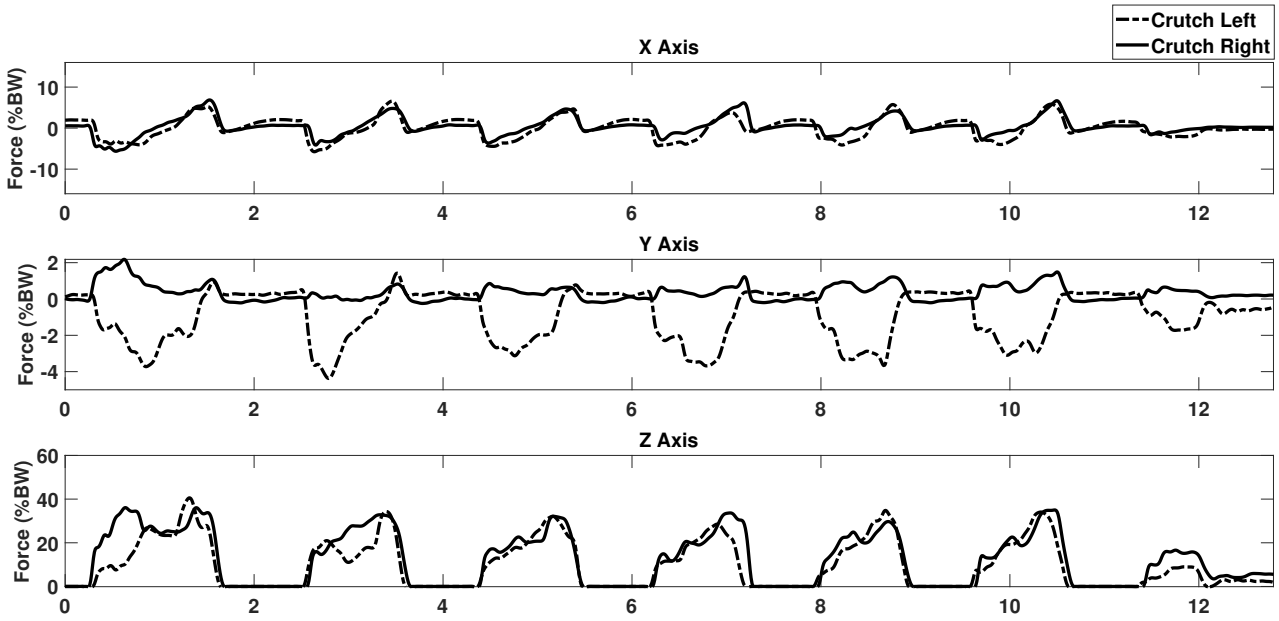

Figure A.16: **Healthy participant 4**. Forces of a healthy person, imitating an impaired right ankle.

Appendix B

Crutch Hardware Design And User Manual

CONTRIBUTION TO MEDICAL DOCUMENTS FOR PHASE II MEASUREMENTS

The instrumented crutches are shown in figure B.1. These prototypes are equipped with Force-Torque (FT) sensors to measure forces and torques present at the crutch tip. Additionally, a 3D Inertial Measurement Unit (IMU) is present on every crutch to measure motion and orientation. An electric circuit board manages the data streams and wireless transmission. Transmission is done via Bluetooth and power is supplied by a rechargeable Li-ion battery. The wirelessly transmitted data is stored locally on a PC.

Sensing Capabilities
Two regular forearm crutches were cut just above the crutch tip and a force torque (FT) sensor was placed in between, as seen in figure B.1. ATI mini 45 FT sensors of type SI-580-20 are used, with six silicon half-bridge strain gauges. The FT18679 in the left crutch and FT05489 in the right crutch. The mini 45 has a total of eight connection wires, one ground, one supply connected to the reference voltage, and six signal lines. A DIN connector with screw mount is used to connect the sensor to an amplifier. Specifications of the ATI mini 45 are found in table B.1.
Both crutches are equipped with a MEMS IMU to keep track of movements. An MPU9250 IMU Breakout PCB is used, which measures linear acceleration, angular acceleration and magnetic data in three axes. The full scale range of the accelerometer can be manually set to ±2g, ±4g, ±8g or ±16g at 16 bit. Gyroscope range can be manually set to a full scale range of ±250°/s, ±500°/s, ±1000°/s or ±2000°/s at 16 bit. The magnetometer has a range of ±4800uT. A temperature sensor with a range of -40 to 85 °C is present for offset calibration. In the design, the magnetometer is disabled and ranges of the accelerometer and gyroscope are set to ±16g and ±2000°/s respectively.

Hardware Architecture
An ESP32-E microcontroller of DFRobot is used. Readings from the FT sensor are lowpass filtered by a first-order filter (f_c = 234 Hz) to prevent aliasing. A custom-made force amplifier is used, where all six channels of the FT sensor are separately amplified by a INA333 instrumentation amplifier (InAmp). Sensor readings are linked to the non-inverting input of the InAmp. The inverting input is linked to a Digital-to-Analogue converter (DAC) that allows the user to apply voltage offsets. Applying offsets changes the baseline level output of the InAmp when the FT sensor is unloaded. An Analogue-to-Digital converter (ADC) is placed after the six InAmps. It has a range between 0 and 2.7V and to stay in this range, voltage offsets of the InAmps can be set.

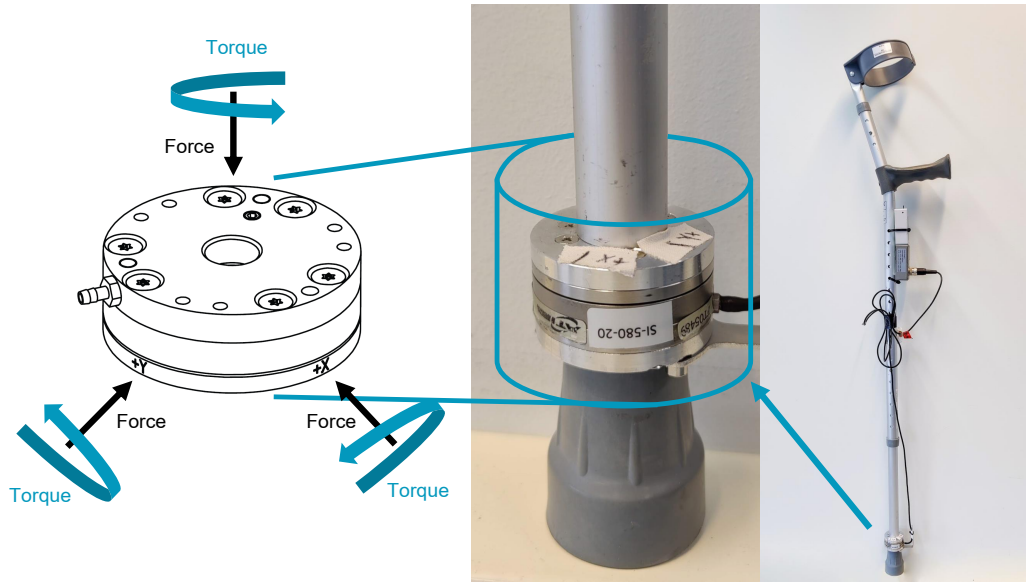

Figure B.1: Overview of an instrumented crutch and the 6 DOF force torque sensor. An ATI Mini 45 force-torque sensor is used. Internal axes of the FT sensor do not match the orientation on a crutch and therefore need to be determined.

Table B.1: Metric specifications of ATI Mini 45 SI-580-20. Adapted from [18].

Fx,Fy	**Fz**	**Tx, Ty**	**Tz**	**Fx, Fy**	**Fz**	**Tx, Ty**	**Tz**
580 N	1160 N	20 Nm	20 Nm	1/4 N	1/4 N	1/188 Nm	1/376 Nm
Sensing range				Resolution			

The rechargeable internal battery can be charged using USB-C and allows 8.5 hours of use. The ESP32 module runs on C++. The processor unit in the custom made force amp runs on C. Hard-coded voltage offsets to the inverting input of the InAmps can be set here. A Python script is used to wirelessly connect the crutches to a PC and transfer data. When starting the script, the battery voltage of the internal battery is shown. In addition, voltage offsets can be sent to temporally overwrite the hard-coded set offsets.

Force torque sensor

The ATI Mini 45 FT sensor uses six silicon strain gauges. Specifications can be found in table **??**. When the silicon deforms, resistance of the strain gauges changes which is read out as a change in voltage. As a load is placed on the sensor, compressive strain is put on a member of a gauge pair, while an equal tensile strain is put on the other member. See figure B.2 for an overview of the transducer equivalent schematic. As the strain gauges are not placed in an orthogonal axis system, a 6x6 calibration matrix is needed to transform the voltages to forces. Image B.3 shows the basic principle of force measurements, where there is always a step in between needed to go from the force domain to the electric domain.

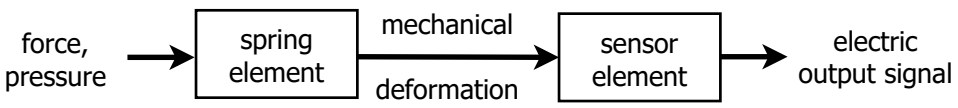

Figure B.3: Basic principle of force measurements. Adapted from [56].

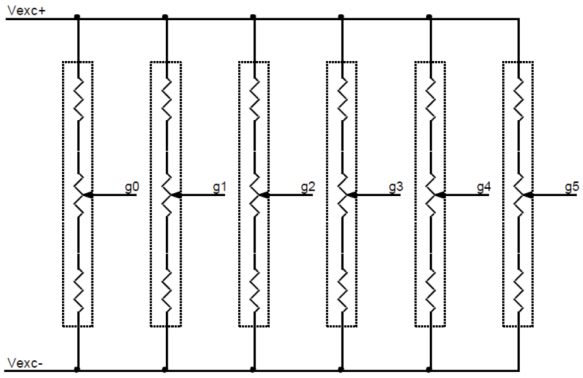

Figure B.2: Strain gauge transducer equivalent schematic. A total of six strain gauges is used. Adapted from

A 6x6 matrix is used to convert sensor readings V_0 - V_5 to actual forces. This matrix is specific per sensor and is supplied by the manufacturer. Conversion is done by multiplying the voltages with the matrix:

$$\mathbf{F = C\ V} \tag{B.1}$$

Where **F** is the array of 3D forces and 3D torques, **C** is the 6x6 calibration matrix and **V** are the voltages measured from the strain gauges. Written out:

$$\begin{pmatrix} Fx \\ Fy \\ Fz \\ Tx \\ Ty \\ Tz \end{pmatrix} = \begin{pmatrix} FxG0 & FxG1 & FxG2 & FxG3 & FxG4 & FxG5 \\ FyG0 & FyG1 & FyG2 & FyG3 & FyG4 & FyG5 \\ FzG0 & FzG1 & FzG2 & FzG3 & FzG4 & FzG5 \\ TxG0 & TxG1 & TxG2 & TxG3 & TxG4 & TxG5 \\ TyG0 & TzG1 & TyG2 & TyG3 & TyG4 & TyG5 \\ TzG0 & TzG1 & TzG2 & TzG3 & TzG4 & TzG5 \end{pmatrix} \begin{pmatrix} V_0 \\ V_1 \\ V_2 \\ V_3 \\ V_4 \\ V_5 \end{pmatrix} \tag{B.2}$$

Where $F_{x,y,z}$ are the forces in x, y and z direction and $T_{x,yz}$ are the torques around the x, y and z direction. The specific calibration matrix used in this report for both FT sensors is:

$$C = - \begin{pmatrix} -2.11240 & 32.15269 & 0.96205 & -34.17360 & 0.01723 & 0.30383 \\ -1.95287 & 18.87434 & -0.55920 & 19.27552 & 2.37414 & -36.52639 \\ -19.14735 & 0.85372 & -18.49781 & 0.48799 & -18.97113 & 0.74205 \\ 35.98018 & -1.59886 & -34.23936 & 1.08167 & -0.66967 & -0.06261 \\ 20.57191 & -1.12269 & 19.78786 & -0.61574 & -39.59170 & 1.86745 \\ -1.29831 & 17.79016 & -0.96511 & 18.70644 & -0.77576 & 17.41219]; \end{pmatrix} \tag{B.3}$$

This matrix is originally provided by ATI in 2004 for sensor FT05489, corresponding to the sensor in the right crutch. In this report, this matrix is used for both FT sensors.

Appendix C

ATI MINI 45 Drift

Figure C.1 shows the drift over time of the ATI Mini 34 F/T sensor. Drift is shown per channel in mV over a time of 7.5 hours. The artifact of the drift suddenly going down around 0.3 and 2.6 hours is caused by accidental touches of the crutches.

Remarkable is that the drift continues and stability appears to only be reached after 7 hours of run time.

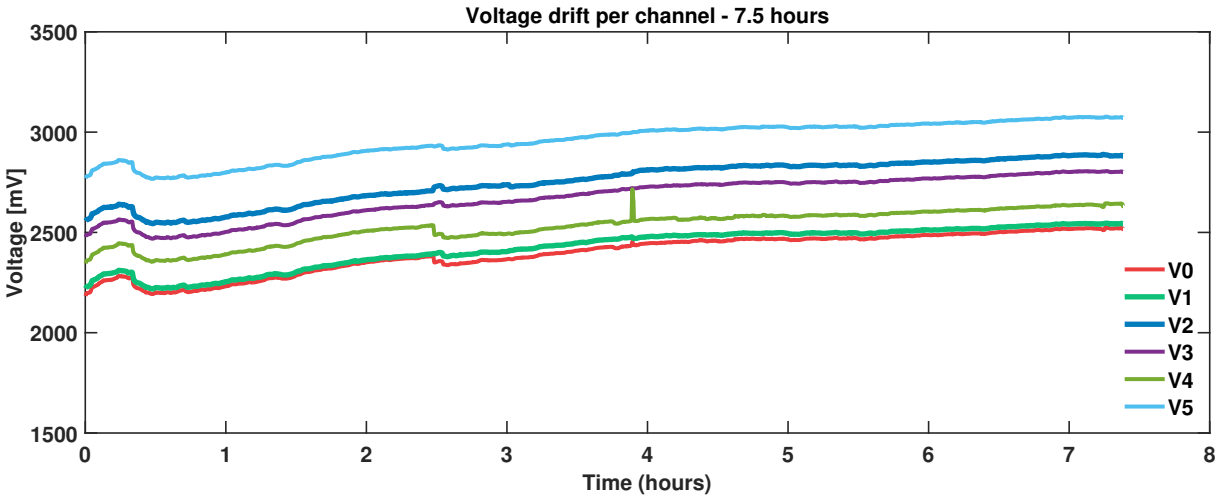

Figure C.1: Voltage drift per channel in a time span of 7.5 hours.

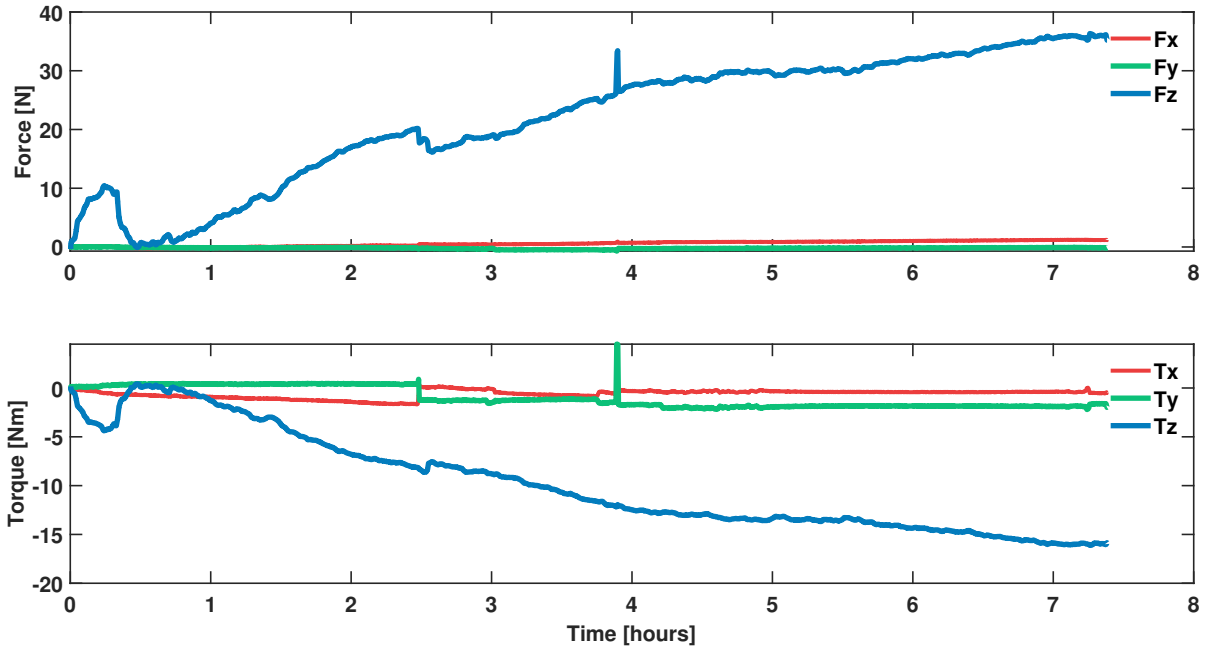

Figure C.2: Force and torque drift per direction in a time span of 7.5 hours.

Figure C.2 shows the drift in terms of force. The drift appears to be steady after 7 hours. The drift effect is 30N in this period.

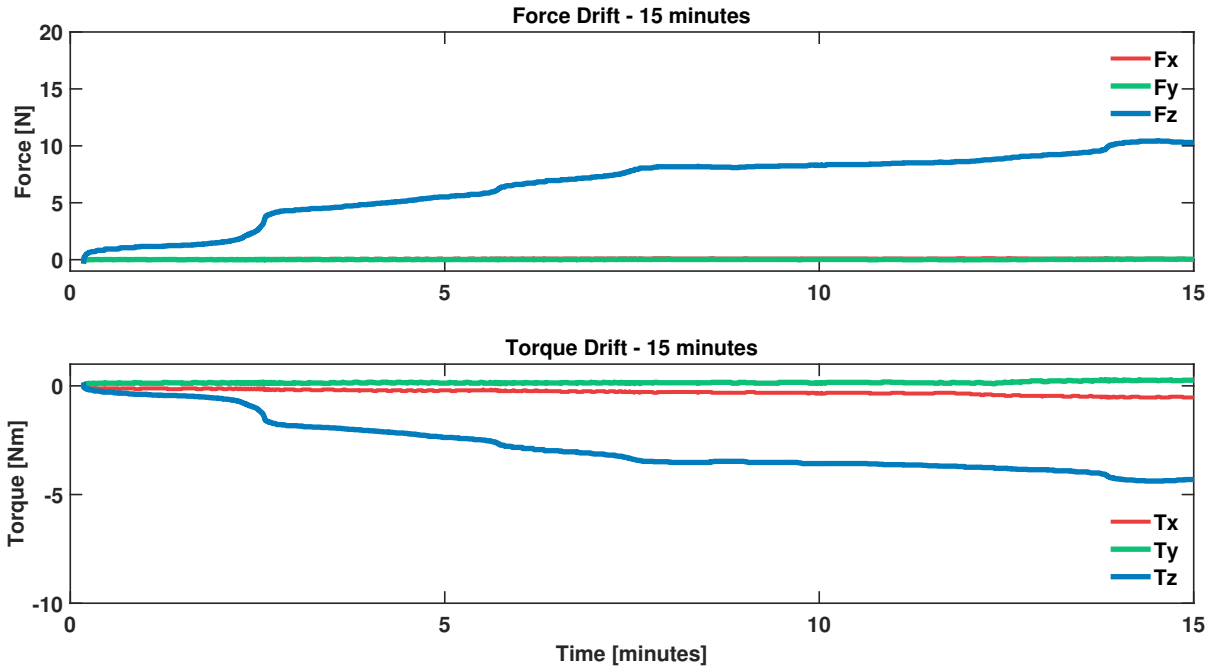

Figure C.3: Force and torque per direction in the first 15 minutes.

Figure C.3 shows the drift in terms of force. The drift is zoomed in on the first 15 minutes, where drift effects were most present. The drift effect is 10N in this period.

Appendix D

Crutch GRFs using Optical Marker Orientation

D.1 Introduction

A calibration and validation is described to relate forces measured by the crutches to forces measured by a force plate. An optical marker system is used to determine the orientation of the crutches.

Both crutches are equipped with an ATI Mini 45 (SI-580-20) Force Torque (FT) sensor at the tip, of which specifications can be found in table B.1. The FT sensor makes use of six silicon strain gauges and a calibration matrix supplied with the sensor allows the measured voltages to be converted into forces. Sensor readings need to be calibrated and validated to relate values measured by the strain gauges to actual forces. An Analog-to-digital converter (ADC) is used to convert force sensor voltages to digital values. This introduces a linear scaling factor. In addition, the tip of the crutch is made out of rubber, which could act as a damper and introduce non-linearity by absorbing energy. In the same way, hysteresis or other non-linearity could be present due to the behaviour of the force sensors or bending of the crutch when force is applied. Calibrated force plates in combination with a VICON optical marker system were used as reference. Cyclic loading tests as well as walking tests have been performed to evaluate forces in different situations. This is line with literature about calibrating crutch forces, where cyclic loading tests and real-life scenarios are used as well [16, 57].
The goal of this crutch calibration experiment is to verify correctness of the calibration matrix, determine offset and scaling factors due to the ADC, determine influence of the rubber tip and investigate if other non-linearities are present.

Reference frames and quaternions
The forces measured at the tip of the crutch need to be related to the forces measured by the force plate. The crutch measures forces in the frame of reference of the crutch (ψ_{crutch}), meaning the z-direction force is always in the direction of shaft of the crutch. The force plate however has a different frame of reference (ψ_{FP}), with the z-direction being perpendicular to Earth. See figure D.1 for a more detailed overview. Therefore, data needs to be transformed to be in the same frame of reference. This can be done using a rotation matrix:

$$\psi_{FP} = \boldsymbol{R} * \psi_{crutch} \tag{D.1}$$

With $\boldsymbol{R}$ being a rotation matrix describing the transformation from ψ_{crutch} to ψ_{FP}. Such that forces in x, y and z directions can be converted:

$$\begin{bmatrix} F_{x'} \\ F_{y'} \\ F_{z'} \end{bmatrix} = R \begin{bmatrix} F_x \\ F_y \\ F_z \end{bmatrix} \tag{D.2}$$

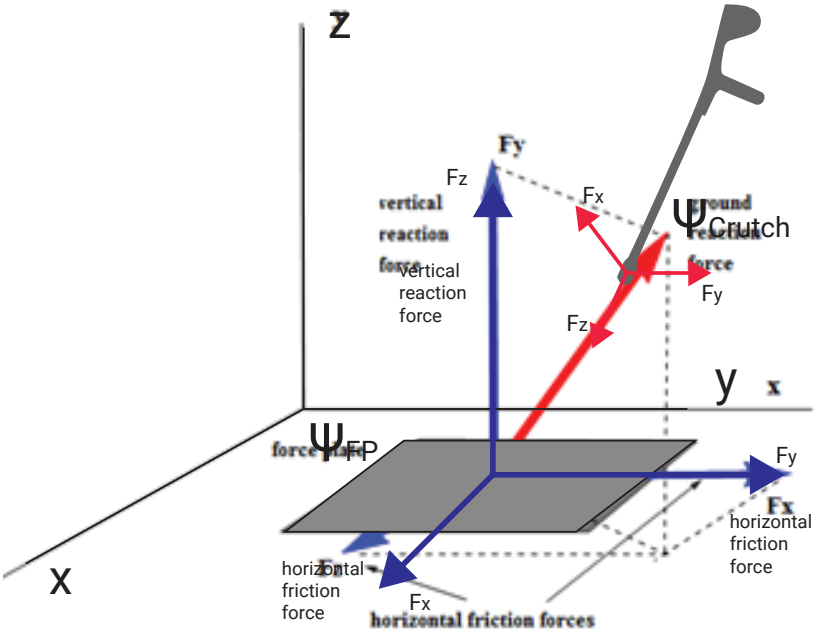

Figure D.1: Reference system of the force plate (ψ_{FP}) and crutch (ψ_{crutch}).

A common method to perform this transformation are Euler angles. These describe the rotation around the x, y and z axis when the angle of rotation is known:

$$\boldsymbol{R_x(\theta)} = \begin{bmatrix} \mathbf{1} & \mathbf{0} & \mathbf{0} \\ \mathbf{0} & \mathbf{\cos\theta} & \mathbf{-\sin\theta} \\ \mathbf{0} & \mathbf{\sin\theta} & \mathbf{\cos\theta} \end{bmatrix} \tag{D.3}$$

$$\boldsymbol{R_y(\theta)} = \begin{bmatrix} \mathbf{\cos\theta} & \mathbf{0} & \mathbf{\sin\theta} \\ \mathbf{0} & \mathbf{1} & \mathbf{0} \\ \mathbf{-\sin\theta} & \mathbf{0} & \mathbf{\cos\theta} \end{bmatrix} \tag{D.4}$$

$$\boldsymbol{R_z(\theta)} = \begin{bmatrix} \mathbf{\cos\theta} & \mathbf{-\sin\theta} & \mathbf{0} \\ \mathbf{\sin\theta} & \mathbf{\cos\theta} & \mathbf{0} \\ \mathbf{0} & \mathbf{0} & \mathbf{1} \end{bmatrix} \tag{D.5}$$

Euler angles introduce gimbal lock however when two axis line up, causing the loss of one degree of freedom. Therefore, another common method is used based on quaternions. Quaternions are an extension of the complex numbers. Next to the complex number *i*, *j* and *k* are introduced. Quaternions are written as:

$$\boldsymbol{q = w + xi + yj + zk} \tag{D.6}$$

Where $\boldsymbol{w}$ is the scalar part indicating the rotation and $\boldsymbol{xi\ yj\ zk}$ the vector part. They follow calculating principles similar to $\boldsymbol{i}$:

$$\mathbf{i}^2 = \mathbf{j}^2 = \mathbf{k}^2 = \mathbf{ijk} = -\mathbf{1} \tag{D.7}$$

And

$$(w_1 + x_1\mathbf{i} + y_1\mathbf{j} + z_1\mathbf{k}) + (w_2 + x_2\mathbf{i} + y_2\mathbf{j} + z_2\mathbf{k}) = (w_1 + w_2) + (x_1 + x_2)\,\mathbf{i} + (y_1 + y_2)\,\mathbf{j} + (z_1 + z_2)\,\mathbf{k} \tag{D.8}$$

When expressing spatial orientations, unit quaterions are often used. A unit quaternion is made by normalizing a quaternion:

$$\mathbf{U}q = \frac{q}{\|q\|} \tag{D.9}$$

Following the rule:

$$w^2 + x^2 + y^2 + z^2 = 1 \tag{D.10}$$

Unit quaternions can be produced by and extension of Euler's formula:

$$\mathbf{q} = e^{\frac{\theta}{2}(u_x\mathbf{i} + u_y\mathbf{j} + u_z\mathbf{k})} = \cos\frac{\theta}{2} + (u_x\mathbf{i} + u_y\mathbf{j} + u_z\mathbf{k})\sin\frac{\theta}{2} \tag{D.11}$$

To transform a vector p to another vector p', the quaternion and inverse quaternion can be used:

$$\mathbf{p}' = \mathbf{qpq}^{-1} \tag{D.12}$$

When implementing this in a program, p is a quaternion where the real part equals 0 and the vector is placed at i, j, and k. The resulting p' has the outcome vector again at i, j, and k and the real part being zero. A vector v_1 = [2 3 4] will be written as quaternion q = [0 + $2i$+$3j$+$4k$], becoming the unit quaternion q = [0 + $0.3714i$+$0.5571j$+$0.7428k$].
An efficient way to determine the vector part of the quaternion $q.ijk$ and the real part of the quaternion $q.w$ is the following:

$$q.ijk = \vec{v_1} \times \vec{v_2} \tag{D.13}$$

$$q.w = \sqrt{v1.length^2 * v2.length^2} + \vec{v_1} \cdot \vec{v_2} \tag{D.14}$$

Where $\times$ denotes the cross product and $\cdot$ the dot product. When we take $\vec{v_1}$ being [0 0 1], and $\vec{v_2}$ the normalized vector that arises from VICON 3D marker data, we obtain the quaternions to rotate our crutch to the reference frame of the force plate ψ_{FP}.

D.2 Method

Data Collection
Each crutch was equipped with six reflective markers as can be seen in figure D.2. Marker data was recorded at 100 Hz with a 6 camera motion capture system (Vicon, Inc. USA). Ground reaction contact forces were recorded at 1 kHz using two force plates (OR6 series, AMTI, Canada). Crutches were set to measure acceleration, angular velocity and FT-sensor readings at 1 kHz.
Data collection was split into three parts: measurement with the left crutch, right crutch, and both at the same time. In the measurement with both crutches at the same time, a walking setting was reproduced and in the test with the individual crutches, dynamic loading was performed by pushing on the crutch under a set angle. During the dynamic loading, axes of the

force sensor were aligned with the axes of the force plate. Linear models were calculated for force in the x, y and z direction based on force plate readings. Cyclic loading tests were used to determine the linear fit and the parameters were tested on the walking test.

Figure D.2: The crutches in the lab with optical markers for the VICON system attached.

Cyclic loading

1. Crutch upright (90°w.r.t ground)
2. Crutch tilted towards x-direction of force plate (80°)
3. Crutch tilted towards y-direction of force plate (80°)
4. Crutch tilted towards x-direction of force plate (70°)
5. Crutch tilted towards y-direction of force plate (70°)

Every experiment was done twice and performed for both the left and right crutch.

Walking test

1. Performing swing phase with the crutches. Partly move weight on the crutches. When crutches hit the force plates, they are pulled back and movement is performed again.
2. Walking with crutches

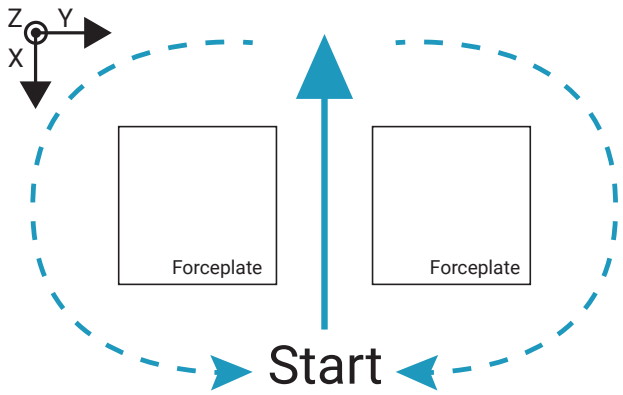

Figure D.3: Top view of stepping on force plates. Each trial consisted of placing a crutch on either force plate and swinging forward. The person then swung backward along the dashed line. This was repeated 14-20 times per trial.

Every experiment was done twice while using both crutches.

Analysis
Data was analysed using *MATLAB* (Mathworks, USA). Data of the VICON system was upsampled to 1 kHz to match the sample frequency of the force plate and crutches. Measurement data of the crutch was made equidistant and voltage readings from the force sensor were multiplied by the calibration matrix. Orientation of the crutches was determined using 3D marker data and expressed by quaternions using formula D.13 and D.14. Forces in the local reference frame of the crutches ψ_{crutch} were converted to the reference frame of the force plates ψ_{FP}. During the cyclic loading experiments, the axes of the force sensor were lined up with with the axes of the force plate. During the walking experiments, this was not the case and an additional rotation was performed using rotation matrix $\boldsymbol{R_z(\theta)}$ as described in equation D.5. Finally, a linear fit was determined for every cyclic loading experiment to relate force plate measurements to FT-sensor data. This was done using *polyfit* and *polyval* functions in *MATLAB*. The resulting linear fit equations are subsequently evaluated on walking test data. Scoring metrics to evaluate the data fit are the Root Mean Square Error (RMSE), R^2, and Pearson correlation score.

Appendix E

Models of walking with crutches

Using crutches allows for different walking patterns. Depending on the type of injury or disability the foot placement and number of ground contact points can be altered. Swing-through without weight bearing (WB) is when the impaired side is not used at all and both crutches are placed on the ground simultaneously, alternating with the non-impaired side [6]. Swing-through Partial Weight Bearing (PWB) is when both the impaired and non-impaired side are both used. Consecutively, both feet and both crutches are placed on the ground with a swing phase in between. 3-point PWB is the type used in this research and is typical for ankle fracture patients in the partial loading phase. Three simultaneous contact points of both crutches and the impaired side are alternated with the non-impaired side. The three simultaneous contact points with the ground allow for a range of PWB. Figure E.1 shows a an overview of this.

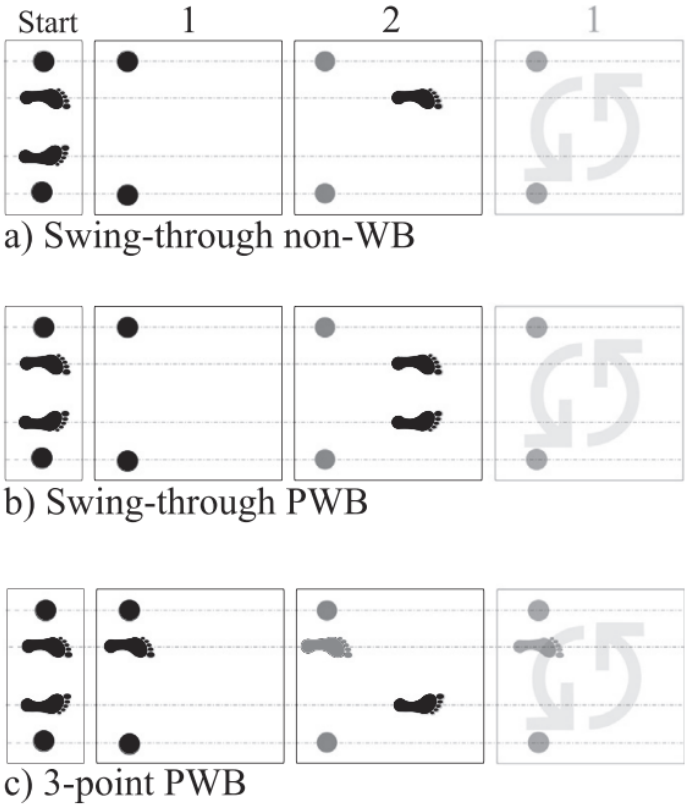

Figure E.1: Overview of the three most common crutch gait types. Adapted from [6].

Appendix F

Ankle Fracture Types

The Weber classification system consist of three types of ankle fractures [58]. Dependent on the location of the fibular fracture with respect to the syndesmosis, these are called class A, B or C. Class A describes an avulsion of the lateral malleolus, i.e. a fracture in the lower part of the fibula, below the syndesmosis (ankle ligament). Type B describes an oblique fracture at the height of the syndesmosis. Type C is a fracture higher in the fibula, above the syndesmosis. See figure F.1 for an overview of the three fracture types.
A more comprehensive version of Weber is Lauge-Hansen [58]. It specifies the three type of Weber fractures by adding information about the position of the foot during time of the injury and the deforming force on the ankle. Additionally, further complications and stability. Weber A is called supination adduction and is divided into two stages. Weber B and C are called supination exorotation and pronation exorotation respectively and are both divided into four stages. See table F.1 for a more detailed overview of the Weber and Lauge-Hansen classification systems.

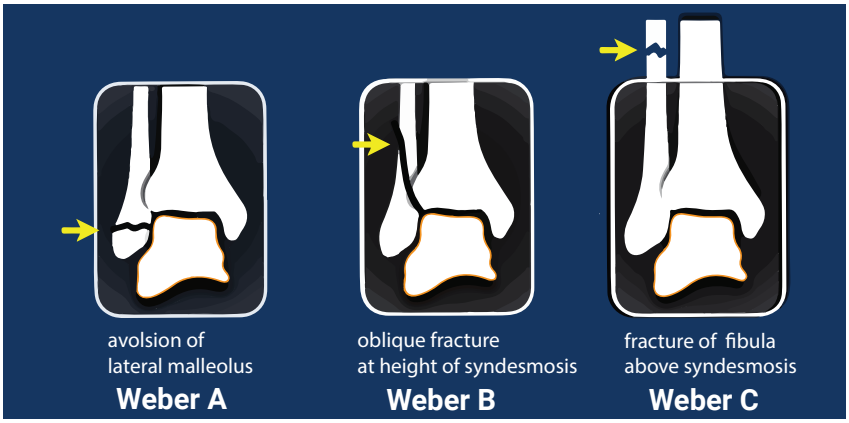

Figure F.1: The three types of ankle fractures according to Weber. Picture adapted from [59].

Table F.1: Classification system for ankle fractures. Information adapted from the Radiology Department of the Rijnland Hospital, Leiderdorp, The Netherlands [59, 60].

Ankle Fracture Classification System			
Weber	**Lauge-Hansen**	**Description**	**Stage**
A (infrasyndesmotic)	Supination adduction	Avulsion of the lateral maleolus	1. Avulsion of the lateral malleolus 2. Oblique fracture of the medial malleolus (uncommon)
B (transsyndesmotic)	Supination exorotation	Oblique fracture at the level of the syndesmosis	1. Rupture of the anterior syndesmosis 2. Oblique freacture of the fibula 3. Rupture of the posterior syndesmosis or fracture of the posterior malleolus 4. Avulsion of the medial malleolus or rupture of the medial bands
C (suprasyndesmotic)	Pronation exorotation	Fibula fracture above the syndesmosis	1. Avulsion of the medial malleolus or ligamentous rupture 2. Rupture of the anterior syndesmosis 3. Fibula fracture above the level of the syndesmosis 4. Avulsion of the posterior malleolus or rupture of the posterior syndesmosis

Stage 2 of Weber type A and stage 3-4 of Weber stage B and C are considered unstable. In case of an unstable fracture, surgery is needed in nearly all cases. Afterwards, an immobility phase of six weeks takes place. Consecutively, a rehabilitation phase starts where the patient is allowed to gradually increase partial weight bearing again. As a rule of thumb, the first two weeks are 25% PWB, the following two weeks are 50% PWB and the final two weeks are 100% PWB.

Appendix G

Ethical approval

The following section contains the ethical approval of the METC Oost-Nederland and Ziekenhuisgroep Twente (ZGT) hospital.

Titel van het onderzoeksprotocol: Evaluatie van het gebruik van geïnstrumenteerde krukken, drukzolen en bewegingssensoren als meetinstrumenten voor het bepalen van de belasting op de enkel bij een populatie van gezonde proefpersonen en proefpersonen 7-12 weken na een enkelfractuur

Dossiernummer METC Oost-Nederland: 2022-13615

Naam hoofdonderzoeker: Felix Dransfeld, mede namens Han Hegeman (ZGT, UT), Bert-Jan van Beijnum (UT), Jorinde Spook (ZGT, UT) en Roelien Russcher (UT)

Naam onderzoekscentrum: University of Twente (BSS), Enschede i.s.m. consortium van Han Hegeman ZGT.

Naam indiener: Felix Dransfeld

Datum indiening: 27 mei 2022

Geachte Felix Dransfeld,

U heeft de commissie verzocht een uitspraak te doen over of bovengenoemd onderzoek onder de Wet medisch-wetenschappelijk onderzoek met mensen (WMO) valt en op grond daarvan door een erkende medisch-ethische toetsingscommissie beoordeeld moet worden.

De onderzoeksdeelnemers worden niet aan WMO-plichtige handelingen onderworpen en aan hen worden geen WMO-plichtige gedragingen opgelegd.

Op grond hiervan verklaart de commissie dat het onderzoek niet onder de WMO valt. Voor de uitvoering ervan is derhalve geen positief oordeel vereist van de METC Oost-Nederland of een andere erkende medisch-ethische toetsingscommissie (in de proefpersoneninformatie kan daarom niet worden vermeld dat de METC Oost-Nederland het onderzoek heeft goedgekeurd).
De commissie heeft uw onderzoek alleen beoordeeld op WMO-plicht en niet aan een inhoudelijk oordeel onderworpen (in de proefpersoneninformatie kan daarom niet worden vermeld dat het onderzoek is goedgekeurd door een METC).

Dit oordeel is tot stand gekomen na bestudering van de volgende documenten:

- Aanbiedingsbrief d.d. 27 mei 2022
- Onderzoeksprotocol d.d. 27 mei 2022
- Proefpersoneninformatie patient versie 12 mei 2022
- Proefpersoneninformatie gezond versie 27 mei 2022

Voor zover u dit nog niet heeft gedaan raad ik u aan in de deelnemende centra na te gaan of voor de uitvoering van uw niet-WMO-onderzoek een beoordeling door de niet-WMO-toetsingscommissie ter plekke vereist is.

Ik vertrouw erop u met dit bericht van dienst te zijn.

Met vriendelijke groet,

Prof. Dr. Richard Dekhuijzen, voorzitter

METC Oost-Nederland
METCoost-en-CMO@radboudumc.nl
T (024) 3613154

Radboud universitair medisch centrum
Tandheelkunde gebouw
Philips van Leydenlaan 25 (route 348), Nijmegen
www.radboudumc.nl
www.metc-oost-nederland.nl

Topzorg voor uw levenskwaliteit

Mevrouw dr. H.M. Dijstelbloem
Voorzitter Raad van Bestuur

POSTADRES
Postbus 546
7550 AM Hengelo

UW KENMERK	ONS KENMERK	DOORKIESNUMMER	DATUM
	ZGT22-30 niet wmo	06 - 82 77 65 18	5 september 2022

ONDERWERP
Advies niet WMO-plichtig onderzoek

Geachte mevrouw Dijstelbloem,

In overleg met de Adviescommissie Lokale Uitvoerbaarheid Wetenschappelijk Onderzoek d.d. 5 september 2022 is de melding experimenteel onderzoek getiteld:

'*Balanced Rehabilitation After an Ankle Fracture Operation - BRAFO*'

besproken. De studie zal worden uitgevoerd in ZGT. De lokale onderzoekscoördinator is de heer H. Hegeman, traumachirurg en lokale onderzoeker is de heer H. Faessen, fysiotherapeut. De studie is door de METC CMO Nijmegen/Arnhem niet WMO-plichtig bevonden. De Adviescommissie Lokale Uitvoerbaarheid Wetenschappelijk Onderzoek ZGT sluit zich hierbij aan en ziet geen bezwaren tegen de uitvoering van deze studie binnen de ZGT op voorwaarde dat de openstaande actiepunten met betrekking tot de medische technologie volledig zijn afgerond en afgehandeld.

Vertrouwende u hiermee voldoende te hebben geïnformeerd.

Met vriendelijke groet,
Namens de Adviescommissie Lokale Uitvoerbaarheid
Wetenschappelijk Onderzoek

Ilonka Dijkhuis
Secretaresse ZGT Academie

Kopie:
- De heer H. Hegeman, traumachirurg, hoofdonderzoeker, coördinator onderzoek
- De heer H. Faessen, fysiotherapeut lokale onderzoeker ZGT
- Mevrouw R. Russcher, junior onderzoeker Utwente
- Mevrouw J. Spook, centrum voor Geriatrische Traumatologie, onderzoeker
- De heer E. Monteban, bedrijfskundig manager cluster snijdend
- De heer J. Raymakers, medisch manager cluster
- Mevrouw O. Boutens, bedrijfskundig clustermanager van cluster medisch ondersteunend
- Mevrouw E. Markink

Appendix H

Measurement Protocol

The following section details the measurement protocol in the Dutch., providing the procedures and methodologies used during the measurements.

	Naam/functie:
Eigenaar in ZGT:	Helena Chon, Manager wetenschap en innovatie, ZGT Academie
ZGT specifiek aanpassingen t.o.v. STZ SOPS	DMP onderdeel in bijlage 9 ´ Voorbeeld van een onderzoeksprotocol voor een niet-WMO plichtige studie´ vervangen door de notitie: Stuur met de indiening bij de ALU een ingevuld datamanagementplan mee (zie bijlage SOP VC11): 1. Indien retrospectief dossier onderzoek: gebruik datamanagementplan 'Retrospectief dossieronderzoek'. 2. Indien prospectief onderzoek: gebruik datamanagementplan 'Prospectief onderzoek'.
Revisiedatum ZGT: Januari 2024	
Voorstellen ter verbetering kunt u door middel van een e-mail kenbaar maken bij de eigenaar met vermelding van de code van het document, uw naam, afdeling en datum.	

Standard Operating Procedure

STZ SOP: **VC1 Ontwikkelen onderzoeksprotocol**

Auteur

STZ PWO werkgroep SOP's

Distributielijst : STZ
Datum : 22-12-2021
Revisiedatum : 22-12-2024

Veranderingen ten opzichte van versie 31-12-2018			
Hoofdstuk	*Soort aanpassing*	*Reden*	*Aanpassing*
5	Tekstueel	De oude bijlage 9.1 is verwijderd en vervangen door een nieuwe bijlage 9.1. De oude bijlage betrof het standaardmodel onderzoeksprotocol WMO plichtig onderzoek. De meest recente versie is altijd terug te vinden op de CCMO website. De nieuwe bijlage is een template voor een niet-WMO plichtig onderzoeksprotocol. Hier is geen standaard voor.	Verwijzing naar de oorspronkelijke bijlage verwijderd en een naar de nieuwe bijlage toegevoegd.
7	Tekstueel	De bijlage 9.1 is verwijderd. Hierin was een verwijzing naar SOP VC7, VC9, VC11 en VC12 opgenomen.	SOP VC7, VC9, VC11 en VC12 als referentie verwijderd
9	Tekstueel	De bijlage 9.1 is verwijderd en vervangen door een andere bijlage	Bijlage 9.1 heet nu: Voorbeeld van een onderzoeksprotocol voor een niet-WMO plichtige

			studie

1. Doel

Het beschrijven van de inhoud van een onderzoeksprotocol. Doel van een onderzoeksprotocol is gedetailleerd te beschrijven hoe de studie wordt uitgevoerd en uniformiteit te creëren bij het uitvoeren van de studie.

2. Afkortingen, definities en termen

Zie lijst met afkortingen, definities en termen STZ-Kwaliteitshandboek SOP's.

3. Verantwoordelijkheden

Hieronder worden de verantwoordelijkheden van de verschillende partijen met betrekking tot deze STZ SOP VC1 'Ontwikkelen onderzoeksprotocol' benoemd.

Sponsor/verrichter is eindverantwoordelijk voor:

- Een duidelijk omschreven onderzoeksprotocol;
- Het tijdig betrekken van andere afdelingen, die, indien nodig, een bijdrage moeten leveren aan het schrijven van een protocol (bijvoorbeeld: apotheek, afdeling beeldvormende technieken, functieafdelingen, laboratorium). Zie hiervoor ook STZ SOP U6 'Studie medicatie' en STZ SOP U7 'Ondersteunende diensten'.

4. Stroomdiagram

-

5. Werkwijze

De CCMO heeft een model onderzoeksprotocol ontwikkeld in het Engels. Deze is te downloaden via de website www.ccmo.nl. Ga vervolgens naar Onderzoekers → Standaardonderzoeksdossier → C. Protocol → C1. Onderzoeksprotocol, of typ 'model onderzoeksprotocol' in de zoekbalk. Raadpleeg deze website voor de meest recente versie van het model.
In geval van een WMO-plichtig onderzoek dient het protocol, samen met overige relevante studiedocumentatie, ter beoordeling te worden voorgelegd aan een erkende METC. Deze procedure is beschreven in STZ SOP VC6 'Beoordeling toetsende commissie (centraal)'. Als een protocol in de loop van de studie gewijzigd wordt dan dient deze wijziging, in de vorm van een amendement, te worden beschreven en voorgelegd aan de erkende METC. Zie hiervoor ook STZ SOP VC8 'Beoordeling amendement toetsende commissie (centraal)' en STZ SOP VL5 'Beoordeling amendement raad van bestuur (lokaal)'.
Voor een voorbeeld van een onderzoeksprotocol voor een niet-WMO plichtige studie zie bijlage 9.1. (STZ werkgroep Lokale Uitvoerbaarheid)

6. Archivering

Het goedgekeurde getekende onderzoeksprotocol dient gearchiveerd te worden in de Investigator site file en Trial Master File (zie STZ SOP VL4 'Studiedossiers (ISF/TMF')).
Zie verder voor archivering STZ SOP A2 'Archiveren studie'

7. Referenties

Richtsnoer voor Good Clinical Practice (CPMP/ICH/135/95), officiële Nederlandse vertaling
Wet Medisch-wetenschappelijk Onderzoek met mensen

Website van de CCMO (www.ccmo.nl)
STZ SOP VC6: Beoordeling toetsende commissie (centraal)
STZ SOP VC8: Beoordeling amendement toetsende commissie (centraal)
STZ SOP VL4: Studiedossiers (Investigator Site File/ Trial Master File)
STZ SOP VL5: Beoordeling amendement raad van bestuur (lokaal)
STZ SOP U6: Studie medicatie
STZ SOP U7: Ondersteunende diensten
STZ SOP VL5: Amendement (lokaal)
STZ SOP A2: Archiveren studie

8. Literatuur

Richtsnoer voor Good Clinical Practice (CPMP/ICH/135/95), officiële Nederlandse vertaling
Website van de CCMO (www.ccmo.nl)

9. Bijlage

9.1 Voorbeeld van een onderzoeksprotocol voor een niet-WMO plichtige studie.

9.1 Voorbeeld van een onderzoeksprotocol voor een niet-WMO plichtige studie.

Template onderzoeksprotocol niet WMO-plichtig onderzoek

De grijze teksten in onderstaand template omvatten extra informatie als hulpmiddel bij het invullen van de verschillende paragrafen. Deze kunnen in de definitieve versie van het protocol verwijderd worden.

STUDIEGEGEVENS			
Titel onderzoek	Balanced Rehabilitation after an Ankle Fracture Operation		
Acroniem/ korte studie titel	BRAFO		
Datum / Versie	27-05-2022 v1.0		
Soort studie	☐ Retrospectief onderzoek (dossier-/statusonderzoek) ☑ (Deels) prospectief onderzoek ☐ Anders, namelijk		
Opdrachtgever / verrichter *De opdrachtgever/ verrichter is de instelling (ziekenhuis, bedrijf, etc) die opdracht heeft gegeven voor de organisatie en/of uitvoering van het onderzoek*	Samenwerkingsverband tussen de Universiteit Twente en Ziekenhuisgroep Twente.		
Leden onderzoeksteam *Indien noodzakelijk kunnen er natuurlijk regels worden toegevoegd of verwijderd*	Gegevens *Noteer hier de naam, functie, vakgroep/afdeling en instelling van elk lid van het onderzoeksteam*		Rol *Bijvoorbeeld lokale hoofdonderzoeker, coördinerend onderzoeker, onderzoeksverpleegkundige, supervisoropleiding,…*
	1	Dr. J. H. Hegeman (traumachirurg ZGT/universitair hoofddocent, UT)	Hoofdonderzoeker/ Betrokken chirurg
	2	Ir. Roelien Russcher (junior-onderzoeker Biomedische Signalen en Systemen, Universiteit Twente)	Coördinerend onderzoeker
	3	Felix Dransfeld (afstudeer masterstudent Biomedical	Master afstudeerder

		Engineering, Universiteit Twente)	
	4	Dr. Ir. B.J.F. van Beijnum (universitair hoofddocent, Biomedische Signalen en Systemen, UT)	Hoofdonderzoeker
	5	Prof. Dr. Jaap Buurke (fysiotherapeut, hoogleraar Biomedische Signalen en Systemen, UT/senior researcher Roessingh Research and Development)	Supervisoropleiding
	6	Dr. J. E. Spook (onderzoekscoördinator ZGT/ universitair docent psychologie, gezondheid en technologie, UT)	Supervisoropleiding
Indiener *(De persoon die de studie indient bij de ZGT)*	Naam: Felix Dransfeld Telefoonnummer: 06 5537 1048 E-mailadres: f.j.m.dransfeld@student.utwente.nl		
(Lokale) hoofdonderzoeker ZGT *(De (lokale) hoofdonderzoeker moet ZGT medewerker zijn en voldoende bewezen onderzoekservaring hebben)*	Naam: Dr. J. H. Hegeman Telefoonnummer: 088-7085233 E-mailadres: h.hegeman@zgt.nl		
Het onderzoek wordt uitgevoerd in het kader van:	☑ Algemeen wetenschappelijk onderzoek (bijv. binnen onderzoekslijn binnen de instelling) ☐ Promotieonderzoek ☑ Wetenschappelijke stage/bachelor- of masterthesis. Naam opleidingsinstituut: Universiteit Twente, Biomedische Signalen en Systemen ☑ Anders, namelijk: Pioneers in Healthcare Voucher 2021		

Inhoudsopgave

SAMENVATTING

Revalidatie na een enkelfractuuroperatie vindt voornamelijk thuis plaats. In de huidige praktijk beginnen patiënten pas zes weken na de operatie met het belasten van hun geopereerde been. Er is inmiddels klinisch bewijs dat dit eerder kan, maar alleen onder de voorwaarde dat patiënten in de thuissituatie nauwlettend in de gaten worden gehouden. Hiervoor wordt een ambulant meetsysteem ontwikkeld dat gebruik maakt van geïnstrumenteerde krukken om belasting op de enkel aan de aangedane zijde te bepalen.
De geïnstrumenteerde krukken bevatten krachtsensoren om de krachten van het lopen te bepalen. Daarnaast zullen er speciale inlegzolen worden gebruikt die druk onder de voet meten en wordt er gebruik gemaakt van bewegingssensoren om bewegingen te volgen. Als referentie voor de krachten op de enkel worden ForceShoes (krachtschoenen) gebruikt. Van de data die uit deze meetapparatuur komt, wordt een model gemaakt om de krachten op de enkel te kunnen schatten. Voor het verkrijgen van deze data zullen er metingen worden gedaan op 10 personen 7-12 weken na een enkelfractuur in het ZGT in Almelo.

INTRODUCTIE

Krukken worden veel gebruikt als ondersteuning bij het lopen met letsel aan de onderste extremiteit. Bij het gebruik van krukken wordt een deel van de belasting van het lichaam overgebracht naar de bovenste ledematen om de onderste ledematen te ontlasten tijdens het lopen en activities of daily living. Krukken stimuleren actief zijn en het lopen in een rechte houding, wat voordelen biedt voor de gezondheid op lange termijn [1]. Enkelfracturen zijn veel voorkomende letsels, met incidentiecijfers tussen 100 en 150 per 100.000 persoonsjaren [2, 3]. In 55% van de gevallen zijn enkelbreuken sport gerelateerd. In geval van een instabiele breuk van de enkel is chirurgische fixatie noodzakelijk. Dit wordt gevolgd door een immobilisatiefase van zes weken waarbij de breuk geneest [4]. Daarna wordt een revalidatieproces gestart, waarin de patiënt de aangetaste enkel geleidelijk mag gaan belasten.

Revalidatie na een enkelfractuuroperatie vindt voornamelijk thuis plaats. In de huidige praktijk beginnen patiënten pas zes weken na de operatie met het belasten van hun geopereerde been. Er is inmiddels klinisch bewijs dat dit eerder kan, maar alleen onder de voorwaarde dat patiënten in de thuissituatie nauwlettend in de gaten worden gehouden [5]. Op dit moment is er geen geschikt ambulant meetsysteem dat de belasting, het looppatroon en de balans bij deze patiënten in het dagelijks leven kan meten, en is er geen kennis over deze grootheden bij deze doelgroep. In dit project wordt een meetsysteem ontwikkeld dat dit wel mogelijk maakt, en bovendien robuust en gebruiksvriendelijk is. Het meetsysteem zal technisch gevalideerd worden. In deze pilotstudie, waarin we dit meetsysteem zullen gebruiken, zullen patiënten in week 7 tot 12 na de fractuur beginnen met het gedeeltelijk belasten van hun enkel. Dit zal de eerste inzichten geven in de toepasbaarheid en klinische mogelijkheden van het nieuwe meetsysteem.

Dit onderzoek richt zich op de krachten op de enkel tijdens het lopen met krukken. Om de belasting volledig in beeld te krijgen, worden zowel de kracht als het moment onderzocht. Krachten en draaimomenten tijdens het lopen met krukken worden gemeten met behulp van de geïnstrumenteerde krukken. Daarnaast worden inlegzolen gebruikt die het massamiddelpunt meten en bewegingssensoren (IMUs) die de beweging meten. ForceShoes (Xsens, Nederland) zijn de gouden standaard voor draagbare loopmetingen en worden in dit onderzoek als referentie gebruikt. Naast het meten van belasting is het ook belangrijk om een model te maken dat belasting kan schatten in geval van 3D krachten. Bij vrij rondlopen en het uitvoeren van activiteiten van het dagelijks leven (ADL-taken) zijn 1D-krachtmetingen niet adequaat.

Bronnen

[1] Haubert LL, Gutierrez DD, Newsam CJ, Gronley JAK, Mulroy SJ, Perry J. A Comparison of Shoulder Joint Forces During Ambulation With Crutches Versus a Walker in Persons With Incomplete Spinal Cord Injury. Archives of Physical Medicine and Rehabilitation. 2006 1;87(1):63-70.
[2] Daly PJ, Fitzgerald RH, Melton LJ, Llstrup DM. Epidemiology of ankle fractures in Rochester, Minnesota. Acta orthopaedica Scandinavica. 1987;58(5):539-44. Available from: https://pubmed.ncbi.nlm.nih.gov/3425285/.
[3] Jensen SL, Andresen BK, Mencke S, Nielsen PT. Epidemiology of ankle fractures. A prospective population-based study of 212 cases in Aalborg, Denmark. Acta orthopaedica Scandinavica. 1998;69(1):48-50. Available from: https://pubmed.ncbi.nlm.nih.gov/9524518/
[4] Moseley AM, Beckenkamp PR, Haas M, Herbert RD, Lin CWC, Evans P, et al. Rehabilitation After Immobilization for Ankle Fracture: The EXACT Randomized Clinical Trial. JAMA. 2015 10;314(13):1376-85. Available from: https://jamanetwork.com/
[5] Smeeing DPJ, Houwert RM, Briet JP, Kelder JC, Segers MJM, Verleisdonk EJMM, et al. Weight-bearing and mobilization in the postoperative care of ankle fractures: a systematic review and meta-analysis of randomized controlled trials and cohort studies. PloS one. 2015 2;10(2). Available from: https://pubmed.ncbi.nlm.nih.gov/25695796/.

ONDERZOEKSVRAAG/ ONDERZOEKSDOEL

De hoofdvraag van dit onderzoek is: Hoe adequaat zijn geïnstrumenteerde krukken, IMU's en drukinlegzolen in combinatie met een wiskundig model in vergelijking met de gouden standaard ForceShoes bij het bepalen van de enkelbelasting in een populatie van patiënten 7-12 weken na een enkelfractuur?

Secundaire onderzoeksvragen:
Voor welke taken zijn 1D voetkracht metingen voldoende en voor welke taken zijn 3D voetkracht metingen nodig?
Welke verschillen in opstelling zijn nodig in gecontroleerd lopen vergeleken met activities of daily living?
Welke parameters zijn er nodig om een klinisch relevante schatting te maken van enkelbelasting?

Is de minimale opstelling van 3 IMUs in combinatie met drukzolen en krachtinformatie onder de kruk voldoende om loopparameters met betrekking tot balans (i.e. staplengte, stapbreedte, positie CoM) te meten?

Omdat het een pilotstudy/proof of principle betreft zullen er 10 patiënten worden geïncludeerd.

METHODEN

In het hoofdstuk methoden komen de onderstaande onderwerpen aan bod. Het aanhouden van onderstaande volgorde van paragrafen is aan te raden.

Mono- of multicenter studie

☑ Monocenter studie

☐ Multicenter studie

Deelnemende centra en lokale hoofdonderzoeker per centrum:

- ZGT Almelo:
    - Dr. J. H. Hegeman, traumachirurg

Studiedesign

Dit protocol wordt gebruikt om te testen of geïnstrumenteerde krukken, samen met drukzolen en bewegingssensoren voldoende zijn om de belasting op de enkel te bepalen tijdens het lopen met krukken. Dit gaat gebeuren bij zowel gezonde proefpersonen als bij patiënten die revalideren van een enkelfractuur. De geïnstrumenteerde krukken zijn standaard onderarmkrukken, aangevuld met een kracht/moment sensor en een standaard inertial measurement unit (IMU). De data van de krukken zullen worden gecombineerd met data van drukinlegzolen (MediLogic, Duitsland), en een set MTw IMUs (Xsens 3D motion tracking, Nederland). Als referentie voor meting van krachten op de voeten zullen de ForceShoes (Xsens 3D motion tracking, Nederland) worden gebruikt.
Lopen met krukken heeft verschillende effecten op het looppatroon. Voorbeelden zijn een verminderde snelheid, veranderingen in plaatsing van de voet en veranderingen in plantaire voetdruk [1]. Smeeing et al. [2] toonden aan dat het vroegtijdig belasten van de enkel het hervatten van werk en dagelijkse activiteiten versnelt in vergelijking met later belasten van de enkel. Dit moet nauwkeurig gecontroleerd worden om overbelasting van de enkel te voorkomen. De huidige studie wil onderzoeken of de geïnstrumenteerde krukken, uitgerust met een krachtsensor en een IMU, in combinatie met MediLogic drukzolen, en een set IMU sensoren op het lichaam de belasting op de enkel kunnen bepalen van patiënten die herstellen van een enkelfractuur en lopen met krukken.
De kracht-/momentsensoren in de krukken (ATI Mini 45 SI-580-20) hebben 6 vrijheidsgraden. De versnellingsmeter en gyroscoop is van het type MPU9250. Daarnaast is een kastje op de kruk aangebracht om draadloos via Bluetooth gegevens door te geven. De drukinlegzolen [3] geven extra informatie over het drukpunt (CoP) en de krachten van de voet tijdens het lopen met de krukken. De ForceShoes [4] geven informatie over kracht en moment van de achter- en voorvoet van de voet tijdens

het lopen. De MTw bewegingssensoren [5] bestaan uit een versnellingsmeter, gyroscoop en magnetometer.

Eerst zullen maximaal 5 gezonde proefpersonen worden gerekruteerd en gemeten volgens het huidige protocol. Om te testen of de meetapparatuur ook voldoende is om te meten aan patiënten, zal er ook onderzoek worden gedaan bij patiënten 7-12 weken na een enkelbreuk. Dit zal gebeuren met 10 patiënten revaliderende van een enkelbreuk. Tijdens de metingen wordt de enkel gedeeltelijk belast onder toezicht van een fysiotherapeut. Aangezien de patiënten een daadwerkelijke beperking hebben, wordt verwacht dat hun looppatroon anders zal zijn, omdat zij niet alle mogelijke compenserende taken kunnen uitvoeren. Daarom is het belangrijk om ook deze doelgroep te meten.
Na de werving wordt de proefpersoon ontvangen op hun reguliere fysiotherapiesessie in ZGT Almelo en wordt het protocol uitgelegd. Als alles duidelijk is voor de proefpersoon, ondertekent de proefpersoon het toestemmingsformulier. Daarna wordt het protocol gestart, dat 30 minuten toevoegt bovenop de reguliere fysiotherapeutische bezoektijd in verband met het bevestigen van de sensoren.
Eerst worden de lengte (met een meetlint) en het gewicht (met een weegschaal) van de deelnemer gemeten. Geslacht, leeftijd, schoenmaat en de aangedane zijde worden ook genoteerd.
De deelnemers zullen in totaal tien draagbare MTw-sensoren van 16 gram per stuk dragen (Xsens 3D Motion tracking, Nederland): één op elke voet, één op elke schenkel, één op elk bovenbeen, één op het bekken, één op het borstbeen en één op de bovenarmen.

Alle gegevens worden via Bluetooth naar een laptop gestuurd en de krukken samplen gegevens op 1000 Hz. De samplefrequentie van de drukinlegzolen, voor het meten van het drukcentrum, de krachtschoenen, voor het meten van de loopkrachten, en de MTw-sensoren, voor het registreren van bewegingen, worden allemaal ingesteld op 100 Hz.

De vier verschillende sensoren in figuur 1 t/m 4, genereren data over belasting van de enkel. De verkregen data van de krukken (figuur 1), de drukzolen (figuur 2) en de bewegingssensoren (figuur 4) wordt gebruikt om de belasting op de enkel te bepalen. De schoenen (figuur 3) worden gebruikt ter referentie.

Figuur 1: Voorbeeld van een geïnstrumenteerde kruk. Het systeem gebruikt 2 van deze krukken.

Figuur 2: De drukzool die in de ForceShoes gelegd zal worden. Het kastje is verbonden aan de zool, hiermee wordt de data opgeslagen.

Figuur 3: De ForceShoes die worden gebruikt om de krachten onder de voeten te meten. Deze worden gedragen tijdens de meting.

Figuur 4: De bewegingssensoren die gedragen worden tijdens de meting. Hiervan worden er een aantal op het lichaam geplaatst.

References
[1] F. Rasouli and K.B. Reed, “Walking assistance using crutches: A state of the art review”, 2020
[2] Smeeing DP, Houwert RM, Briet JP, Kelder JC, Segers MJ, Verleisdonk EJ, Leenen LP, Hietbrink F. Weight-bearing and mobilization in the postoperative care of ankle fractures: a systematic review and meta-analysis of randomized controlled trials and cohort studies. PLoS One. 2015 Feb 19;10(2):e0118320. doi: 10.1371/journal.pone.0118320. PMID: 25695796; PMCID: PMC4335061.
[3] Medilogic, “medilogic WLAN insole”, via: https://medilogic.com/en/medilogic-wlan-insole/
[4] Xsens, “ForceShoes”, via: https://www.xsens.com/press-releases/xsens-technology-launched-outer-space
[5] Xsens, “MTw Awinda”, via: https://www.xsens.com/products/mtw-awinda

Procedure en interventie (indien van toepassing)

De metingen vinden plaats in de oefenzaal van de afdeling fysiotherapie van ZGT in Almelo . De metingen worden uitgevoerd onder begeleiding van een ervaren fysiotherapeut (Hans Faessen).

Na deze eerste voorbereiding en bevestiging van de systemen wordt de proefpersoon gevraagd twee looptaken (10 meter looptest en figuur van 8 looptest) en twee ADL-taken (traplopen en opstaan uit een stoel) uit te voeren. De loop- en ADL-taken zijn zo gekozen dat zij kunnen worden uitgevoerd als onderdeel van de gewone klinische bezoeken van de patiënten.
De proefpersoon moet (ten minste) 1 minuut met de meetapparatuur lopen om eraan te wennen. Pauzes zijn niet vereist maar kunnen worden ingelast wanneer de fysiotherapeut of de proefpersoon dat wenst.

Tabel 1: Schematisch overzicht van het experimentele protocol met tijdsaanduidingen.

SECTIE	**ACTIVITEIT PROEFPERSOON**	**TIJD (minuten)**
I. Voorbereiding	Het protocol zal aan de proefpersoon	10

	worden uitgelegd. Meet lichaamslengte, gewicht en lumbale sensorhoogte. Noteer geslacht, leeftijd, de aangedane enkel. Toon 25% gedeeltelijke gewichtsbelasting (PWB) op een weegschaal (of het maximum dat de fysiotherapeut de patiënt toestaat).	
II. BEVESTIG DRAAGBARE SENSOREN + DRUKZOLEN + KRACHTSCHOENEN	Stil staan of zitten tijdens het plaatsen van de sensoren, en het aantrekken van ForceShoes met inlegzooltjes voor de druk.	8
III. VOER KALIBRATIE EN SYNCHRONISATIE UIT	Voer kalibratiestappen uit van krukken en IMU's. Synchroniseer de hele opstelling. De proefpersoon staat stil.	2
IV. UITVOEREN VAN LOOPOPDRACHT 1 (3x)	Loop 10 meter rechtuit op de gewenste loopsnelheid met 25% PWB (of het maximum dat de fysiotherapeut de patiënt toestaat).	5
V. UITVOEREN VAN LOOPOPDRACHT 2 (3x)	Loop een 8-vorm (f8-test) op de voorkeursloopsnelheid met 25% PWB (of het maximum dat de fysiotherapeut de patiënt toestaat).	5
PAUZE	Neem een pauze en leg de volgende taken uit. (Of wanneer de fysiotherapeut pauze nodig vindt).	3
VI. UITVOEREN VAN ADL-TAAK 1 (3x)	Traplopen met gebruik van de krukken	5
VII. UITVOEREN VAN ADL-TAAK 2 (3x)	Opstaan uit een stoel met gebruik van de krukken	5
VIII. LOSHALEN VAN SENSOREN + DRUKZOLEN + KRACHTSCHOENEN	Staand (of indien gewenst, gedeeltelijk zittend), worden de sensoren door de onderzoekers losgemaakt.	5
OPBOUWTIJD & UITLEG REGULIERE BEZOEK WANDELTIJD (INCL. RUST) AFBREKEN SYSTEEM **GESCHATTE TOTALE TIJD**		20 25 (of reguliere behandeltijd) 10 **45-50 min**

Duur van de studie

Data wordt verzameld in de periode juni t/m november 2022.

Werving en selectie van proefpersonen

Screening/selectie

Bij de eerste controle, 2 weken na het ongeval, c.q. de operatie, wordt de patiënt door een van de traumachirurgen van het ZGT op de hoogte gesteld van het onderzoek. De coördinatie van de werving van patiënten is in handen van J. H. Hegeman, op basis van de in- en exclusiecriteria zoals verderop staat beschreven Tijdens het spreekuur wordt de PIF aan de geïnteresseerden personen meegegeven die binnen de inclusiecriteria vallen. J. H. Hegeman vraagt of het goed is om contactgegevens door te geven aan de onderzoekers. In dat geval mogen de onderzoekers contact opnemen met de persoon. Vervolgens plant fysiotherapeut Hans Faessen de eerste fysioafspraak in met de patiënt.

Studiepopulatie

De studiepopulatie is 10 deelnemers, die 7-12 weken geleden een enkelfractuur hebben gehad. Deze zijn tussen de 18 en 55 jaar oud en spreken Nederlands. In dit onderzoek worden zowel mannen als vrouwen geïncludeerd waarbij wordt gericht op een gelijke verdeling van beide geslachten. De studiepopulatie zal gerekruteerd worden bij het ZGT Almelo, onder mensen die voor een enkelfractuur bij het ZGT zijn geweest.

Inclusiecriteria

Om mee te mogen doen aan dit onderzoek, moet een proefpersoon voldoen aan het volgende criteria:

- In de leeftijdscategorie vallen van 18-55 jaar oud.
- Heeft 7-12 weken geleden een enkelfractuur gehad.
- Heeft geen aandoening/beperking die het looppatroon beïnvloed (anders dan de enkelfractuur).
- Beschikt over voldoende cognitief vermogen om instructies in het Nederlands te volgen.

De leeftijd tussen de 18 en 50 is gekozen omdat ouderen meer moeite hebben met balans houden en een groter risico lopen op complicaties. Daarom zijn ouderen uitgesloten van het onderzoek. Met de brede leeftijdsgroep kunnen de resultaten worden gegeneraliseerd over een bredere populatie. Het criterium 7-12 weken na de fractuur is gekozen omdat na zes weken, de enkel weer gedeeltelijk belast mag worden. Het lopen met krukken vormt dan geen risico. Na 12 weken is de enkelfractuur weer volledig hersteld en daarom zijn resultaten na 12 weken niet meer interessant voor dit onderzoek.
Het is nodig dat de deelnemer geen andere aandoeningen/beperkingen heeft die het looppatroon beïnvloeden, omdat dit de resultaten kan beïnvloeden. Het kunnen volgen van Nederlands is noodzakelijk om communicatie met de fysiotherapeut en onderzoekers goed te laten verlopen.

Exclusiecriteria

Een potentiële proefpersoon die aan een van de volgende criteria voldoet, zal van deelname aan deze pilotstudie worden uitgesloten:

- Heeft een medische aandoening die het onmogelijk maakt de vereiste procedures uit te voeren.
- Deelname wordt door de fysiotherapeut of arts beschouwd als onveilig.

Aantal proefpersonen / steekproefgrootte

Het aantal proefpersonen bedraagt 10 voor deze pilotstudie. Dit is het minimum voor een pilotstudy [1]. Meer patiënten maakt het uitvoeren van de metingen tijdsintensiever.

[1] Hertzog, M. A. (2008). Considerations in determining sample size for pilot studies. Research in Nursing &Health, 31(2), 180–191. https://doi.org/10.1002/NUR.20247

Dataverzameling: variabelen en meetmethoden

Primaire uitkomstmaat (afhankelijke variabele)

De primaire uitkomstvariabelen van dit onderzoek zijn Root Mean Square Error en Pearson Correlation Score.

In dit onderzoek wordt onderzocht in welke mate geïnstrumenteerde krukken, IMUs en drukzolen in combinatie met een wiskundig model de belasting op de enkel kunnen bepalen 7-12 weken na een enkelfractuur. Dit wordt vergeleken met krachtschoenen als referentie.

Overzicht variabelen en meetinstrumenten

Variabele	Meetinstrument/ Bron van de data	Uitkomstwaarden	Meetmoment
Leeftijd	Vragen aan deelnemer	18-50 (jaren)	Aan begin van meting
Schoenmaat	Meten	38-46 (EU schoenmaat)	Wordt van tevoren gevraagd
Gewicht	Meten	0 – 140 (kg)	Aan begin van meting
Lichaamslengte	Meten	(m)	Aan begin van meting
Type Enkelbreuk	Vragen aan deelnemer/arts/ fysiotherapeut	A1-2 of B1-4 of C1-4. (WEBER classificatie)	Aan begin van meting
Hoogte IMU sensoren	Meten	0.50– 1.50 (m)	Aan begin van meting
Acceleratie (m/s^2)	Inertial Measurement Unit	± 160 m/s2	Tijdens meting

	(IMU, bewegingssensor)		
Hoeksnelheid (deg/s)	Inertial Measurement Unit (IMU, bewegingssensor)	± 2000 deg/s	Tijdens meting
Magnetisch veld (Gauss)	Inertial Measurement Unit (IMU, bewegingssensor)	± 1.9 Gauss	Tijdens meting, geen kalibratie vooraf, data wordt niet meegenomen
Druk (kracht/oppervlak)	Drukzool	0,6 - 64 N/cm²	Tijdens meting
Kracht (Newton)	Geïnstrumenteerde krukkken & ForceShoes	± 580 N in x- en y-richting ± 1160 N in z-richting	Tijdens meting
Moment (Newton*meter)	Geïnstrumenteerde krukkken & ForceShoes	± 20 Nm om x, y en z-as	Tijdens meting

Standaardisering

Hoogte van de bewegingssensor (IMU) op de pelvis wordt altijd ten opzichte van de grond gemeten. De andere locaties van bewegingssensoren worden in verhouding gemeten van het lichaamsdeel waar ze opzitten.

Data-analyse

De inhoud van deze paragraaf is afhankelijk van het soort onderzoek en type onderzoeksvra(a)g(en).
Let op: De beschrijving van de data-analyse in een onderzoeksprotocol moet verder gaan dan het benoemen van de software die gebruikt zal worden voor de analyse en het soort analyse. Deze paragraaf moet een globaal overzicht geven van álle stappen die uitgevoerd worden met de verzamelde gegevens in het analyseproces.

Data-inspectie

Krachtdata uit de geïnstrumenteerde krukken bevatten extreme waardes (spikes) die 0.001 seconden duren. Deze worden verwijderd met een low-pass filter of handmatig als ze 2 keer de standaarddeviatie overschrijden. Van elke deelnemer moeten er meetdata en variabele zoals leeftijd en lichaamslengte bepaald worden. Van elke meting bij elke proefpersoon moeten er ten minste twee goede herhalingen zijn om de data te includeren. In geval dat er cruciale meetdata mist zal de proefpersoon worden uitgesloten van het onderzoek. In geval dat er variabele zoals leeftijd en lichaamslengte ontbreken,

worden de resultaten gebruikt tot waar mogelijk en indien niet bruikbaar wordt de proefpersoon uitgesloten van het onderzoek.

Analyses

Kwantitatief onderzoek: lineaire regressie, classificatie modellen, bijvoorbeeld Support Vector Machine (SVM) en multilayer perceptron.

Er wordt een model gemaakt gebaseerd op de data van alle deelnemers samen. Voor het bepalen van de werking van het model wordt een deel van de data gebruikt voor het opstellen van het model en een deel voor het testen van het model. Deze verhouding heeft orde van grootte 80% model maken, 20% model testen.

De scores die gebruikt worden om de meetdata te vergelijken met de referentie zijn de Root Mean Square Error, Pearson Correlation Score, F1-score, accuracy, mean absolute error, mean square error, area under the curve, confusion matrix, R^2, precision en recall, of vergelijkbare uitkomstmaten mocht dat een betere weergave van de resultaten zijn.

Beschrijvende statistiek

De studiepopulatie wordt beschreven door kwantitatieve variabelen zoals leeftijd en gewicht. Deze variabelen worden uitgedrukt met een gemiddelde en de standaarddeviatie. Als variabelen duidelijk niet normaal verdeeld zijn, wordt er gekozen om de mediaan en interquartile range (IQR) weer te geven. Voor de categorische variabele gender wordt gebruik gemaakt van frequentie en percentage per categorie (% M/V).

Statistische analyse

De meetdata wordt geanalyseerd met de scores zoals beschreven bij kwantitatief onderzoek. De beschrijvende statistische variabelen worden niet statistisch geanalyseerd.

Softwareprogramma

Matlab (achteraf, opstellen van het wiskundige model)

Python (geïnstrumenteerde krukken)

MT Manager 4.8 (IMUs)

MT Manager 1.7.4 (ForceShoes)

MediLogic (drukzolen)

ETHISCHE OVERWEGINGEN

Niet WMO verklaring

Een niet-WMO verklaring is verkregen bij de Medisch Ethische Toetsingscommissie Oost-Nederland (Arnhem-Nijmegen). Het dossiernummer 2022-13615 is hieraan toegekend.

Opmerking voor de CMO Arnhem Nijmegen: ervan uitgaande dat het onderzoek niet-WMO is. Het protocol is in het format van de Adviescommissie Lokale Uitvoerbaarheid wetenschappelijk onderzoek van het ZGT.

Belasting en vergoeding voor de proefpersoon

Deelnemers komen twee keer naar het ZGT ziekenhuis in Almelo. De eerste keer voor een normale behandeling met de fysiotherapeut. Hierbij kijkt de fysiotherapeut of de deelnemers daadwerkelijk deel kunnen nemen. In het geval van wel, komen de deelnemers terug naar het ziekenhuis voor een tweede behandeling. Bij deze tweede behandeling zal de meting plaatsvinden, resulterende in 30 minuten extra behandelingstijd. De belasting komt neer op 30 minuten extra behandeltijd en de eventuele extra reistijd om naar het ZGT Almelo toe te komen.
In het geval dat de fysiotherapeut bepaald dat een deelnemer niet geschikt is, kunnen zij naar wens hun fysiotherapietraject hervatten bij het ZGT of een andere locatie.
Voor zowel de eerste als tweede afspraak wordt de behandeling volledig vergoedt.

Toestemming proefpersoon

Bij prospectief niet WMO plichtig onderzoek moet altijd toestemming worden gevraagd aan de proefpersoon. Bij retrospectief niet WMO plichtig onderzoek is dat afhankelijk van de manier van dataverzameling en de verwerking ervan.

Wordt toestemming aan de proefpersoon gevraagd?	☑ Ja (Vul optie A 'Informed Consent Procedure' in) ☐ Nee (Vul optie B 'Toestemming wordt niet gevraagd')
Optie A: Informed Consent procedure	
Benadering proefpersonen	Bij het eerste spreekuur met arts J. H. Hegeman zullen patiënten op de hoogte worden gesteld van het onderzoek. Hierbij wordt ook gevraagd of zij mee willen doen en krijgen ze een PIF mee naar huis.
Informeren proefpersonen	De persoon wordt op de hoogte gesteld van de inhoud van het onderzoek tijdens het spreekuur met J.H. Hegeman. Hierbij is er ook ruimte om vragen te stellen over het onderzoek en krijgt de persoon een PIF mee naar huis. Hierna wordt er door de onderzoekers contact opgenomen met de proefpersoon om te vragen of deze deelneemt. Bij dit contact is er ook ruimte om vragen te stellen. Bij de eerste fysiotherapiebehandeling is er ook ruimte om vragen te stellen aan de fysiotherapeut. In de PIF staan de

	gegevens van betrokken onderzoeken, artsen en mensen onafhankelijk van het onderzoek waar per e-mail of telefoon contact mee opgenomen kan worden.
Bedenktijd	De bedenktijd om te besluiten om mee te doen aan dit onderzoek is 2 weken.
Tekenen toestemmings-verklaring	Het toestemmingsformulier wordt getekend voordat de metingen beginnen, bij de behandeling waar de metingen plaatsvinden.

DATAMANAGEMENT & PRIVACY

Stuur met de indiening bij de ALU een ingevuld datamanagementplan mee (zie bijlage SOP VC11):

1. *Indien retrospectief dossier onderzoek: gebruik datamanagementplan 'Retrospectief dossieronderzoek'.*
2. *Indien prospectief onderzoek: gebruik datamanagementplan 'Prospectief onderzoek'.*

VALORISATIE EN PUBLICATIE

Valorisatie

Revalidatie na een enkelfractuuroperatie vindt voornamelijk thuis plaats. In de huidige praktijk beginnen patiënten pas zes weken na de operatie met het oefenen van hun geopereerde been. Er is inmiddels klinisch bewijs dat dit eerder kan, maar alleen onder de voorwaarde dat patiënten in de thuissituatie nauwlettend in de gaten worden gehouden [5]. Op dit moment is er geen geschikt ambulant meetsysteem dat de belasting, het looppatroon en de balans bij deze patiënten in het dagelijks leven kan meten, en is er geen kennis over deze grootheden bij deze doelgroep. In dit project wordt een meetsysteem ontwikkeld dat dit wel mogelijk maakt, en bovendien robuust en gebruiksvriendelijk is. Het meetsysteem zal technisch gevalideerd worden. In deze pilotstudie, waarin we dit meetsysteem zullen gebruiken, zullen patiënten in week 7 tot 12 na de fractuur beginnen met het gedeeltelijk belasten van hun enkel. Dit zal de eerste inzichten geven in de gebruiksvriendelijkheid, toepasbaarheid en klinische mogelijkheden van het nieuwe meetsysteem.

De geïnstrumenteerde krukken kunnen in de toekomst worden meegegeven aan enkelfractuurpatiënten om revalidatie op maat te bieden. Hiermee zou de patiënt eerder kunnen beginnen met belasten, om zo het revalideren te versnellen.

Publicatie

De resultaten van de studie worden gebruik voor een master afstudeeropdracht en worden uitgeschreven in een afstudeerverslag in artikelvorm. Indien hier resultaten uit voortkomen die publiceerbaar zijn, wordt er een journaal bepaald om dit in te doen.

REFERENTIES

[1] Haubert LL, Gutierrez DD, Newsam CJ, Gronley JAK, Mulroy SJ, Perry J. A Comparison of Shoulder Joint Forces During Ambulation With Crutches Versus a Walker in Persons With Incomplete Spinal Cord Injury. Archives of Physical Medicine and Rehabilitation. 2006 1;87(1):63-70.
[2] Daly PJ, Fitzgerald RH, Melton LJ, Llstrup DM. Epidemiology of ankle fractures in Rochester, Minnesota. Acta orthopaedica Scandinavica. 1987;58(5):539-44. Available from: https://pubmed.ncbi.nlm.nih.gov/3425285/.
[3] Jensen SL, Andresen BK, Mencke S, Nielsen PT. Epidemiology of ankle fractures. A prospective population-based study of 212 cases in Aalborg, Denmark. Acta orthopaedica Scandinavica. 1998;69(1):48-50. Available from: https://pubmed.ncbi.nlm.nih.gov/9524518/
[4] Moseley AM, Beckenkamp PR, Haas M, Herbert RD, Lin CWC, Evans P, et al. Rehabilitation After Immobilization for Ankle Fracture: The EXACT Randomized Clinical Trial. JAMA. 2015 10;314(13):1376-85. Available from: https://jamanetwork.com/
[5] Smeeing DPJ, Houwert RM, Briet JP, Kelder JC, Segers MJM, Verleisdonk EJMM, et al. Weight-bearing and mobilization in the postoperative care of ankle fractures: a systematic review and meta-analysis of randomized controlled trials and cohort studies. PloS one. 2015 2;10(2). Available from: https://pubmed.ncbi.nlm.nih.gov/25695796/.
[6] F. Rasouli and K.B. Reed, “Walking assistance using crutches: A state of the art review”, 2020
[7] Medilogic, “medilogic WLAN insole”, via: https://medilogic.com/en/medilogic-wlan-insole/
[8] Xsens, “ForceShoes”, via: https://www.xsens.com/press-releases/xsens-technology-launched-outer-space
[9] Xsens, “MTw Awinda”, via: https://www.xsens.com/products/mtw-awinda
[10] Hertzog, M. A. (2008). Considerations in determining sample size for pilot studies. Research in Nursing &Health, 31(2), 180–191. https://doi.org/10.1002/NUR.20247